

HYDRAULIC CONDUCTIVITY OF BENTONITE-POLYMER (B-P)
GEOSYNTHETIC CLAY LINERS (GCLS) TO AGGRESSIVE COAL COMBUSTION
PRODUCT (CCP) LEACHATES

by

Binte Zainab
A Thesis
Submitted to the
Graduate Faculty
of
George Mason University
in Partial Fulfillment of
The Requirements for the Degree
of
Master of Science
Civil, Environmental, and Infrastructure Engineering

Committee:

_____	Dr. Kuo Tian, Thesis Director
_____	Dr. Burak F. Tanyu, Committee Member
_____	Dr. Viviana Maggioni, Committee Member
_____	Dr. F. Erol Guler, Committee Member
_____	Dr. Sam Salem, Department Chair
_____	Dr. Kenneth S. Ball, Dean, Volgenau School of Engineering

Date: _____ Fall Semester 2019
George Mason University
Fairfax, VA

Hydraulic conductivity of Bentonite-Polymer (B-P) Geosynthetic Clay Liners (GCLs) to
aggressive Coal Combustion Product (CCP) Leachates

A Thesis submitted in partial fulfillment of the requirements for the degree of Master of
Science at George Mason University

by

Binte Zainab
Bachelor of Science Civil Engineering
University of Engineering and Technology (UET), Lahore Pakistan, 2016

Director: Kuo Tian, Assistant Professor
Department of Civil, Environmental, and Infrastructure Engineering

Fall Semester 2019
George Mason University
Fairfax, VA

Copyright 2019 Binte Zainab
All Rights Reserved

DEDICATION

I dedicate my work to our holy prophet Muhammad ﷺ who taught us to “acquire knowledge and impart it to the people”, my mother Munira, father Abdus Salam, my sisters Ayesha and Fatima and my brothers Abdullah and Ibrahim who have always been an inspiration for me and most importantly, to my beloved husband Saad Ullah who has always been my biggest support and strength and I cannot begin to give you the thanks that you deserve.

ACKNOWLEDGEMENTS

I would like to thank Dr. Kuo Tian my research advisor for providing me the opportunity and trusting in my ability to work on this great project under his supervision. I would also like to thank Dr. Burak Tanyu and Dr. Erol Guler for their great support and guidance throughout the project.

I want to thank Samuel Demeke, Kledi Mita, Andres Cruz, Jorge Briones, Anny Kreiser and Jackeline Gastelo for their great help and assistance in the lab Thanks are extended to all GMU SGI team members who participated in this research voluntarily.

I want to extend my gratitude to Environmental Research & Education Foundation (EREF) for their financial support and CETCO, Minerals Technologies Inc for their generous material donations as this research would not be possible without their support.

TABLE OF CONTENTS

	Page
List of Tables	ix
List of Figures	x
List of Equations	xiv
List of Abbreviations	xv
Abstract	xvi
Chapter 1 : INTRODUCTION.....	1
1.1 Coal Combustion Products (CCPs).....	1
1.1.1 Types of CCPs	2
1.1.2 CCP Leachates.....	3
1.1.3 Effects of CCP Leachates	5
1.1.4 Selection of Synthetic CCP Leachates	7
1.2 Geosynthetic Clay Liners (GCLs).....	8
1.2.1 Sodium Bentonite (Na-B) GCLs	9
1.2.1.1 Swelling of (Na-B) GCLs	9
1.2.1.2 Factors Affecting Swelling of Na-B GCLs.....	10
1.2.1.2a: Ionic Strength (I).....	12
1.2.1.2b: Relative Abundance of Monovalent and Divalent Cations (RMD)...	12
1.2.1.3 Effect of Saline Solutions on Swelling and Hydraulic Conductivity of Na-B GCLs	13
1.2.2 Modified GCLs.....	15
1.2.2.1 Dense Prehydrated GCL	15
1.2.2.2 Multiswellable Bentonite (MSB).....	16
1.2.2.3 Bentonite Polymer Composite (BPC).....	17
1.2.2.3.1 Effect of Saline Solutions on BPC:.....	17
1.2.2.3.2 Bentonite-Polymer (B-P) GCLs.....	19
1.2.2.4 Swelling of Modified GCLs:	22

Chapter 2 : EFFECT OF SAMPLE PREPARATION ON INDEX PROPERTIES OF BENTONITE-POLYMER GCLS	47
2.1 Introduction	48
2.2 Materials and Methods	51
2.2.1 Bentonite-Polymer Composites	51
2.2.2a ASTM Standard Method.....	52
2.2.2b Alternative Methods	52
2.2.3 Swell Index Test	53
2.2.4 Loss on Ignition Tests.....	54
2.3 Results and Discussion.....	55
2.3.1 ASTM Standard Method	55
2.3.1a Swell Index.....	55
2.3.1b Loss on Ignition	56
2.3.2 Alternative Methods	58
2.3.2a Swell Index.....	58
2.3.2b Loss on Ignition	59
2.4 Summary and Conclusion	60
Chapter 3 : HYDRAULIC CONDUCTIVITY OF BENTONITE-POLYMER GEOSYNTHETIC CLAY LINERS TO AGGRESSIVE COAL COMBUSTION PRODUCT LEACHATES	78
3.1 Introduction	79
3.2 Materials.....	82
3.2.1 Geosynthetic Clay Liners	82
3.2.2 Permeant Solutions	83
3.3 Methods.....	86
3.3.1 Hydraulic Conductivity	86
Termination Criteria.....	86
3.3.2 Swell Index	87
3.4 Results and Discussion.....	87
3.4.1 Hydraulic Conductivity	87
3.4.2 Swelling.....	90
3.4.3 Polymer Loading	91
3.4.4 Polymer Type	92

3.4.5 Polymer Elution - Preferential Flow.....	93
3.5 Summary and Conclusions.....	94
Chapter 4 : FINAL REMARKS AND CONCLUSION	110
Future Research.....	111
REFERENCES	112

LIST OF TABLES

Table	Page
Table 1-1: Amount of CCP produced, recycled and disposed of by category. (ACCA, 2015 CCP Production & Use Survey Report).	23
Table 1-2: Chemical composition of CCP leachate based on dominant CCP type.	24
Table 1-3: Concentration of trace heavy metals in the CCP leachates.	26
Table 1-4: Summary of GCLs, leachates and effective stress used by previous researchers.	27
Table 2-1: Amount of Na-B and B-P sample retained and passing #100 sieve after grinding in according to ASTM D5890.....	62
Table 2-2: Sample preparation methods used in this study.	63
Table 2-3: Swell index and loss on ignition (LOI) test results of samples prepared following ASTM standard method.	64
Table 2-4: Swell index and loss on ignition results of Na-B and B-P GCL samples prepared following the alternative methods 1 and 2.	65
Table 3-1: Mass per unit area, initial thickness and polymer loading of sodium bentonite (Na-B) and bentonite-polymer (B-P) GCLs used in this study.	97
Table 3-2. Properties of selected synthetic CCP leachates.	98
Table 3-3. Hydraulic conductivity of GCLs permeated with CCP leachates and DI water.	99

LIST OF FIGURES

Figure	Page
Figure 1-1: Flow diagram of the flue-gas-desulfurization process based on lime (CaO) or limestone (CaCO ₃), which are the sorbents used by 90 percent of FGD systems in the United States (Graded from Kalyoncu and Olson 2016).....	28
Figure 1-2: Box plot for pH of CCP leachates based on dominant CCP type.	29
Figure 1-3: Box plot for major constituents (cations and anions) of CCP leachate based on dominant CCP type.....	30
Figure 1-4: Relationship between ionic strength and RMD of CCP leachate based on dominant CCP type. Source: CCP leachate data (130 U.S disposal sites), Leaching test data, Kolstad 2000 and Chen et al. 2018.	31
Figure 1-5: Hydraulic conductivity of conventional Na-B and B-P GCLs to coal-fired power plant leachates (Data from Benson et al. 2014) (Note: DI water at 0.01 mM).	32
Figure 1-6: Ionic strength versus. RMD relationship for landfill leachates i.e. municipal solid waste (MSW) leachate, coal combustion product (CCP) leachate and low-level radioactive waste (LLW) leachate. Source: CCP leachate data from 130 U.S. disposal sites, Leaching test data, Kolstad 2000, Tian et al 2016 and Chen et al 2018.	33
Figure 1-7: Selection of four synthetic CCP leachates based on their ionic strength and RMD. HI (high ionic strength leachate), LRMD (low RMD/ divalent cations rich leachate), TFGDS (Typical FGD solids leachate i.e. geometric mean of all FGD solids and TCCP (Typical CCP leachate i.e. geometric mean of all CCP leachates. (Note: The maximum RMD observed in case of CCP leachate data was ∞ i.e., only monovalent cations present but to represent that data in figure RMD = 100 has been used.).....	34
Figure 1-8: Selection of two synthetic CCP leachates based on their ionic strength and anion ratio (R). H. R (high anion ratio i.e. Cl ⁻ rich leachate) and L. R (low anion ratio i.e. SO ₄ ²⁻ rich leachate).....	35
Figure 1-9: Comparison of selected synthetic CCP leachate with CCP leachate used by previous researchers (Chen et al. 2018). Note: The maximum RMD observed in case of CCP leachate data was ∞ (i.e. only monovalent cations present) but to represent that data in figure RMD = 100 has been used.....	36

Figure 1-10: Replacement of ions in silicon tetrahedron and aluminium octahedron due to isomorphous substitution.....	37
Figure 1-11: Cations and water molecules attachment on the clay interlayer.	38
Figure 1-12: Step-wise hydration in the crystalline swelling regime (after Likos, 2004). Grabbed from Bouazza, A., & Bowders Jr, J. J. (2009), “Geosynthetic clay liners for waste containment facilities”.....	39
Figure 1-13: Replacement of cations based on lyotropic series.	40
Figure 1-14: Ionic strength versus free swell relationship for Na-B GCLs permeated with deionized water (DI) , monovalent cations leachate (RMD = infinity), divalent cations leachate (RMD = 0), trivalent cations leachate and mix cations leachate. Ref. Jo et al 2001, Kolstad 2004a, Kolstad 2004b, Lee et al. 2005, Katsumi 2008, Scalia et al 2011, Tian et al. 2016, Chen at al. 2018.(Note: DI water at 1.2 mM)	41
Figure 1-15: Ionic strength versus hydraulic conductivity relationship for Na-B GCLs permeated with monovalent cations leachate (RMD = infinity), divalent cations leachate (RMD = 0), trivalent cations leachate and mix cations leachate. Ref. Jo et al 2001, Kolstad 2004a, Kolstad 2004b, Lee et al. 2005, Katsumi 2008, Scalia et al 2011, Tian et al. 2016, Chen at al. 2018.(Note: DI water at 1.2 mM).....	42
Figure 1-16: Free swell versus hydraulic conductivity relationship for Na-B GCLs.	43
Figure 1-17: Ionic strength versus hydraulic conductivity relationship for modified GCLs. DPH = Dense prehydrated, MSB = Multi swellable bentonite and BPC = Bentonite polymer composite.....	44
Figure 1-18: Ionic strength versus hydraulic conductivity relationship for modified GCLs. DPH = Dense prehydrated, MSB = Multi swellable bentonite and BPC = Bentonite polymer composite.....	45
Figure 1-19: Free swell versus hydraulic conductivity relationship for modified GCLs. DPH = Dense prehydrated, MSB = Multi swellable bentonite and BPC = Bentonite polymer composite.....	46
Figure 2-1: Relationship between swell index and hydraulic conductivity of Na-B and B-P GCLs (Note: Na-B GCLs data from Jo et al. 2001; Kolstad et al. 2004; Lee et al. 2005; Katsumi et al. 2008; Scalia et al. 2014; Setz et al. 2017; Tian et al. 2017; and B-P GCLs data from Katsumi et al. 2008; Scalia et al. 2014; Tian et al. 2016; Tian and Benson 2017; Tian et al. 2017)	66
Figure 2-2: Granule size distribution of Na-B and B-P GCL samples used in this study. 67	
Figure 2-3: Comparison of swell indices of B-P7 samples before (a and b) and after (c and d) swell test, prepared following ASTM standard method that includes the specimens passing the #100 sieve (ASTM-P) and remaining on the #100 sieve (ASTM-R).	68

Figure 2-4: Comparison of swell indices of ASTM-P and ASTM-R for the Na-B and B-P samples prepared following ASTM standard method (Note: Swell test not done on Na-B and B-P1-ASTM-R due to limited quantity of sample retained on #100 sieve).....	69
Figure 2-5: Images of ASTM-Remnants #100 (ASTM-R) specimens of B-P3 and B-P7 before (a and b) and after (c and d) swell index test.	70
Figure 2-6: Loss on ignition (LOI) of Na-B and B-P samples prepared following ASTM standard method for the specimen passing the #100 sieve (ASTM-P) and remnants on the #100 sieve (ASTM-R).	71
Figure 2-7: Images of Na-B and B-P6 specimens prepared following ASTM standard method for the specimens passing the #100 sieve (ASTM-P) and remnants on the #100 sieve (ASTM-R) before and after loss on ignition test.....	72
Figure 2-8: Comparison of swell indices of Na-B and B-P samples prepared following ASTM standard method (ASTM-P) with the alternative method 1 (AL1-As-is) and alternative method 2 passing #100 (AL2-P) and retained #100 (AL2-R). ..	73
Figure 2-9: Images of Na-B, B-P3 and B-P7 prepared following the ASTM standard method (ASTM-P) and the alternative method 1 (AL1-As-is) after swell index test on specimens.	74
Figure 2-10: Comparison of loss on ignition values of Na-B and B-P samples prepared following ASTM standard method (ASTM-P) with the alternative method 1 (AL1-As-is) and alternative method 2 [i.e. passing #100 (AL2-P) and retained #100 (AL2-R)]......	75
Figure 2-11: Images of B-P6 specimens prepared following alternative method 1(AL1-As-is) and alternative method 2 (AL2-P and AL2-R) before and after loss on ignition test.....	76
Figure 2-12: Comparison of loss on ignition (LOI) of Na-B and B-P samples prepared following the alternative method 1 (AL1-As-is), prepared following ASTM standard method (ASTM-P), and the alternative method 2 passing (AL2-P) and retained (AL2-R) on #100 sieve.	77
Figure 3-1: Grain size distribution of sodium bentonite (Na-B) and bentonite polymer (B-P) GCLs used in this study. Note: Na-B = conventional sodium bentonite GCL with polymer loading = 0%, P = polymer loading.	100
Figure 3-2: Comparison of selected synthetic CCP leachate with CCP leachate used by previous researchers (Chen et al. 2019). Note: The maximum RMD observed in case of CCP leachate data was ∞ (i.e. only monovalent cations present) but to represent that data in figure RMD = 100 has been used.....	101
Figure 3-3: Hydraulic conductivity, ratio of inflow to outflow (Q_{in}/Q_{out}), pH, and EC from test on B-P-0.5 permeated to LRMD-96 leachate.	102
Figure 3-4: Hydraulic conductivity of GCLs as a function of ionic strength.	103

Figure 3-5: Hydraulic conductivity versus swell index of Na-B and B-P GCLs in CCP leachates and DI water.....	104
Figure 3-6: Hydraulic conductivity of GCLs as a function of polymer loading.....	105
Figure 3-7: Images of two different types of polymers found in BP-GCLs. (a) B-P-3.7 and (b) B-P-5.5.....	106
Figure 3-8: Comparison of hydraulic conductivity of B-P GCLs with similar polymer loading but different polymer type (linear vs. crosslinked polymers).....	107
Figure 3-9: (a) Temporal behavior of B-P-0.5 permeated to LR-2577 leachate (b) dye test conducted on B-P-0.5 (LR-2577) indicating preferential flow on the effluent side of GCL (c) polymer elution from B-P GCL during permeation with CCP leachate (d) Temporal behavior of B-P-3.4 permeated with LR-2577 and (e) dye test on B-P-3.4 (LR-2577) showing uniform flow distribution on effluent side of GCL.	108
Figure 3-10: Polymer elution from B-P GCL during permeation with CCP leachate....	109

LIST OF EQUATIONS

Equation	Page
Equation 1-1: Ionic Strength.....	6
Equation 1-2: RMD.....	6
Equation 1-3: Anion Ratio.....	7
Equation 3-1: Ionic strength.....	83
Equation 3-2: RMD.....	84

LIST OF ABBREVIATIONS

American Coal Ash Association.....	ACAA
Anion Ratio.....	R
Bentonite Polymer Composite.....	BPC
Bentonite Polymer.....	B-P
Coal Combustion Product.....	CCP
Compacted Clay Liner.....	CCL
Dense Prehydrated.....	DPH
Flue Gas Desulphurization.....	FGD
Geosynthetic Clay Liner.....	GCL
Ionic Strength.....	I
Low Level Radioactive Waste.....	LLW
Multiswellable Bentonite.....	MSB
Municipal Solid Waste.....	MSW
Polymer Loading.....	P
Relative Abundance of Monovalent and Divalent Cations.....	RMD
Sodium Bentonite.....	Na-B
Spray Dryer Ash.....	SDA
United States Environmental Protection Agency.....	USEPA

ABSTRACT

HYDRAULIC CONDUCTIVITY OF BENTONITE-POLYMER (B-P) GEOSYNTHETIC CLAY LINERS (GCLS) TO AGGRESSIVE COAL COMBUSTION PRODUCT (CCP) LEACHATES

Binte Zainab, M.S.

George Mason University, 2019

Thesis Director: Dr. Kuo Tian

Coal Combustion Products (CCPs) also known as coal ash/residues are generated when coal is burnt to generate electricity or steam. CCPs include fly ash, bottom ash, flue gas desulfurization (FGD) materials (FGD solids, FGD Gypsum), spray dryer ash etc. In 2012, approximately 40 percent of the CCPs generated in United States were beneficially used while the remaining 60 percent of CCPs were disposed in surface impoundments and landfills. According to American Coal Ash Association (ACAA), the production of CCPs has grown from 59.5 million Mg in 1974 to 114.7 million Mg in 2013.

The leachates produced at the CCP landfills may contain high concentration of toxic substances such as heavy metals, very high and low pH conditions and high salinity. Therefore, United States Environmental Protection Agency (USEPA) require the CCP disposal facilities to have a composite liner consisting of a geomembrane overlying a 0.6 m thick compacted clay liner (CCLs) to prevent the potential contamination of groundwater. Hydraulic conductivity of CCLs should be $\leq 1 \times 10^{-9}$ m/s. The regulation

allows the use of alternative materials (e.g., Geosynthetic Clay Liners, GCLs) in *lieu* of CCLs, provided that they have equal or lower hydraulic conductivity than CCLs.

Conventional sodium bentonite (Na-B) GCLs consist of a thin layer of sodium bentonite sandwiched between two geotextiles. GCLs are easy to install, save air space due to less thickness (5 to 10 mm), and have low hydraulic conductivity ($< 10^{-10}$ m/s). The low hydraulic conductivity of Na-B GCLs is due to swelling of bentonite layer that clogs the void spaces and results in narrower and tortuous flow paths. However, aggressive leachates with high salinity, polyvalent cations or extreme pH can inhibit the swelling of Na-B GCLs leading to high hydraulic conductivity. Studies have shown that polymer modified GCLs consisting of bentonite-polymer (B-P) mixtures have higher chemical compatibility and lower hydraulic conductivity to aggressive leachates than Na-B GCLs.

Recently, the CCP leachate data collected from more than 130 CCP disposal facilities have shown much more aggressive leachates than those studied by previous researchers. Therefore, the purpose of this study was to evaluate the hydraulic performance of B-P GCLs to new CCP leachates. Index properties and hydraulic conductivity of B-P GCLs was studied in detail. Swell index and hydraulic conductivity tests were conducted on six B-P GCLs permeated to six synthetic CCP leachates. B-P GCLs were selected with varying polymer loading ranging from 0.5% to 12.7%, to evaluate the effect of polymer loading on the hydraulic conductivity of B-P GCLs. The six synthetic CCP leachates were created based on data collected from more than 130 CCP disposal facilities to represent the typical and worse scenarios observed in the field.

CHAPTER 1 : INTRODUCTION

1.1 Coal Combustion Products (CCPs)

Coal Combustion Products (CCPs) also known as coal ash, are the solid minerals left when coal is burnt to generate electricity or steam. In 2012, 470 coal-fired electric utilities generated about 100 million Mg of coal ash (USEPA). The production of CCPs has grown from 59.4 million Mg in 1974 to 114.7 million Mg in 2013 (ACAA 2015).

CCPs can be disposed in off-site landfills or disposed in on-site landfills or surface impoundments. In 2012, approximately 40 percent of the CCPs generated in U.S. were beneficially used (e.g., in concrete products, gypsum panels, waste stabilization, agriculture etc.) while the remaining 60 percent of CCPs were disposed in surface impoundments and landfills. Of that 60 percent, approximately 80 percent was disposed in on-site disposal units. CCPs disposal currently occurs at more than 310 active on-site landfills, averaging more than 0.5 km² in size with an average depth of over 12 meters, and at more than 735 active on-site surface impoundments, averaging more than 0.2 km² in size with an average depth of 6 meters (USEPA 2017). According to a survey conducted by American Coal Ash Association (ACAA) in 2015, out of 106 million Mg of total CCP produced approximately 51 million Mg is disposed of in landfills and impoundments. Table 1-1, shows the survey results of ACCA for different CCP types produced, recycled and disposed in the year of 2015.

1.1.1 Types of CCPs

Various types of CCPs are generated during the combustion of coal including:

- Bottom Ash
- Boiler Slag
- Fly Ash
- Flue Gas Desulphurization (FGD) Materials
- Spray Dryer Ash

Coarse and heavier portion of coal ash that settles at the bottom of the combustion chamber is termed as bottom ash. Boiler slag is the melted coal ash. Fly ash is the fine and light form of coal ash that floats into the exhaust stacks and is removed from the flue gas by electrostatic precipitators or other gas-scrubbing systems.

Flue Gas Desulphurization (FGD) method is used to remove sulphur oxides (SO_x) from flue gas using either calcium oxide (CaO) or calcium carbonate (CaCO_3). This removal of sulphur generally results in formation of hydrous calcium sulfate ($\text{CaSO}_4 \cdot 2\text{H}_2\text{O}$) also known as FGD Gypsum that can be used in various application such as agriculture, gypsum panel products, highway construction, mining applications, cement production, water treatment and glass making. FGD sludge also contain high concentrations of calcium sulfite (CaSO_3), which requires fixation/stabilization treatment. One of the treatment methods is forced oxidation that converts calcium sulfite (CaSO_3) into calcium sulfate (CaSO_4) a relatively more stable product. The final stabilized material is known as Fixated FGD.

Spray Dryer Absorber (SDA) is also a FGD technology that captures SO₂ from flue gas and the material collected through this process is termed as SDA material or dry FGD. (Heebink, et al. 2007). Figure 1-1 shows the flow diagram for a typical FGD process, also showing the production of other CCP types.

1.1.2 CCP Leachates

CCP leachates are produced when water percolates through the coal residues (CCPs) present in the CCP landfill or disposal site and extracts the contaminants out of it. Chemical characterization of CCP leachate data collected from more than 130 CCP disposal units (landfills and impoundments) located within United States and on leaching analysis tests (LT) conducted at geo-environmental lab have been presented in Table 1-2 and Fig. 1-3. Leachate characterization is based on dominant CCP type (bottom ash, fly ash, FGD materials, mixed coal ash etc.) and the master variables known to affect the hydraulic properties of GCL i.e., major cations (Na⁺, K⁺, Mg²⁺, Ca²⁺), major anions (Cl⁻, SO₄²⁻), ionic strength (I), pH, relative abundance of monovalent and divalent cations (RMD) and anion ratio (Cl⁻/SO₄²⁻).

pH of all the CCP leachates is shown in Figure 1-2 which indicates that most of the CCP leachate is basic in nature with mean pH ranging from 7.44 to 9.32. Out of total samples collected, approximately 50% comprised of mixed coal ash. Table 1-2 and Fig. 1-3 represents the relative abundance of all the chemical constituents present in the CCP leachate. It has been observed that leaching test (LT) samples possess higher relative abundance of all chemical constituents in comparison to rest of the leachate data obtained (see Fig. 1-3). The CCP leachate data obtained from disposal sites (landfills and

impoundments) showed that out of all four major cations, Na^+ (1831.81 mM) and K^+ (23.8 mM) displayed highest and lowest concentration respectively (see Fig 1-3, FGD Solids). The CCP leachate data obtained from LT also proclaims similar relationship between Na^+ and K^+ cations, i.e., highest and lowest concentration respectively. However, the concentration of Na^+ (3448.7 mM) and K^+ (1395.1 mM) in case of L.T samples is relatively much higher compared to the data obtained from disposal sites.

The maximum concentration of divalent cations Mg^{2+} and Ca^{2+} , observed in CCP leachate data obtained from disposal sites is 140.12 mM (FGD Solids) and 41.33 mM (Fixated FGD) respectively. On contrary the data obtained from LT represents much higher concentration for both Mg^{2+} and Ca^{2+} i.e., 507.5 mM and 538.1 mM respectively.

Similarly, major anions concentration has also been analyzed to understand complete picture of the CCP leachate. The CCP leachate data shows that for most of the leachates the concentration of Cl^- is higher than SO_4^{2-} . The data obtained from LT depict that Cl^- and SO_4^{2-} has a maximum concentration of 4366 mM and 696.4 mM respectively (see Fig. 1-3/Table 1-2, Leaching Test). However maximum Cl^- and SO_4^{2-} concentration obtained from disposal sites is 1195.5 mM (see Fig. 1-3/Table 1-2, Mixed Coal Ash) and 990.83 mM respectively (see Fig. 1-3/Table 1-2, FGD Solids).

In case of bulk properties, RMD ranges from a minimum value of $0.002 \text{ M}^{1/2}$ (Mixed Coal Ash and Fly Ash) to a maximum of infinity (LT), because one leachate sample had no divalent cations present. Anion ratio ($\text{Cl}^-/\text{SO}_4^{2-}$) ranges from 0.01 to 122.30 (LT). Maximum Ionic strength is 4685.00 mM and 3177.69 mM for LT sample and leachate

collected from disposal sites (FGD Solids) respectively. The relationship between bulk properties i.e., ionic strength versus RMD of different CCP leachate types is shown in Fig. 1-4.

1.1.3 Effects of CCP Leachates

The CCP disposal sites (landfills and impoundments) can be a threat to humans and environment if not regulated properly. The CCP leachates produced at the disposal sites contain high concentration of toxic substances such as heavy metals (Table 1-3), very high and low pH conditions (Fig. 1-2) and high salinity (Fig. 1-3, Table 1-2). Therefore, if CCPs are disposed of at the disposal sites without any lining or cover system these toxic substances can percolate into the ground water and into the atmosphere affecting the quality of drinking water, food and air. Table 1-3 shows that the concentration of all the heavy metals are beyond the USEPA standard limit for drinking water.

New regulations established for disposal of CCPs require that disposal facilities include a composite liner consisting of a geomembrane overlying a 0.6-m-thick clay liner. Alternative liner configurations are also permissible including use of GCLs in lieu of a CCLs. GCLs are a popular lining material because they save airspace, easy to install, have relatively low cost and hydraulic conductivity ($< 10^{-10}$ m/s) in comparison to CCLs.

The Electric Power Research Institute (EPRI) sponsored a study in 2014 to assess whether GCLs have sufficiently low hydraulic conductivity when permeated with CCP leachate (Benson et al. 2014). EPRI's study showed that conventional GCLs could be used

for more dilute CCP leachates, whereas more resilient GCLs with bentonite-polymer (B-P) composites are needed for more concentrated leachates, Fig. 1-5.

The hydraulic conductivity and swelling of GCLs is sensitive to the concentration of the permeant solution and the cation valence. In general, higher hydraulic conductivity and lower swell of GCLs is related to high ionic strength (I) and low relative abundance of monovalent and divalent cations (RMD) of permeant solutions. (Kolstad et al. 2004a). Ionic strength (I) is defined as

$$I = \frac{1}{2} \sum_{i=1}^n c_i z_i^2 \quad \text{Equation 1-1: Ionic Strength}$$

Where, c_i is the concentration of the i^{th} ionic specie, z_i is the valence of the i^{th} specie, and n is the number of cation and anion specie in the leachate. RMD is defined as (Kolstad et al. 2004a).

$$\text{RMD} = \frac{M_m}{\sqrt{M_d}} \quad \text{Equation 1-2: RMD}$$

Where, M_m is the total molar concentration of monovalent cations in the leachate and M_d is the total molar concentration of divalent cations in the leachate. Ionic strength describes the overall strength of a solution and RMD describes the relative abundance of monovalent and divalent cations in a solution.

Tian et al. (2017), also relates the sensitivity of the B-P GCL to anion ratio ($\text{Cl}^-/\text{SO}_4^{2-}$) as it is attributed to the collapse of the polymer. When the Cl^- concentration increases, it opens the intergranular pores and results in higher hydraulic conductivity.

$$R = \frac{[Cl^-]}{[(SO_4)^{2-}]}$$

Equation 1-3: Anion Ratio

1.1.4 Selection of Synthetic CCP Leachates:

A comparison between ionic strength and RMD of different types of landfill leachates is shown in Fig. 1-6. Most of municipal solid waste (MSW) and CCP leachate overlap each other but the highest ionic strength and lowest RMD is given by CCP leachate in comparison to MSW and low level radioactive (LLW) leachate.

To identify the most aggressive and typical CCP leachates for evaluating the chemical compatibility of B-P GCLs, the CCP leachate data has been organized in terms of ionic strength and RMD in Fig. 1-7. Four synthetic CCP leachates based on their ionic strength and RMD have been selected as shown in Fig. 1-7. HI represent the highest ionic strength leachate reported out of 130 U.S. disposal sites. LRMD is the lowest RMD leachate or divalent cations rich leachate (geometric mean of all FGD gypsum). TFGDS is the typical FGD solids leachate (geometric mean of all FGD solids) that is the representative of most aggressive CCP type and TCCP is the typical CCP leachate (geometric mean of all CCP leachates) that is representative of most commonly seen CCP leachate in the U.S disposal sites.

To identify the most aggressive CCP leachates in terms of anion ratio for evaluating the chemical compatibility of B-P GCLs to chloride and sulphate rich leachates, the leachate data has been organized and in terms of ionic strength and anion ratio ($R = Cl^- / SO_4^{2-}$) in Fig. 1-8. Fig. 1-8 shows the selection of two synthetic CCP leachates based on their ionic strength and anion ratio (R). HR is the high anion ratio leachate i.e., Cl^- rich

leachate and LR is the low anion ratio leachate i.e., SO_4^{2-} rich leachate. HI is also shown in Fig. 1-8 as the leachate with moderate anion ratio (R).

The new CCP leachate data has been compared with the CCP leachate data used by previous researchers in Fig. 1-9. The comparison showed that the new CCP leachate is much more aggressive than the one used by previous researchers both in terms of higher ionic strength ($I \approx 5 \text{ M}$ versus $I = 1 \text{ M}$) and low RMD ($\text{RMD} = 0.005$ versus $\text{RMD} = 0.01$). It shows that there is a need to check whether the commercially available GCLs are effective against the selected synthetic CCP leachates or not. Table 1-6 shows the summary of bulk properties of the six synthetic CCP leachates selected for testing and evaluation of geosynthetic clay liners (GCLs).

1.2 Geosynthetic Clay Liners (GCLs)

Geosynthetic clay liners (GCLs) are composed of a thin layer of bentonite sandwiched between two geotextile layers held together by needle punching or stitching (Shackelford et al. 2000). GCLs have been increasingly used in the liner and cover systems of waste disposal facilities (landfills and impoundments) because of their low hydraulic conductivity ($< 10^{-10} \text{ m/s}$), ease of installation and relatively low cost (Shackelford et al. 2000; Jo et al. 2001, 2005; Kolstad et al. 2004a; Benson et al. 2010). GCLs can be categorized into two main types i.e., (1) conventional sodium bentonite (Na-B) GCLs and (2) modified GCLs (e.g., dense prehydrated (DPH), multiswellable bentonite (MSB) and bentonite-polymer (B-P) GCLs).

1.2.1 Sodium Bentonite (Na-B) GCLs

The conventional sodium bentonite geosynthetic clay liners (Na-B GCLs) mainly consist of sodium bentonite as the impermeable layer controlling the hydraulic conductivity of the GCLs. The sodium bentonite contains sodium ions (Na^+) as the dominant cations surrounding the negatively charged clay surface. Na-bentonite is composed primarily of mineral Na-montmorillonite (65 to 90 %). The mineral montmorillonite is responsible for the significantly large swelling of bentonite clay due to its large specific surface area (as high as $800 \text{ m}^2/\text{g}$), high charge deficiency (0.5–1.2 per unit cell), high cation exchange capacity (80–150 meq/100 g), and ability for interlayer swelling (Shackelford et al. 2000). When bentonite absorbs water, it swells and fill up the voids between bentonite granules. Swelling of bentonite leads to narrower and tortuous flow paths for the mobile water and resulting in low hydraulic conductivity (Shackelford et al. 2000; Jo et al. 2001, 2005; Ashmawy et al. 2002; Kolstad 2004a; Guyonnet et al. 2005; Scalia et al. 2011; Bradshaw et al. 2014; Chen et al. 2014; Athanassopoulos et al. 2015; Tian et al. 2016; Setz et al. 2017; Ören and Akar 2017; Chen et al. 2019).

1.2.1.1 Swelling of (Na-B) GCLs

As discussed in previous section Na-bentonite mainly consists of mineral Na-montmorillonite which is a member of the smectite family. It is a 2:1 clay, it consists of an alumina octahedral layer sandwiched between two silica tetrahedral layers (Fig. 1-10).

Montmorillonite gets a negative charge due to a phenomenon called isomorphous substitution. Due to isomorphous substitution the Si^{4+} of the tetrahedron is replaced by Al^{3+} or the Al^{3+} of the octahedron is replaced by Mg^{2+} (Fig. 1-10) resulting in an overall negative

charge on the montmorillonite mineral. This negative charge plays a very important role as it leads to the adsorption of cations (typically Na^+) and water molecules onto the surface and interlayers of Na-montmorillonite mineral and results in the swelling of bentonite clay.

Overall water is a neutral molecule, consisting of one oxygen atom covalently bonded with two hydrogen atoms but because of the high electronegativity of oxygen it attracts the shared pair of electrons more toward itself. Which leads to unequal sharing of electrons between oxygen and hydrogen atoms making water a dipolar molecule with oxygen having a partial negative charge and hydrogen having a partial positive charge. Dipolar water molecules can attach to the negatively charged clay particles in two ways i.e., either the partial negative oxygen of water can attach to the already attached positively charged cations or the partial positive hydrogen atom of water can directly attach itself to the negatively charged clay particles (Fig.1-11). The interlayer swelling occurs in two phases: firstly, the crystalline (or hydration) phase takes place when several layers of water molecules hydrate the clay from completely dry state and results in small amount of swelling called “crystalline swelling”. Fig. 1-12 shows the step-wise hydration in the crystalline phase. Secondly, osmotic swelling results in additional molecular layers of water and larger interlayer distances. Osmotic hydration is responsible for significant amount of immobile water molecules, larger swelling (osmotic swelling) and lower hydraulic conductivity.

1.2.1.2 Factors Affecting Swelling of Na-B GCLs

Factors (such as small particle size, interlayer swelling, and thick layer of bound water associated with montmorillonite particles) that are responsible for the low hydraulic

conductivity of sodium bentonite (Na-B) GCLs, also make it more susceptible to chemical interactions. Especially when they are permeated with landfill leachates such as municipal solid waste (MSW), coal combustion product (CCP), and low level radioactive waste (LLW) etc. produced in the landfills and disposal sites. Therefore, these factors can also lead to increase in hydraulic conductivity of GCLs.

Several studies have investigated the effect of chemicals on the hydraulic conductivity of geosynthetic clay liners (Jo et al. 2001; Kolstad 2004a; Lee et al. 2005; Katsumi 2008; Scalia et al 2011; Tian et al. 2016; Chen et al. 2018). It has been seen that the chemical characteristics of the permeant solution (leachate) such as ionic strength (i.e., concentration of ions), relative abundance of monovalent and divalent cations (i.e., associated with valence of cations presents in the leachate), and pH are the main factors affecting the swelling and hydraulic conductivity of Na-B GCLs (Jo et al 2001; Kolstad 2004a; Lee et al. 2005; Katsumi 2008; Scalia et al 2011). Lower swell is generally associated with an increase in concentration, an increase in cation valence, or very low or very high pH of the permeant solution (Jo et. al. 2001). Moreover, if multivalent cations (i.e., valence $\geq 2+$) dominate the exchange complex, or if the hydrating solution has high ionic strength, swelling of sodium bentonite decreases. (Shackelford et al. 2000; Jo et al. 2001, 2005; Kolstad et al. 2004a; Katsumi et al. 2008). These trends observed for bentonites are likely to be much stronger than those for other clayey soils that have lower montmorillonite content. Changes in the swelling behavior of bentonite can lead to various problems towards its application as a hydraulic barrier. The following sections explain the factors affecting the swelling behavior of sodium bentonite GCLs in detail.

1.2.1.2a: Ionic Strength (I)

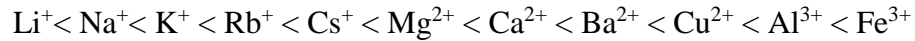
To understand the effect of ionic strength of the surrounding solution on the swelling of the sodium bentonite, we can consider the phenomena of osmosis, in which water (solvent) starts moving from regions of low concentration of ions (solutes) to a region of high concentration of ions (solutes) through a semi-permeable membrane (that allows movement of water but not the solute particles) to bring the system to equilibrium with equal concentration of water (solvent) on both sides. In clays (bentonite), the effect of a semi-permeable membrane is introduced by the limitation in ion movement that the negatively charged clay particles impose on the interlayer cations in overlapping double layers. Once sufficient separation distances between unit layers are achieved during crystalline swelling (for Na⁺-smectite, this is ~20 Å), attractive forces no longer dominate, and the interlayer can be considered a region of high electrolyte concentration compared to the external bulk solution. If the concentration of cations present in the interlayer region is greater than the bulk solution, osmotic pressure arises from the difference in concentration of ions, thus causing water molecules to be drawn into the zone of relatively high concentration of ions. The volume change associated with this process is referred to as osmotic swelling (Bouazza, A., & Bowders Jr, J. J., 2010).

1.2.1.2b: Relative Abundance of Monovalent and Divalent Cations (RMD)

To understand how RMD can affect the swelling of sodium bentonite, Fig. 1-13 is shown that if a solution having high concentration of divalent cations (e.g., Ca²⁺ and Mg²⁺) comes in contact with sodium bentonite then according to a series called lyotropic

series, the ions present on the right side of the series can replace the ions present on the left side of the series.

The preference for replacement as per the lyotropic series is as follows:



As Ca^{2+} and Mg^{2+} are present on the right side of Na^+ , they can replace the Na^+ of the Na-B. To keep the system neutral as a whole one $\text{Ca}^{2+} / \text{Mg}^{2+}$ will replace two Na^+ because of double the positive charge present on it. Now because of the replacement of two Na^+ by one $\text{Ca}^{2+} / \text{Mg}^{2+}$, the number of water molecules attached to the cations will reduce because earlier two cations were holding water molecules separately and now only one cation is holding the water molecules. Moreover due to high positive charge on $\text{Ca}^{2+} / \text{Mg}^{2+}$ in comparison to Na^+ ion, it attracts the opposite interlayer surfaces with greater force and results in shrinkage of the bentonite.

1.2.1.3 Effect of Saline Solutions on Swelling and Hydraulic Conductivity of Na-B

GCLs

The ionic strength versus free swell relationship for Na-B GCLs permeated with leachates containing monovalent cations (RMD = infinity), divalent cations (RMD = 0), trivalent cations and with mix of all these cations is shown in Fig. 1-14. The mix cations also include the synthetic leachates that are representative of field conditions. Data collected from Jo et al 2001; Kolstad 2004a; Lee et al. 2005; Katsumi 2008; Scalia et al 2011; Tian et al. 2016; Chen et al. 2018.

Monovalent cations with RMD = infinity showed highest value of free swell but with the increase in concentration of ions (ionic strength) the free swell of monovalent

cations gradually decreased to same level as of the multivalent cations (at $I = 1000 \text{ mM}$). The multivalent cations i.e. divalent and trivalent showed a rapid decrease in swell value with fairly consistent value from 100 to 1000 mM ionic strength. Moreover trivalent cations showed lower swell than the divalent cations. In general the swelling of Na-B is dependent on valence at low concentrations ($< 100 \text{ mM}$). For ionic strength equal to 100 mM to 1000 mM the effect of valence becomes negligible.

The ionic strength versus hydraulic conductivity relationship for Na-B GCLs permeated with monovalent cations (RMD = infinity), divalent cations (RMD = 0), trivalent cations and mix cations leachate is shown in Fig. 1-15. Data obtained collected from Jo et al 2001; Kolstad 2004a; Lee et al. 2005; Katsumi 2008; Scalia et al 2011; Tian et al. 2016; Chen et al. 2018.

The GCLs permeated with monovalent solutions showed hydraulic conductivity similar to that of DI water for ionic strength less than 100 mM i.e. approximately 10^{-11} m/s . The hydraulic conductivity of GCLs permeated with divalent solutions are higher than that of permeated with monovalent solutions and the values increased significantly for ionic strength greater than 30 mM. In case of ionic strength greater than 1000 mM, the GCLs permeated with divalent solutions showed hydraulic conductivity of higher than 10^{-7} m/s .

The free swell versus hydraulic conductivity relationship for Na-B GCLs is shown in Fig. 1-16. Hydraulic conductivity shows an inverse relationship with free swell. That is in case of Na-B GCLs higher the swell lower will be hydraulic conductivity. Therefore, swell index test can be used as a quick test to predict the hydraulic conductivity of Na-B GCLs.

1.2.2 Modified GCLs

Previous researches have shown that the swelling of conventional Na-B GCLs significantly reduces when exposed to leachates having high ionic strength or preponderance of multivalent cations (Jo et al 2001; Kolstad 2004a; Lee et al. 2005; Katsumi 2008; Scalia et al 2011). The reduction in swelling ultimately leads to an increase in the hydraulic conductivity of the GCLs, making GCLs unsuitable as hydraulic barriers for the liner and cover systems for waste containment facilities. Therefore, different methods have been adopted to improve the effectiveness of GCLs as liner systems. Table 1-4 shows a summary of GCL and leachates used by previous researchers.

1.2.2.1 Dense Prehydrated GCL:

Kolstad et al. (2004b), suggested the use of dense prehydrated (DPH) GCLs to achieve low permeability. DPH-GCL consisted of bentonite prehydrated using a dilute aqueous solution of carboxymethyl cellulose (CMC) and methanol and then calendered to achieve a uniform thickness (5 mm) and void ratio (1.2). He compared the swelling and hydraulic conductivity of conventional Na-B and DPH GCLs using different aqueous solutions (1 M CaCl₂, 1 M NaCl, HCL with pH 1.2 and NaOH with pH 13.1) as permeant liquids. Kolstad et al. (2004b) reported that the two GCLs gave comparable swell in NaCl, CaCl₂ and acidic (HCl) solutions. However, the bentonite from DPH-GCL showed 90% more swell than Na-B GCL when permeated with NaOH (pH = 13.1). Moreover, the hydraulic conductivity of DPH GCL was found to be lower in all permeant solutions than Na-B GCL. For example, the hydraulic conductivity of DPH-GCL and Na-B GCL to 1 M CaCl₂ was 3.7×10^{-12} m/s and 9.1×10^{-7} m/s respectively. In case of DI water DPH-GCL

showed three times lower hydraulic conductivity (4.1×10^{-12} m/s) than Na-B GCL (1×10^{-11} m/s). According to Kolstad et al. (2004b) DPH-GCLs may be more resistant to chemical interactions than Na-B GCLs. The hydraulic conductivity tests discussed in the paper were conducted for less than a year whereas the GCLs in the field are expected to function for several decades. Therefore, the long-term behavior of DPH-GCLs in the field may vary from the results obtained in the paper.

1.2.2.2 Multiswellable Bentonite (MSB):

Katsumi et al. (2008) studied the long-term hydraulic conductivity of two modified materials, a multiswellable bentonite (MSB) containing 25 % propylene carbonate (PC) by weight to sodium bentonite (Na-B) and a dense prehydrated GCL (DPH-GCL) containing factory prehydrated–consolidated Na-B. Tests were also conducted on pure sodium bentonite (Na-B) and conventional Na-B GCL as control materials. The GCLs were permeated with Deionized (DI) water, inorganic salt solutions of NaCl, CaCl₂ and NaCl-CaCl₂ for a maximum of 7 years. The ionic strength (0.05 to 2 M) and RMD (0 to ∞) of the salt solutions was varied to see their effect on the performance of GCLs. Free swell and liquid limit tests were also conducted in addition to hydraulic conductivity tests. The experimental results showed that MSB has lower hydraulic conductivity (1.0×10^{-11} m/s) in comparison to Na-B when permeated with NaCl solutions of molar concentration less than 1.0 M. However, the hydraulic conductivity of MSB was identical to Na-B when the molar concentration of NaCl was 2.0 M. Similarly, DPH-GCL also showed lower hydraulic conductivity (1.0×10^{-12} m/s) in comparison to non prehydrated GCL when permeated with

CaCl₂ solutions. However, the hydraulic conductivity tests on DPH-GCL was conducted for 3 years in comparison to tests conducted on MSB which were conducted for 7 years.

1.2.2.3 Bentonite Polymer Composite (BPC)

In recent years, the conventional sodium bentonite GCLs have been modified using different organic molecules and polymers. These bentonite polymer composites (B-P) are expected to have better chemical resistance and lower hydraulic conductivity when permeated with aggressive leachates (Onikata et al. 1999; Ashmawy et al. 2002; Kolstad et al. 2004b; Katsumi et al. 2008; Shackelford et al. 2010; Scalia et al. 2014; Tian et al. 2016; Chen et al. 2019).

1.2.2.3.1 Effect of Saline Solutions on BPC:

Onikata et al. (1999), studied the effect of propylene carbonate (PC) on montmorillonite clay to improve its swelling behavior. Complexes of montmorillonite clay were prepared with varying PC content (1.5 to 4.4 moles of PC/kg of clay). Powdered X-ray diffraction, Fourier transform infrared (FTIR) and Thermogravimetric analyses (TGA) was carried out on complexes to better understand the adsorption of water molecules to montmorillonite clay particles. Onikata et al. (1999) concluded that montmorillonite saturated with Li⁺, Na⁺, K⁺, NH₄⁺, Mg²⁺, Ca²⁺, Ba²⁺, or Ni²⁺ ions can form complexes with propylene carbonate (PC) by intercalation. Moreover, stated that osmotic swelling can be achieved even in case of electrolytic solutions.

Emidio et al. (2015), developed an engineered clay (hyper clay) through treatment of sodium bentonite with carboxy methyl cellulose (CMC), an anionic polymer. The clay was treated with various polymer dosages (2%, 4%, 8% and 16%). Atterberg limits, x-ray

diffraction, swell index, chemico-osmotic and hydraulic conductivity tests were conducted on treated (hyper clay) and untreated clay samples. KCl and CaCl₂ solutions of varying concentration (0.001 to 0.5 M) were used as permeant solutions to study the effect of concentration and valence on the swelling of the polymer treated bentonite. Whereas, deionized water (as control solution) and 0.005 M CaCl₂ was used as permeant solution for chemico-osmotic and hydraulic conductivity tests. X-ray diffraction analysis showed the intercalation of polymer in the interlayer region of clay, inducing a dispersed clay structure. An increase in the swell index and liquid limit was observed with the increase in polymer dosage. Hyper clay and untreated clay showed comparable hydraulic conductivity (6.4×10^{-12} versus 6.5×10^{-12} m/s respectively) in deionized water. However, after 300 days both the prehydrated (with deionized water) samples were permeated with 5 mM CaCl₂ solution. The hydraulic conductivity of untreated clay increased (from 10^{-12} to 10^{-11} m/s) whereas hyper clay maintained its hydraulic conductivity to 10^{-12} m/s. Moreover, the hydraulic conductivity of hyper clay remained one order of magnitude lower than untreated clay even in case of salt solutions.

Scalia et al (2014), polymerized acrylic acid within the bentonite slurry to create a bentonite polymer composite (BPC) that can give low hydraulic conductivity even when permeated with aggressive inorganic solutions. Swell index and hydraulic conductivity tests were conducted on BPC as well as on pure Na-B and sodium polyacrylate (SAP) using deionized water (as control solution), CaCl₂ (5 to 500 mM), NaOH (1 M with pH 13.1) and HNO₃ (1 M with pH 0.3) as permeant solutions. CaCl₂ was used to investigate the impact of ionic strength and divalent cations on swelling and hydraulic conductivity of GCLs.

Whereas, NaOH and HNO₃ were used as extreme pH solutions. BPC in deionized water swelled 3.8 times more than the Na-B (73 versus 19 mL/2 g). However, in case of 500 mM CaCl₂ solution both BPC and Na-B showed similar swell (< 10 mL/2 g). On contrary to the classical hydraulic conductivity-swell index relationship (i.e., low swell-high hydraulic conductivity and vice versa), BPC maintained low hydraulic conductivity ($k < 10^{-11}$ m/s) in all permeant solutions even in case of 500 mM CaCl₂ solution that resulted in significantly low swell index. Whereas, Na-B and SAP showed hydraulic conductivity that was higher by three orders of magnitude in all permeant solutions (except < 5 mM CaCl₂). Soluble cations, bound cations and cation exchange capacity (CEC) of all the samples was also measured. Clogging of effluent line due to polymer elution was observed during the hydraulic conductivity tests. Loss on ignition test (LOI) was conducted before and after the permeation test to do polymer quantification. Polymer elution was observed for all permeant solutions. The observed trend showed that polymer elution decreased with an increase in CaCl₂ concentration.

1.2.2.3.2 Bentonite-Polymer (B-P) GCLs

After Scalia et al. (2014) many researchers evaluated the performance of polymer modified (B-P) GCLs under varying conditions and leachate properties. For example Athanassopoulos et al. (2015) studied the effect of high pH solutions on the hydraulic conductivity of B-P GCLs. Hydraulic conductivity tests were performed on polymer modified GCLs with two synthetic solutions having very high pH, trona ash leachate (pH = 11, I = 1.05 M) and bauxite residue liquor (pH = 13, I = 2.35 M) representing leachate conditions at trona ash landfill and bauxite residue storage facility respectively. The GCL

evaluated in this study was manufactured using granular sodium bentonite ($D_{50} \approx 1 \text{ mm}$) and was blended with several proprietary water-swelling polymers. The solutions with extreme pH ($11 < \text{pH} < 3$) greatly effects the hydraulic conductivity of conventional Na bentonite GCLs hence there was a need to investigate the performance of modified GCLs in case of extreme pH conditions. The hydraulic conductivity tests with bauxite liquor and trona ash leachate showed that polymer-modified bentonites developed for leachate environments with high pH and high ionic strength have hydraulic conductivity four to five orders of magnitude lower than the hydraulic conductivity of a conventional GCL with granular Na bentonite. The conventional Na-B when permeated with bauxite liquor showed hydraulic conductivity of $1.8 \times 10^{-8} \text{ m/s}$ where the polymer modified GCL showed hydraulic conductivity of $4.4 \times 10^{-12} \text{ m/s}$. Similarly when permeated with trona ash leachate the conventional NaB and polymer modified GCL showed hydraulic conductivity of $1.2 \times 10^{-6} \text{ m/s}$ and $5.2 \times 10^{-12} \text{ m/s}$ respectively.

Tian et al. (2016) studied the effect of two low level radioactive leachates (LLW) on eight commercially available B-P GCLs and compared their hydraulic conductivity and swell with the conventional Na-B GCLs permeated with the same leachates. The difference between the two LLW leachates was that one had no radionuclides (a.k.a. nonradioactive synthetic leachate, NSL) and the other had radionuclides (radioactive synthetic leachate, RSL). The ionic strength and RMD of both the leachates was 43.6 mM and $0.077 \text{ M}^{1/2}$ respectively. The B-P GCLs were classified into two different categories based on their polymer loading. GCLs with polymer loading ranging from 1.2 to 3.3% were classified as low polymer loading GCLs and the one with polymer loading greater than 5 % as high

polymer loading GCLs. It was found that the low polymer loading GCLs gave hydraulic conductivity same as of conventional sodium bentonite GCL (i.e., 10^{-10} to 10^{-11} m/s). Whereas, the hydraulic conductivity of high polymer loading GCLs with the two leachates was found to be similar to that of deionized water (DI) i.e. in order of 10^{-12} m/s. All the GCLs showed similar hydraulic conductivities with the two different LLW leachates (i.e., RSL and NSL). The hydraulic conductivity of Na-B GCLs gradually increased by a factor of 5 to 25 due to the replacement of native bound sodium by the divalent cations present in the leachate. Swell index test were also conducted on the GCLs with DI water and leachates. Swelling of all the GCLs decreased when permeated with LLW leachates in comparison to that of DI water. Moreover Tian et al. (2016) also presented a conceptual model based on scanning electron microscopic (SEM) image analysis for the low hydraulic conductivity of the B-P GCLs to LLW leachates. That is, polymer hydrogels present in the B-P GCLs result in the blockage of the void spaces and therefore even in case of low swell index to LLW leachates the B-P GCLs were able to give low hydraulic conductivity.

Chen et al. (2019) studied the effect of CCP leachates on the hydraulic conductivity of B-P GCLs and found that the hydraulic conductivity of B-P GCLs with polymer loading ≥ 1.9 % was primarily controlled by polymer hydrogel instead of bentonite swell. Hydraulic conductivity of conventional Na-B GCLs was $> 10^{-10}$ m/s with all the CCP leachates ($I = 39.5$ mM to 755 mM). B-P GCLs with $P < 1.9$ % to CCP leachates was similar to the hydraulic conductivity of Na-B GCL ($\geq 10^{-10}$ m/s) whereas B-P GCL with $P \geq 1.9$ % typically showed low hydraulic conductivity ($< 10^{-10}$ m/s) to CCP leachates ($I = 39.5$ mM to 755 mM).

1.2.2 4 Swelling of Modified GCLs:

The ionic strength versus free swell relationship for modified GCLs (i.e., for DPH, MSB and BPC) is shown in Fig. 1-17. It shows that with the increase in ionic strength the free swell decreases similar to the trend observed for conventional Na-B GCLs. Whereas, Fig. 1-18, shows the ionic strength versus hydraulic conductivity relationship for the modified GCLs. It can be seen that even for high ionic strength (≈ 1000 mM) most of the B-P GCLs are able to give low hydraulic conductivity ($\approx 10^{-10}$ m/s) that is much less than the hydraulic conductivity seen for the conventional Na-B GCLs for the same ionic strength.

Fig. 1-19, shows the free swell versus hydraulic conductivity relationship for the modified GCLs. It can be seen that in case of modified GCLs there does not exist a clear relationship between free swell and hydraulic conductivity as it exist for the conventional sodium bentonite GCLs. That also limits the application of free swell test as an index test for the B-P GCLs.

Tables:

Table 1-1: Amount of CCP produced, recycled and disposed of by category. (ACCA, 2015 CCP Production & Use Survey Report).

CCP Type	Total Amount of CCP (Million Mg)		
	Produced	Recycled	Disposed
Fly Ash	40.25	21.83	18.42
Bottom Ash	10.90	4.37	6.52
Boiler Slag	2.02	1.70	0.33
FGD Gypsum	29.63	15.48	14.15
FGD Materials	11.64	1.38	10.26
Others	11.97	10.63	1.33
Sum of all CCP Types	106.40	55.38	51.02

Table 1-2: Chemical composition of CCP leachate based on dominant CCP type.

CCP Type	Major Components	Unit	N _m /N _T	Range	Mean	COV	
FGD Solids	Major Cations	Na ⁺	mM	9/9	22.75–1831.81	402.06	1.53
		K ⁺	mM	9/9	0.44–23.80	7.29	1.05
		Mg ²⁺	mM	9/9	3.05–140.12	56.61	0.98
		Ca ²⁺	mM	9/9	0.57–31.13	14.98	0.53
	Major Anions	Cl ⁻	mM	9/9	9.74–1067.95	221.29	1.61
		SO ₄ ²⁻	mM	9/9	27.24–990.83	200.22	1.51
	Bulk Properties	Cl/SO ₄ ²⁻	-	9/9	0.09–6.21	1.28	1.49
		RMD	M ^{1/2}	9/9	0.11–30.55	4.07	2.45
		I	mM	9/9	116.03–3177.69	858.94	1.16
		pH	-	9/9	6.10–8.88	7.44	0.12
Mixed Coal Ash	Major Cations	Na ⁺	mM	62/63	0.18–999.35	37.57	3.81
		K ⁺	mM	43/63	0.068–12.63	1.64	1.49
		Mg ²⁺	mM	61/63	0.0026–62.59	2.74	2.93
		Ca ²⁺	mM	63/63	0.18–32.11	5.72	0.94
	Major Anions	Cl ⁻	mM	63/63	0.07–1195.50	21.73	6.93
		SO ₄ ²⁻	mM	62/63	0.49–276.34	20.63	2.15
	Bulk Properties	Cl/SO ₄ ²⁻	-	62/63	0.0043–∞ ¹	0.35	2.61
		RMD	M ^{1/2}	62/63	0.002–6.05	0.37	2.47
		I	mM	63/63	2.46–1638.18	87.29	2.66
		pH	-	62/63	5.54–12.23	8.54	0.18
Bottom Ash	Major Cations	Na ⁺	mM	11/11	0.25–240.95	31.21	2.29
		K ⁺	mM	10/11	0.02–4.47	0.75	1.81
		Mg ²⁺	mM	10/11	0.04–10.27	1.35	2.22
		Ca ²⁺	mM	11/11	0.10–16.14	5.13	1.01
	Major Anions	Cl ⁻	mM	11/11	0.07–52.87	9.59	1.91
		SO ₄ ²⁻	mM	11/11	0.10–141.63	19.25	2.16
	Bulk Properties	Cl/SO ₄ ²⁻	-	11/11	0.04–2.44	0.78	1.11
		RMD	M ^{1/2}	11/11	0.01–1.68	0.25	1.98
		I	mM	11/11	0.71–467.90	72.20	1.90
		pH	-	10/11	5.10–10.84	8.17	0.26
Fly Ash	Major Cations	Na ⁺	mM	25/25	0.07–239.91	26.16	2.13
		K ⁺	mM	24/25	0.07–4.61	1.20	1.00
		Mg ²⁺	mM	25/25	0.0028–10.03	1.08	1.88
		Ca ²⁺	mM	25/25	0.16–15.43	4.97	0.94
	Major Anions	Cl ⁻	mM	23/25	0.05–38.37	2.55	3.09
		SO ₄ ²⁻	mM	25/25	0.93–140.55	18.10	1.69
	Bulk Properties	Cl/SO ₄ ²⁻	-	23/25	0.01–1.86	0.23	1.78
		RMD	M ^{1/2}	25/25	0.0023–7.25	0.61	2.58
		I	mM	25/25	3.68–464.41	63.12	1.56
		pH	-	20/25	4.16–11.18	7.76	0.24

CCP Type	Major Components	Unit	N _m /N _T	Range	Mean	COV	
Fixated FGD	Major Cations	Na ⁺	mM	12/12	0.07–100.43	27.22	0.99
		K ⁺	mM	8/12	0.52–17.19	10.18	0.61
		Mg ²⁺	mM	11/12	0.0012–3.56	1.14	0.87
		Ca ²⁺	mM	12/12	0.10–41.33	19.10	0.64
	Major Anions	Cl ⁻	mM	12/12	0.30–96.73	39.60	0.79
		SO ₄ ²⁻	mM	12/12	0.01–49.06	19.48	0.62
	Bulk Properties	Cl ⁻ /SO ₄ ²⁻	-	12/12	0.28–30.60	4.65	1.80
		RMD	M ^{1/2}	12/12	0.01–1.43	0.28	1.36
I		mM	12/12	0.42–196.42	116.02	0.51	
	pH	-	9/12	7.39–10.65	8.54	0.14	
FGD Gypsum	Major Cations	Na ⁺	mM	5/5	0.07–3.57	1.39	1.07
		K ⁺	mM	1/5	0.27	0.27	-
		Mg ²⁺	mM	5/5	0.94–38.47	11.83	1.30
		Ca ²⁺	mM	5/5	14.02–22.76	17.00	0.21
	Major Anions	Cl ⁻	mM	5/5	0.94–54.09	23.64	1.15
		SO ₄ ²⁻	mM	5/5	14.95–23.98	17.38	0.21
	Bulk Properties	Cl ⁻ /SO ₄ ²⁻	-	5/5	0.06–3.62	1.31	1.18
		RMD	M ^{1/2}	5/5	0.004–0.02	0.01	0.57
I		mM	5/5	64.54–188.47	104.96	0.51	
pH		-	5/5	6.82–11.96	8.34	0.25	
Spray Dryer Ash	Major Cations	Na ⁺	mM	3/4	4.7–86.68	53.53	0.81
		K ⁺	mM	2/4	0.26–2.74	1.50	1.17
		Mg ²⁺	mM	3/4	0.14–3.17	1.35	1.19
		Ca ²⁺	mM	2/4	1.85–13.17	7.51	1.07
	Major Anions	Cl ⁻	mM	4/4	0.55–3.86	2.21	0.82
		SO ₄ ²⁻	mM	4/4	4.93–42.76	24.45	0.71
	Bulk Properties	Cl ⁻ /SO ₄ ²⁻	-	4/4	0.04–0.15	0.10	0.50
		RMD	M ^{1/2}	3/4	0.04–2.66	1.55	0.88
I		mM	4/4	10.25–134.78	80.00	0.68	
pH		-	4/4	8.04–10.65	9.32	0.15	
Leaching Test (LT)	Major Cations	Na ⁺	mM	11/11	1.10–3448.70	551.34	1.92
		K ⁺	mM	11/11	0.10–1395.10	134.82	3.10
		Mg ²⁺	mM	10/11	0.30–507.50	80.37	1.93
		Ca ²⁺	mM	10/11	0.66–538.10	109.73	1.66
	Major Anions	Cl ⁻	mM	11/11	0.93–4366.00	660.58	1.95
		SO ₄ ²⁻	mM	11/11	0.90–696.40	157.16	1.63
	Bulk Properties	Cl ⁻ /SO ₄ ²⁻	-	11/11	0.01–122.30	27.57	1.60
		RMD	M ^{1/2}	10/11	0.01–∞ ²	1.36	2.21
I		mM	11/11	4.88–4685.00	1332.63	1.09	
pH		-	11/11	5.40–12.00	8.17	0.25	

Note: Dominant CCP type unknown for leaching test conducted in lab; I = Ionic Strength; N_m/N_T = Number of measurable data points/Total no. of data points; ∞¹ = concentration of SO₄²⁻ is zero, ∞² = concentration of divalent cations is zero, RMD = Relative abundance of monovalent and divalent cations.

Table 1-3: Concentration of trace heavy metals in the CCP leachates.

Element	Leachate Data (µg/L)			USEPA (µg/L) Drinking Water Standard	
	No. of Site	Range	Mean		
As	109	0.67–3132	98.82	3.26	10
Pb	56	0.07–490	12.00	5.44	15
Hg	64	0.00–31	0.85	4.65	2
Cr	99	0.16–4885	105.45	5.10	100
Be	25	0.04–5	1.60	1.14	4
Cd	83	0.10–237	7.61	3.57	5
Tl	47	0.05–36	2.23	2.46	2

Note: USEPA = United States Environmental Protection Agency

Table 1-4: Summary of GCLs, leachates and effective stress used by previous researchers.

Material	Modification	Permeant solution properties		Avg. effective stress (kPa)	Reference
		Solutions	Ionic strength		
Granular Na-B	None	DI water, NaCl, KCl, LiCl, CaCl ₂ , MgCl ₂ , ZnCl ₂ , CuCl ₂ , and LaCl ₃	0.005 to 1 M	20	Jo et al. (2001)
Granular Na-B	None	DI water, Li-Ca, Na-Mg, Li-Na and Ca-Mg	0.05, 0.1, 0.2 and 0.5 M	20	Kolstad et al. (2004a)
Na-B and DPH	DPH: prehydrated to a water content of 43% using a dilute aqueous solution containing sodium carboxymethyl cellulose (CMC) and methanol.	DI water, NaCl, CaCl ₂ , HCl and NaOH	NaCl (1M & pH 6.8), CaCl ₂ (1M & pH 6.9), HCl (pH 1.2), and NaOH (pH 13.1).	20	Kolstad et al. (2004b)
High quality and Low-quality Bentonite	None	DI water and CaCl ₂	5, 10, 20, 50, 100, and 500 mM.	23.5 and 16.2	Lee et al. (2005)
Na-B, MSB and DPH-GCL	MSB: 25 % propylene carbonate (PC) by weight to sodium bentonite (Na-B) and DPH-GCL: factory prehydrated-consolidated Na-B	DI water, NaCl, CaCl ₂ and NaCl – CaCl ₂	0.05 to 2 M	20-30	Katsumi et al. (2008)
Na-B and BPC	BPC: Polyacrylic acid (PAA)	DI water and CaCl ₂	5, 50 and 500 mM	20	Scalia et al. (2011)
BPC, Na-B and SAP	BPC: Polyacrylic acid (PAA)	DI water and CaCl ₂	5, 20, 50, 200, and 500 mM	20	Scalia et al. (2013)
Na-B and BPC	BPC: Proprietary polymer	DI water, RSL and NSL	RSL (43.6 mM) and NSL (43.6 mM)	20	Tian et al. (2016)
Na-B	None	DI water, Typical CCP, Low RMD, FGD, High strength and Trona	Typical CCP (39.5 mM), Low RMD (48 mM), FGD (96.8 mM), High strength (177 mM) and Trona (755 mM)	20, 100, 250 and 450	Chen et al. (2018)

Figures:

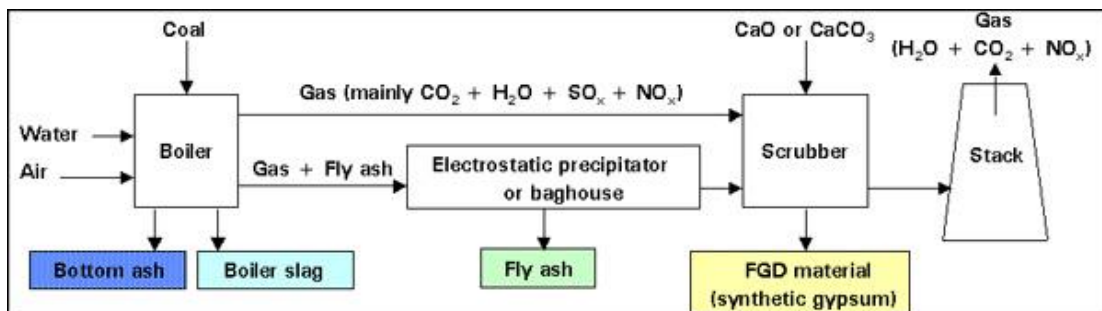


Figure 1-1: Flow diagram of the flue-gas-desulfurization process based on lime (CaO) or limestone (CaCO₃), which are the sorbents used by 90 percent of FGD systems in the United States (Grabed from Kalyoncu and Olson 2016)

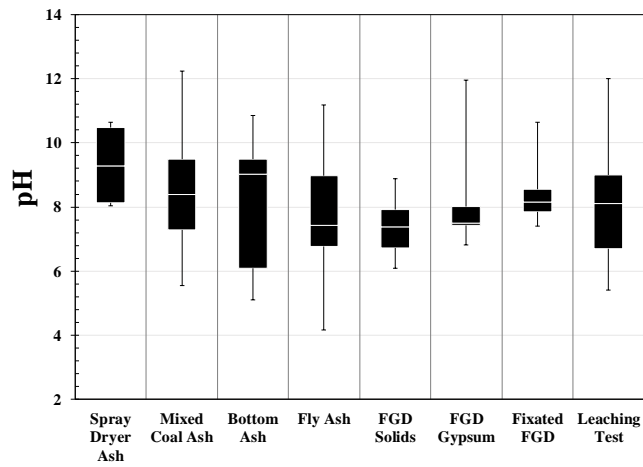


Figure 1-2: Box plot for pH of CCP leachates based on dominant CCP type.

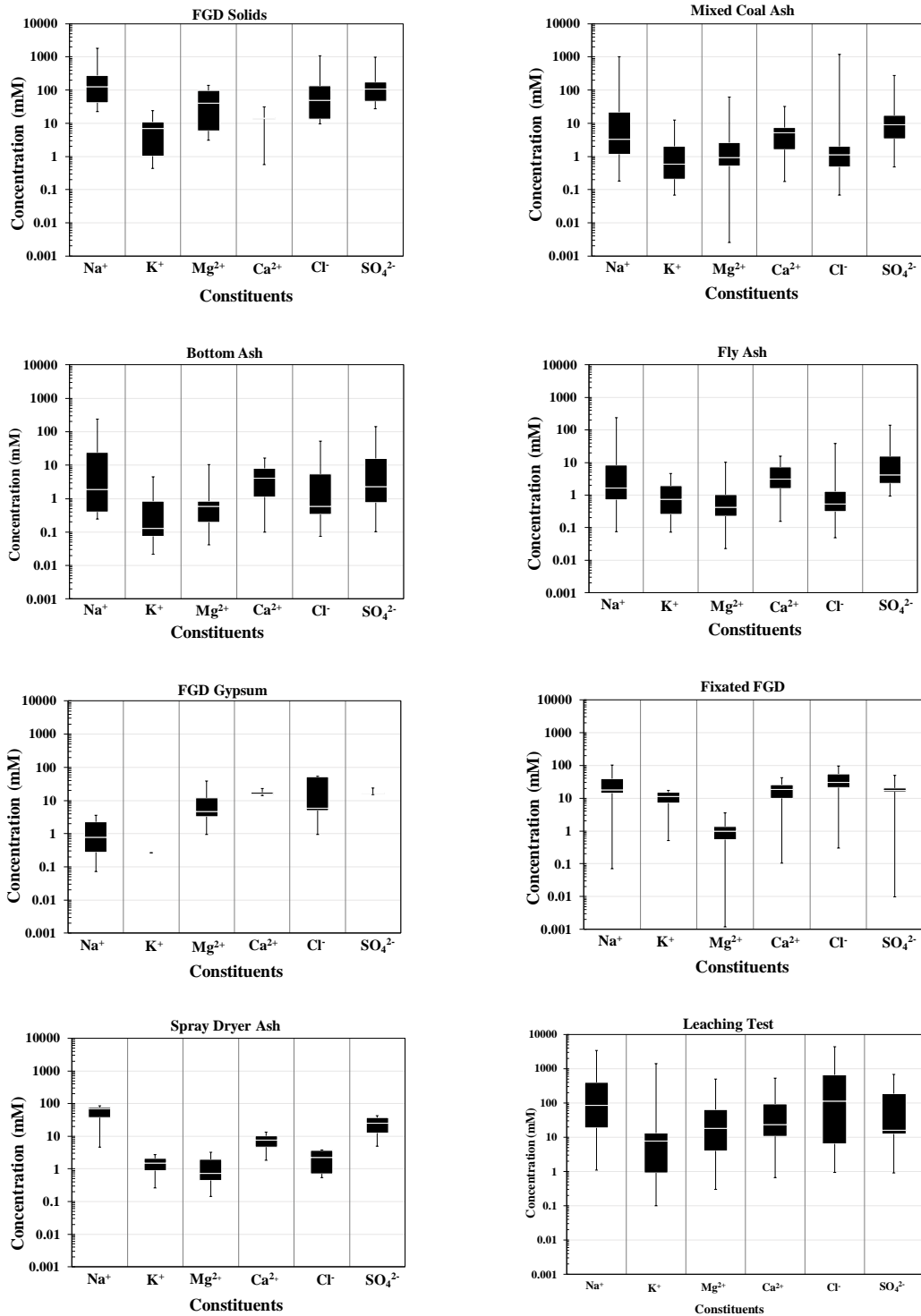


Figure 1-3: Box plot for major constituents (cations and anions) of CCP leachate based on dominant CCP type.

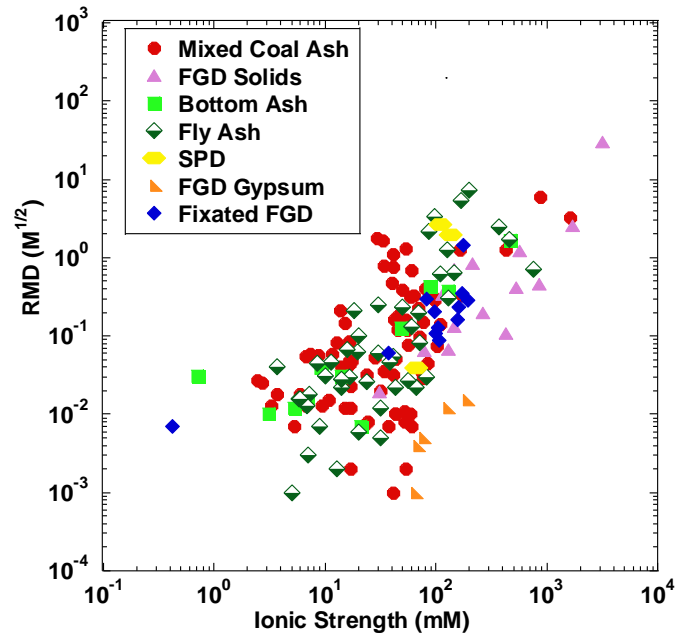


Figure 1-4: Relationship between ionic strength and RMD of CCP leachate based on dominant CCP type. Source: CCP leachate data (130 U.S disposal sites), Leaching test data, Kolstad 2000 and Chen et al. 2018.

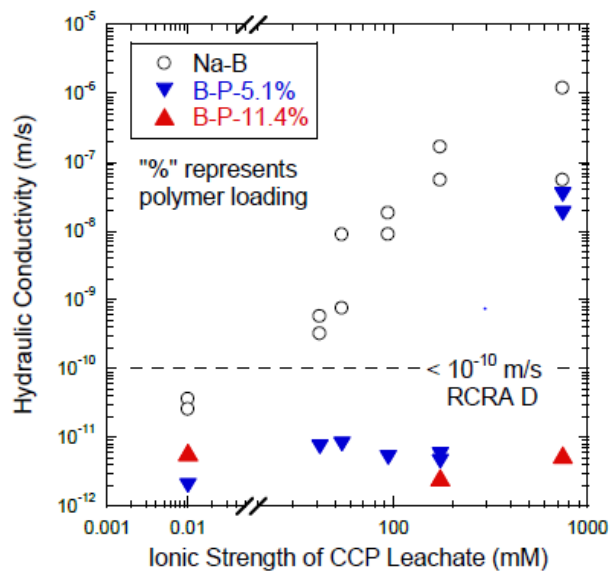


Figure 1-5: Hydraulic conductivity of conventional Na-B and B-P GCLs to coal-fired power plant leachates (Data from Benson et al. 2014) (Note: DI water at 0.01 mM).

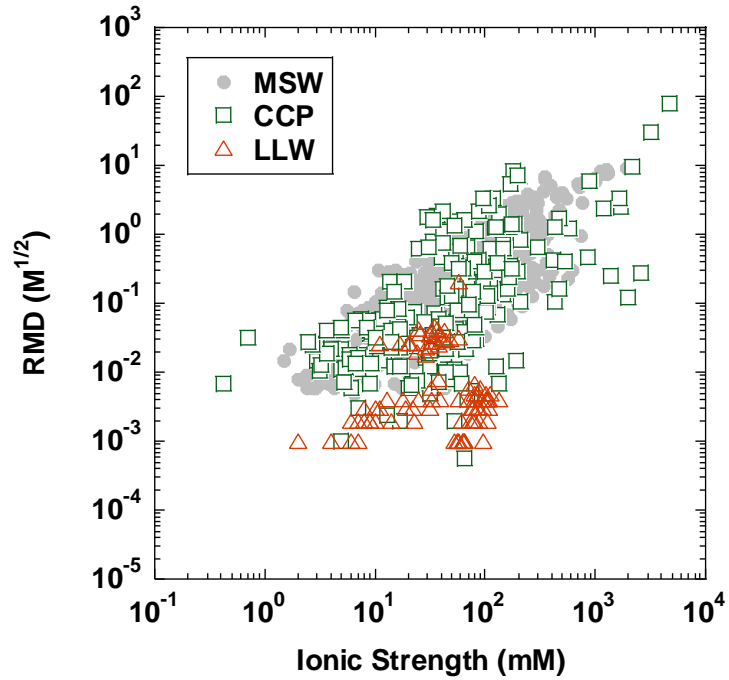


Figure 1-6: Ionic strength versus. RMD relationship for landfill leachates i.e. municipal solid waste (MSW) leachate, coal combustion product (CCP) leachate and low-level radioactive waste (LLW) leachate. Source: CCP leachate data from 130 U.S. disposal sites, Leaching test data, Kolstad 2000, Tian et al 2016 and Chen et al 2018.

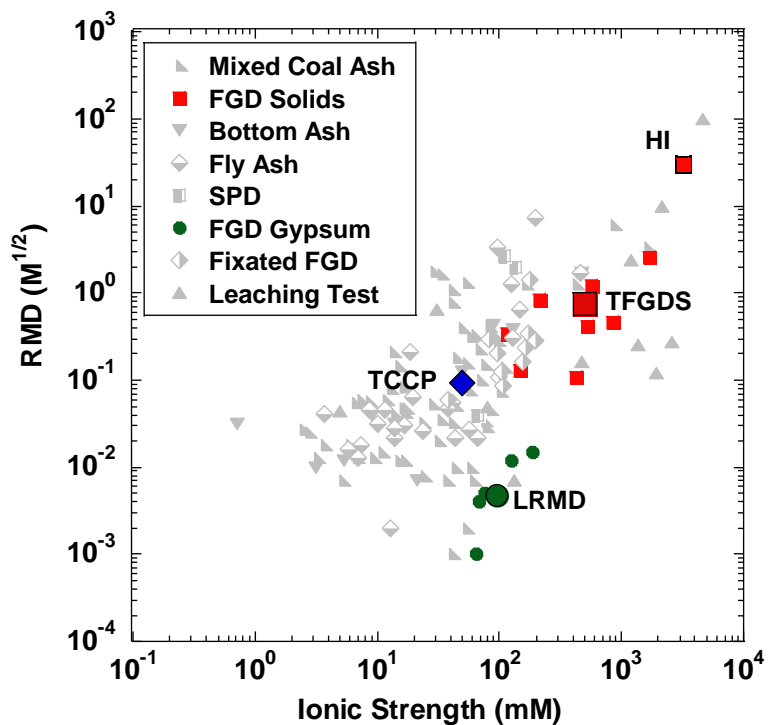


Figure 1-7: Selection of four synthetic CCP leachates based on their ionic strength and RMD. HI (high ionic strength leachate), LRMD (low RMD/ divalent cations rich leachate), TFGDS (Typical FGD solids leachate i.e. geometric mean of all FGD solids and TCCP (Typical CCP leachate i.e. geometric mean of all CCP leachates. (Note: The maximum RMD observed in case of CCP leachate data was ∞ i.e., only monovalent cations present but to represent that data in figure RMD = 100 has been used.)

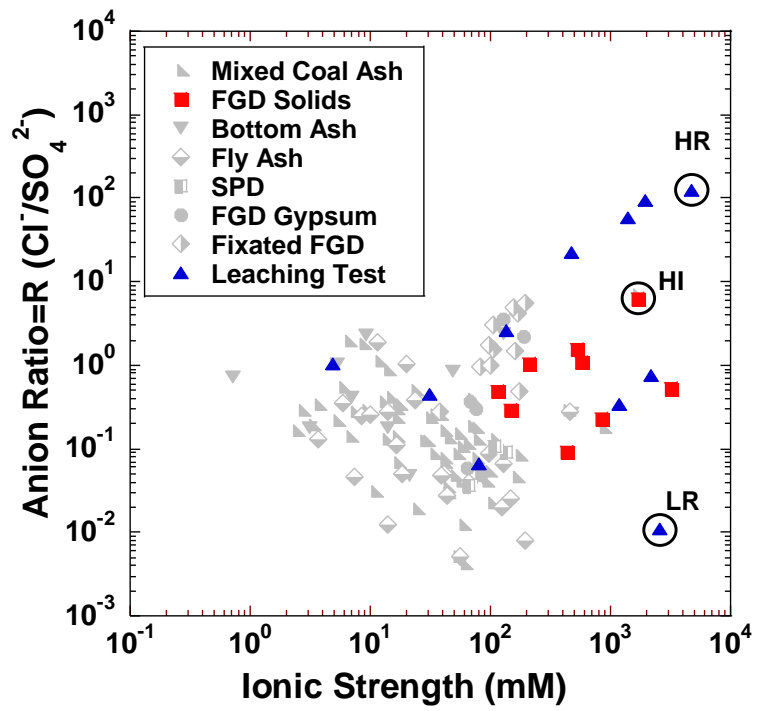


Figure 1-8: Selection of two synthetic CCP leachates based on their ionic strength and anion ratio (R). H. R (high anion ratio i.e. Cl⁻ rich leachate) and L. R (low anion ratio i.e. SO₄²⁻ rich leachate).

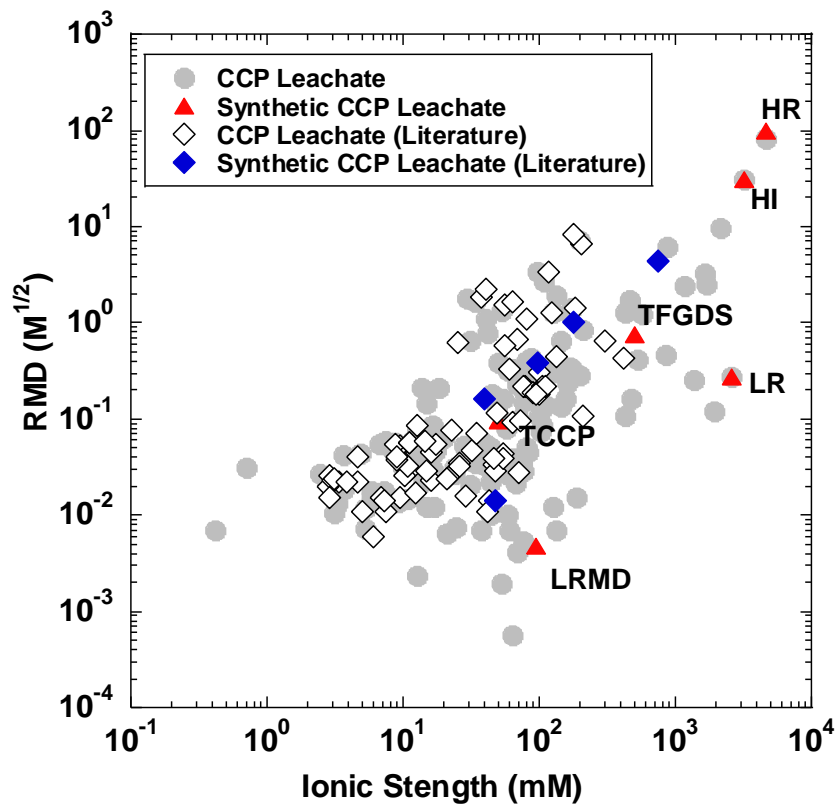
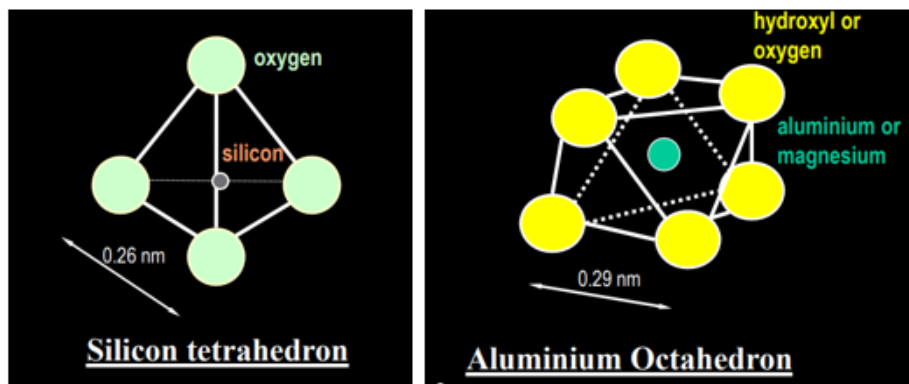


Figure 1-9: Comparison of selected synthetic CCP leachate with CCP leachate used by previous researchers (Chen et al. 2018). Note: The maximum RMD observed in case of CCP leachate data was ∞ (i.e., only monovalent cations present) but to represent that data in figure RMD = 100 has been used.



Isomorphous substitution = Si^{+4} Replaced by Al^{+3} OR Al^{+3} Replaced by Mg^{+2}

Figure 1-10: Replacement of ions in silicon tetrahedron and aluminium octahedron due to isomorphous substitution.

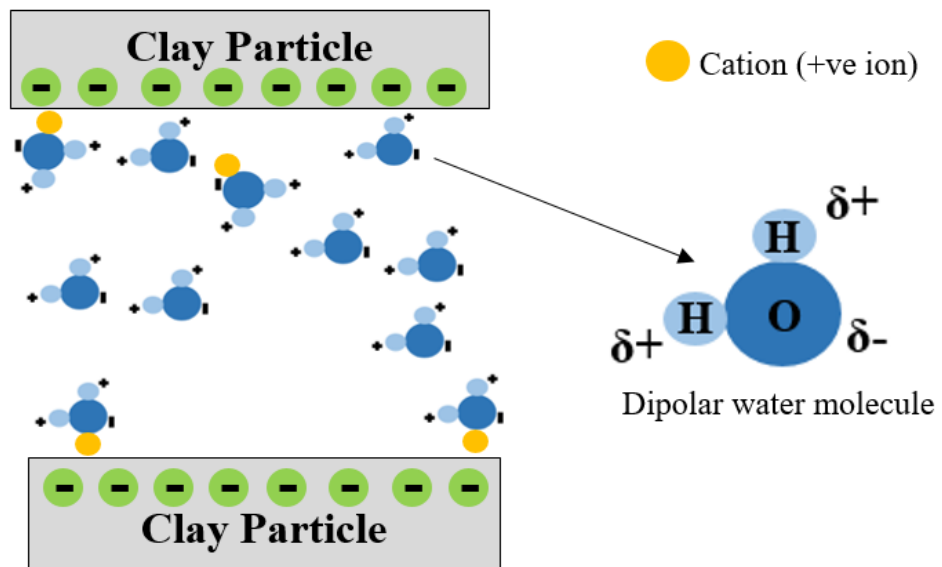


Figure 1-11: Cations and water molecules attachment on the clay interlayer.

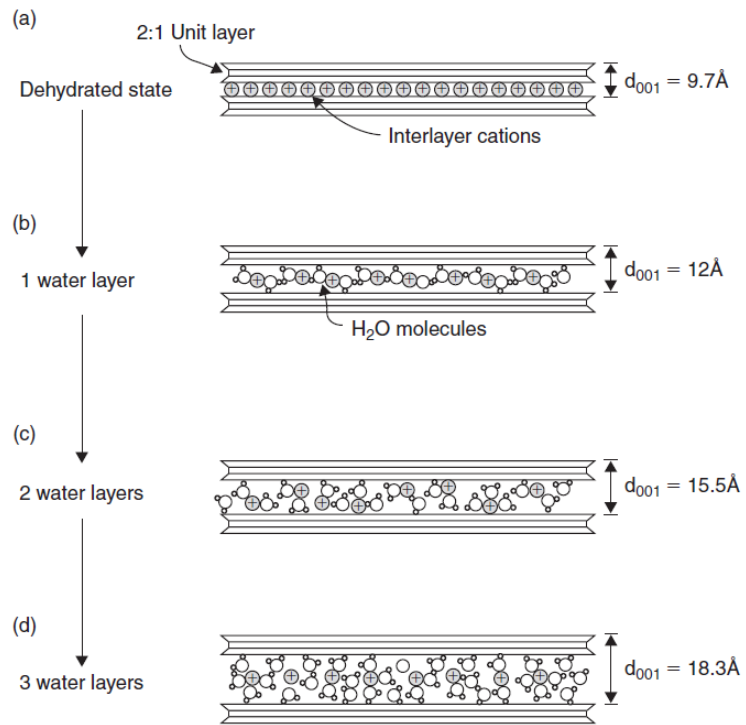


Figure 1-12: Step-wise hydration in the crystalline swelling regime (after Likos, 2004). Grabbed from Bouazza, A., & Bowders Jr, J. J. (2010), "Geosynthetic clay liners for waste containment facilities".

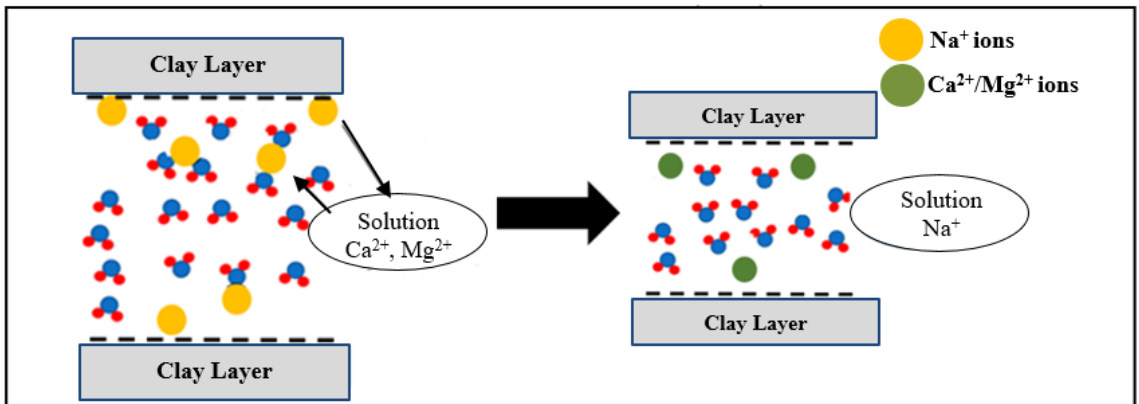


Figure 1-13: Replacement of cations based on lyotropic series.

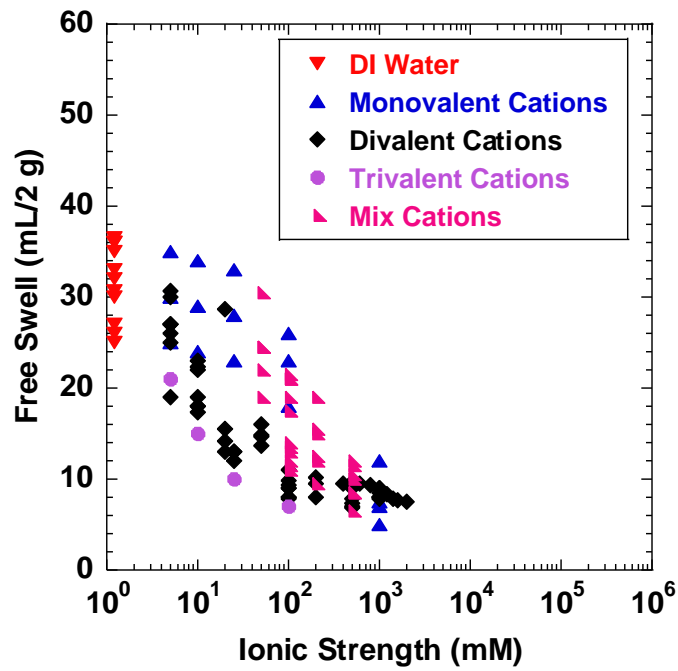


Figure 1-14: Ionic strength versus free swell relationship for Na-B GCLs permeated with deionized water (DI), monovalent cations leachate (RMD = infinity), divalent cations leachate (RMD = 0), trivalent cations leachate and mix cations leachate. Ref. Jo et al 2001; Kolstad 2004a; Kolstad 2004b; Lee et al. 2005; Katsumi 2008; Scalia et al 2011; Tian et al. 2016; Chen et al. 2018. (Note: DI water at 1.2 mM)

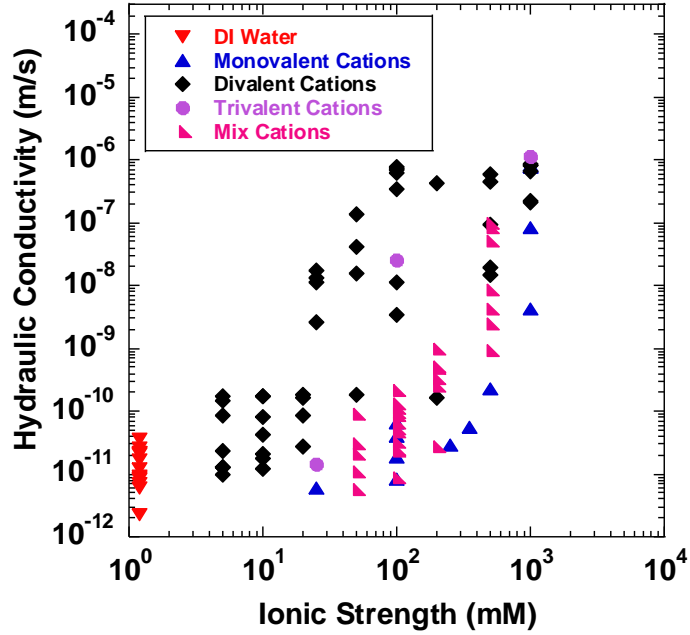


Figure 1-15: Ionic strength versus hydraulic conductivity relationship for Na-B GCLs permeated with monovalent cations leachate (RMD = infinity), divalent cations leachate (RMD = 0), trivalent cations leachate and mix cations leachate. Ref. Jo et al 2001; Kolstad 2004a; Kolstad 2004b; Lee et al. 2005; Katsumi 2008; Scalia et al 2011; Tian et al. 2016; Chen et al. 2018. (Note: DI water at 1.2 mM)

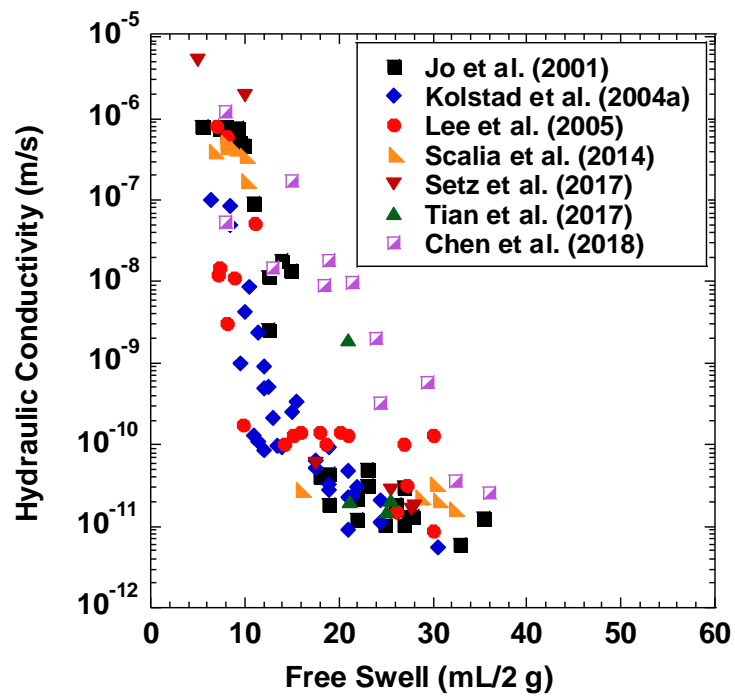


Figure 1-16: Free swell versus hydraulic conductivity relationship for Na-B GCLs.

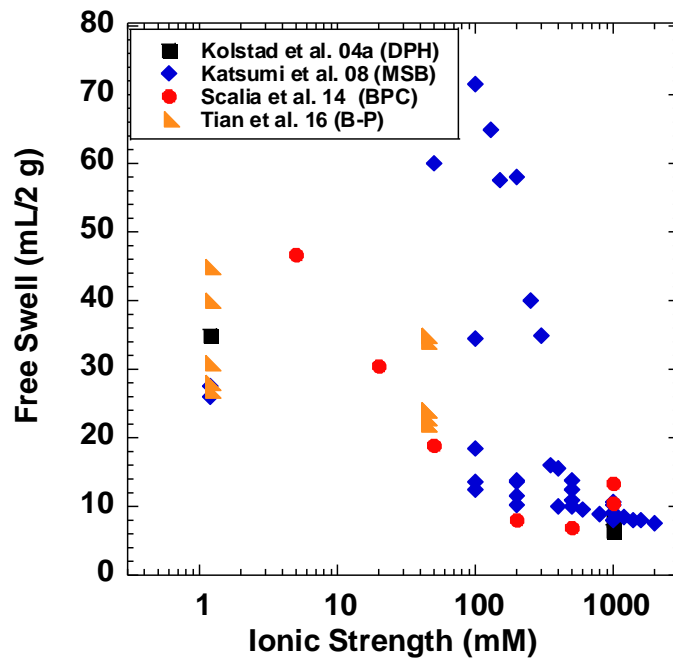


Figure 1-17: Ionic strength versus hydraulic conductivity relationship for modified GCLs. DPH = Dense prehydrated, MSB = Multi swellable bentonite and BPC = Bentonite polymer composite. (Note: DI at 1.2 mM)

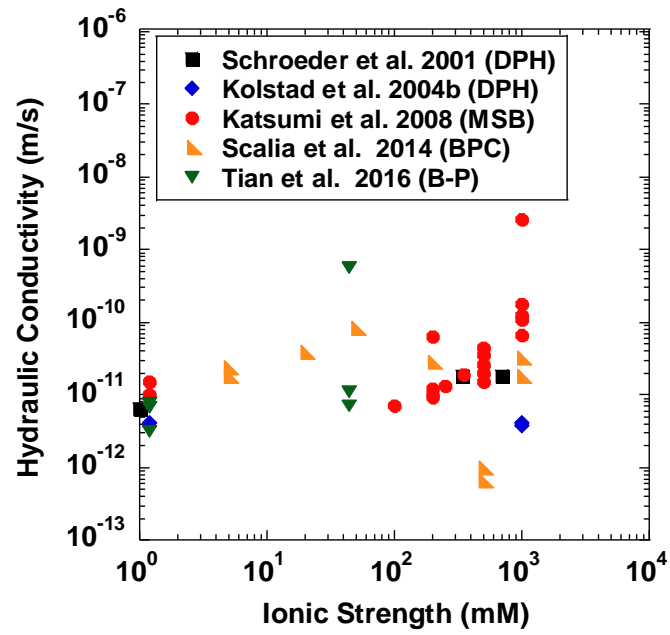


Figure 1-18: Ionic strength versus hydraulic conductivity relationship for modified GCLs. DPH = Dense prehydrated, MSB = Multi swellable bentonite and BPC = Bentonite polymer composite. (Note: Ionic strength for DI water taken as 1.2mM).

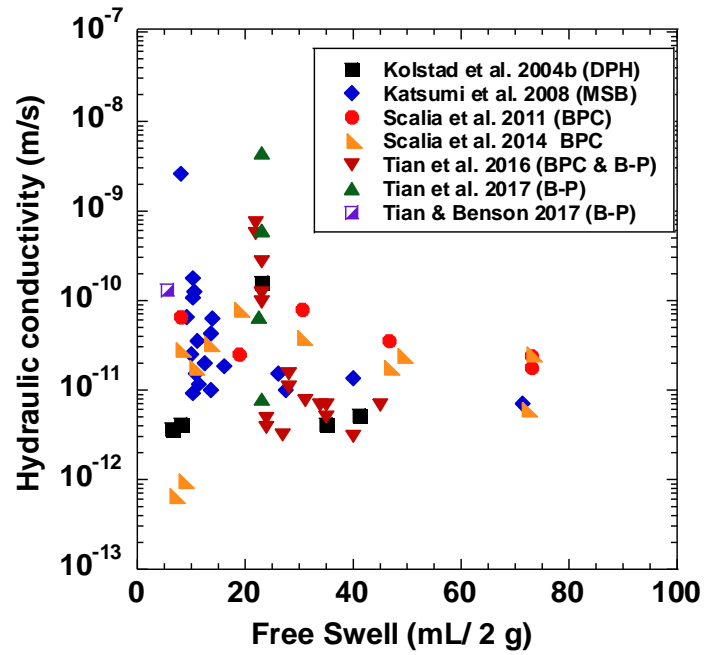


Figure 1-19: Free swell versus hydraulic conductivity relationship for modified GCLs. DPH = Dense prehydrated, MSB = Multi swellable bentonite and BPC = Bentonite polymer composite.

CHAPTER 2 : EFFECT OF SAMPLE PREPARATION ON INDEX PROPERTIES OF BENTONITE-POLYMER GCLS

Experiments were conducted on seven bentonite-polymer (B-P) composite geosynthetic clay liners (GCL) to evaluate the effects of crushing and sieving on the swell index (SI) and loss on ignition (LOI) test. SI tests were conducted with type II deionized (DI) water according to ASTM D5890. LOI tests were conducted to determine the polymer loading in the B-P composites. Control tests were conducted on conventional sodium bentonite (Na-B) GCL. Three different methods of sample preparation were adopted to evaluate the SI and LOI of B-P composites: (1) the standard method for SI test, ASTM D5890, (2) alternative method 1 with no crushing and sieving (AL1-As-is) and (3) alternative method 2 (AL2) with 50% of total material passing #100 sieve (AL2-P) and 50% of total material retained #100 sieve (AL2-R). For samples prepared in according to ASTM D5890, a small portion of B-P composites (0.1% to 4% by mass) cannot pass the #100 sieve no matter how much crushing was performed using pestle and mortar. SI and LOI tests were conducted on the B-P composites passing (ASTM-P) and retained (ASTM-R) on #100 sieve. Test results showed that ASTM-R had much higher SI and LOI than ASTM-P, indicating that the ASTM-R primarily may consist of the polymer. The segregation of polymer and bentonite may be attributed to the large size of polymer used in B-P composite. Crushing with pestle and mortar would not break down the polymer into small piece effectively, and thus the polymer was retained by #100 sieve. Two alternative sample preparation methods were conducted to further investigate the segregation phenomena and to provide appropriate sample preparation method to measure the

representative SI and LOI of B-P composites. Test results indicated that the sample prepared using AL1-As-is method was more appropriate to characterize the index properties of B-P GCL.

2.1 Introduction

Geosynthetic clay liners (GCLs) are factory-manufactured products that consist of a thin layer of sodium bentonite (Na-B) sandwiched between two geotextiles (Shackelford et al. 2000; Koerner 2012; Scalia et al. 2014; Tian et al. 2016). GCLs are widely used as hydraulic barriers in waste containment applications in lieu of compacted clay liners due to ease of installation, save air-space (due to 5 to 8 mm thickness), and low hydraulic conductivity to water ($<10^{-10}$ m/s) (Koerner 2012; Scalia et al. 2014; Tian et al. 2016). Na-B used in GCLs primarily consists of montmorillonite, which is mainly responsible for the low hydraulic conductivity of Na-B GCLs. (Shackelford et al. 2000; Jo et al. 2001; Kolstad et al. 2004a). Na-B has high swelling capacity when hydrated, resulting in tortuous and narrow intergranular flow channels for liquids (Mesri and Olson 1971; Jo et al. 2001; Kolstad et al. 2004a; Scalia et al. 2014). Additionally, the high swelling potential of Na-B allows GCLs to have self-healing ability to seal small defects, such as punctures that may be incurred during installation (Sari and Chai 2013).

However, leachates with high ionic strength, predominant polyvalent cations, and/or extreme pH can inhibit the swelling of Na-B, resulting in open and large intergranular flow channels and high hydraulic conductivity of Na-B GCL ($>10^{-10}$ m/s) (Petrov and Rowe 1997; Shackelford et al. 2000; Jo et al. 2001; Katsumi et al. 2008; Jo et al. 2004; Kolstad et al. 2004a; Jo et al. 2005; Lee et al. 2005; Bradshaw and Benson 2014;

Bradshaw et al. 2016). Recognition of this limitation, tremendous researches have focused on improving the chemical compatibility of Na-B GCLs to aggressive leachates by amending bentonite with organic molecules. For example, Onikata et al. (1999) modified montmorillonite with propylene carbonate (PC) to improve its swelling behavior. Katsumi et al. (2008) investigated the long-term hydraulic conductivity of a multiswellable bentonite (MSB) permeated with inorganic salt solutions. The experimental results showed that MSB had lower hydraulic conductivity ($k = 1.0 \times 10^{-11}$ m/s) in comparison to Na-B ($k = 2.3 \times 10^{-10}$ m/s) when permeated with NaCl solutions less than 1.0 M. Scalia et al. (2014) reported that bentonite-polymer (B-P) composite GCL, created by polymerizing acrylic acid within a bentonite slurry, can maintain low hydraulic conductivity ($<10^{-11}$ m/s) when permeated with 500 mM CaCl_2 solution, whereas the Na-B GCL showed three orders of magnitude higher hydraulic conductivity ($\sim 10^{-7}$ m/s). Athanassopoulos et al. (2015) report that B-P GCLs had hydraulic conductivity ($< 1 \times 10^{-11}$ m/s) to bauxite liquor (pH = 13, ionic strength = 2.35 M). Tian et al. (2016) reported that the hydraulic conductivity of B-P GCLs (with polymer loading $> 5\%$) to LLW leachates can maintain low hydraulic conductivity (e.g., $< 10^{-12}$ m/s). Most commercially modified GCLs contain a dry mixture of bentonite and proprietary polymer (Salihoglu et al. 2016; Tian et al. 2016; Tian and Benson 2017 and Tian et al. 2017). These GCLs are collectively referred to herein as B-P GCLs.

Hydraulic conductivity test is conducted in the laboratory as per ASTM D5084 and ASTM D6766 to predict the hydraulic barrier performance of GCLs in the field. The hydraulic conductivity tests is continued until reaching hydraulic and chemical equilibrium to reflect long-term hydraulic conductivity of GCL, which generally take a few months to

years (Petrov and Rowe 1997; Shackelford et al. 2000; Jo et al. 2001; Kolstad et al. 2004; Jo et al. 2005). The time required to reach chemical equilibrium can be even longer for B-P GCLs (Scalia et al. 2014; Razakamanantsoa and Djeran-Maigre 2016; Tian et al. 2016; Donovan et al. 2017). Hence, quick and inexpensive index tests are often performed on the bentonite component of GCLs to assess chemical and hydraulic compatibility of the GCL with the permeant liquid (Jo et al. 2001; Lee et al. 2005).

Swell index (SI) test is one of the most commonly used tests due to its easy, inexpensive, and quick to assess the hydraulic performance and the chemical compatibility of GCLs to liquid solutions. SI test is performed in accordance with ASTM D5890. 2 g of bentonite is ground until 100 % passing No. (#) 100 mesh, and a minimum of 65% passing #200 mesh U.S. standard sieve. Studies have shown a correlation exists between hydraulic conductivity and SI of Na-B as shown (Jo et al. 2001; Kolstad et al. 2004a; Lee et al. 2005; Katsumi et al. 2008; Scalia et al. 2014; Tian et al. 2016; Setz et al. 2017; Tian and Benson 2017; Tian et al. 2017). For Na-B GCLs, $SI > 14 \text{ mL/2 g}$ generally correlates to hydraulic conductivity $< 10^{-10} \text{ m/s}$, while $SI < 14 \text{ mL/2 g}$ correlates to hydraulic conductivity $> 10^{-10} \text{ m/s}$. However, SI and hydraulic conductivity of B-P GCL are not as correlated as Na-B GCL. B-P GCLs with $SI < 10 \text{ mL/2 g}$ can still maintained low hydraulic conductivity $< 10^{-10} \text{ m/s}$ (Fig. 2-1) (Scalia et al. 2014; Salihoglu et al. 2016; Tian et al. 2016; Chen et al. 2018). On the other hand, the hydraulic conductivity of B-P GCL can be higher than 10^{-10} m/s when SI of B-P exceed 20 mL/2g . The poor correlation between hydraulic conductivity and SI for B-P GCLs may be an indication that methods and sample preparation during SI test might not be appropriate for B-P GCLs. For example, the polymer in B-P become

transparent when hydrated, resulting in underestimated SI of B-P. Additionally, the grinding and sieving process during sample preparation may also affect the polymer loading in the B-P because the size of dry polymer hydrogel can range from 10 to 1000 μm (Yun et al., 2017), which may not pass #200 sieve (opening 75 μm) completely, resulting in separating from the B-P samples.

Consequently, the objective of this study is to investigate the influence of crushing and sieving on the swell index (SI) and loss on ignition (LOI) tests of B-P composites. Tests were conducted with seven B-P GCL samples prepared according to the ASTM standard method (D5890) and two other alternative methods (Table 2-2). SI tests were performed using type II deionized (DI) water. LOI tests were conducted to quantify the polymer loading of all portions of the samples prepared using the different methods.

2.2 Materials and Methods

2.2.1 Bentonite-Polymer Composites

Seven B-P composites from commercial B-P GCLs were evaluated in this study. All the B-P composites consist of a dry mixture of Na-B and proprietary polymer. Pure Na-B that used to produce B-P composites was used in this study as a control material². The granule size distributions of the B-P composites were obtained through mechanical sieve analysis following ASTM C136/C136M, as shown in Fig. 2-2. The grain size distribution of the seven B-P composites and Na-B falls into a narrow range, i.e., medium to fine sand ($D_{50} = \sim 0.9 \text{ mm}$) as shown in Fig. 2-2. The seven B-P composites used in this study are designated herein as B-P1, B-P2, B-P3, B-P4, B-P5, B-P6, and B-P7.

2.2.2a ASTM Standard Method

The Na-B and B-P samples were first prepared following the ASTM standard for SI test (ASTM D5890). Twenty-five (25) g of each sample was ground using conventional pestle and mortar to pass the #100 sieve. However, after extensive and iterative grinding and sieving, a small portion of B-P cannot be passed through the #100 sieve. The portion that passed the #100 sieve is referred to herein as “ASTM-Passing #100 (ASTM-P)”, whereas the portion that retained on the #100 sieve is referred to herein as “ASTM-Remnants #100 (ASTM-R).” For the portion that passed the #100 sieve, the B-P composites continued to be ground until at least 65% passed the #200 sieve, as required by the ASTM D5890. The amount of ASTM-P and ASTM-R of seven B-P composites are shown in Table 2-1. The ASTM-R ranged from 0.1 to 4% for the Na-B and B-P samples.

2.2.2b Alternative Methods

Observations made on the specimens prepared following the ASTM standard method revealed that crushing and sieving the B-P composites, as required by ASTM D5890, resulted in the segregation of some material on the #100 sieve, as shown in Table 1. Hence, alternative methods 1 and 2 (Table 2-2) were explored as possible sample preparation methods for SI testing of B-P GCLs.

For alternative method 1, specimens obtained from the B-P and Na-B samples were not subjected to any grinding and sieving to prevent the potential separation of polymer and bentonite, i.e., the samples were used as they were received from the manufacturer. Specimens prepared using this method are referred to herein as “Alternative method 1-As-is (AL1-As-is)”.

For alternative method 2, 50 g of each sample was ground and sieved until approximately 50% (e.g., 25 g) of the sample passed the #100 sieve. This method was developed to assess the influence of the #100 sieve of polymer segregation. The portion that passed the #100 sieve is referred to as “Alternative method 2-Passing #100 (AL2-P),” and the portion that retained on the #100 sieve is referred to as “Alternative method 2-Retained #100 (AL2-R).”

2.2.3 Swell Index Test

SI tests on the ASTM-P, AL1-As-is, AL2-P and AL2-R specimens were performed in according to ASTM D5890. 2 g of the specimen was oven-dried and added into a 100 mL graduated cylinder filled with 90 mL of type II DI water. The sample was added in graduated cylinder with an increment of 0.1 g. After adding 2 g of sample, the cylinder was filled to the 100 mL with DI water. The SI was measured as the volume of the swollen specimen in the graduated cylinder after 24 h (in mL/2 g). Tests were conducted in triplicates, and averages were reported in this study.

The procedure adopted for the SI tests of the ASTM-R samples was different from due to the small quantity (<0.3g) of ASTM-R samples (Table 2-1). SI tests for the ASTM-R specimen were performed by first adding 0.2 g (instead of 2 g) of the specimen into a 100 mL graduated cylinder and then gradually adding DI water in increments of 1 mL every 10 min. The tests were performed until no swelling was observed after adding the water and the SI was then recorded as the final volume of the swollen specimen (in mL/0.2 g). The SI of ASTM-R were estimated by multiply a factor of 10 to convert the unit to mL/2 g.

2.2.4 Loss on Ignition Tests

Loss on ignition (LOI) test has been adopted by many researchers to determine polymer content in B-P composite (Scalia et al. 2014; Tian et al. 2016, Tian et al. 2017). During the LOI test, polymer additives are assumed to be only contained organic compounds that are combusted completely. The polymer loading can be calculated using the LOI and discounting the LOI of the conventional Na-B, as suggested by Scalia et al. (2014) and Tian et al. (2016). The samples obtained from each preparation method was first oven-dried to constant mass at 105 ± 5 °C. The samples were then ignited at 550 ± 5 °C for 4 h using a Gilson HM-378 binder ignition system. The percentage of mass loss was reported as the LOI.

Similar to SI tests, LOI tests were conducted to determine the polymer loading in the specimens prepared by different methods (e.g., ASTM-P, ASTM-R, AL1-As-is, AL2-P, and AL2-R). For the ASTM-P, AL1-As-is, AL2-P, and AL2-R samples, triplicate tests were done using approximately 5 g for each sample. However, the mass of the ASTM-R samples used for the LOI tests varied from 0.1 to 0.2 g due to the limited quantity of the sample available, as shown in Table 2-1

LOI tests were conducted on ASTM-P and ASTM-R samples to quantify the polymer loading in the B-P samples segregated by #100 sieve when following the ASTM D5890. Comparative LOI tests were conducted on samples prepared by alternative method 1 (AL1-As-is) to minimize the disturbance of B-P specimens. Alternative method 2 was adopted that includes 50% sample passing #100 sieve (AL2-P) and 50% retained on #100 sieve (AL2-R) to further evaluate the segregation of #100 sieve on polymer and bentonite.

2.3 Results and Discussion

2.3.1 ASTM Standard Method

SI and LOI results for Na-B and B-P samples prepared following the ASTM standard method (ASTM-P and ASTM-R) are summarized in Table 2-3. LOI test was conducted on ASTM-P and ASTM-R samples to quantify the polymer loading in different portions of samples. To compare the SI results of ASTM-P and ASTM-R samples, the estimated SI of ASTM-R (mL/2 g) for B-P samples in Table 2-3 was determined by multiplying the experimentally measured SI of 0.2 g of the sample by a factor of 10 to obtain SI of 2 g of the sample (mL/2 g).

2.3.1a Swell Index

SI tests were conducted on both the ASTM-P and ASTM-R samples for all the B-P composites using type-II DI water. An example of SI test of ASTM-P and ASTM-R of B-P7 is shown in Fig. 2-3. ASTM-P consists of powder (Fig. 2-3a) whereas the ASTM-R has the white granules (Fig 2-3b). ASTM-P had SI of 43.6 mL/2 g (Fig. 2-3c) ASTM-R has a swell index of 55 mL/0.2 g, which was estimated to be 550 mL/2 g (Fig. 2-3d). ASTM-R formed a clear gel, whereas the ASTM-P formed a gray color gel. The ASTM-R after swelling looked like the polymer hydrogel.

All SI of Na-B and B-P samples are shown in Fig. 2-4. The ASTM-P of B-P1 to B-P5 had similar swelling in comparison with ASTM-P of Na-B. The SI of ASTM-P of B-P6 and B-P7 samples were higher than that of Na-B (~50 mL/2 g vs. 30 mL/2 g). In contract, the SI of ASTM-R were much higher (2 to 11 times) than the SI of ASTM-P samples. For B-P6, the SI of ASTM-R was approximately 400 mL/2 g whereas the SI of

ASTM P was approximately 50 mL/2 g. Similarly, the SI of ASTM-R of B-P7 was much higher than that of ASTM-P (550 mL/2 g vs. 46 mL/2 g). The high SI of ASTM-R were contributed to polymer hydrogel, as Scalia et al. (2014) reported that the super absorbent polymers (SAP) had super high swelling in DI water (~1790 mL/2 g). Consequently, these observations indicate that the B-P composites retained on #100 sieve (ASTM-R) were primarily polymer particles.

Visual examination of the ASTM-R samples before and after the swell test further revealed that B-P samples used in this study may contain two distinct types of polymers. The polymer found in B-P1 to B-P4 had slightly bigger size than the polymer found in the B-P5 to B-P7 composites. For example, the features of ASTM-R of B-P3 and B-P7 are shown in Figs. 2-5a and b. The ASTM-R of B-P3 is bigger than that of B-P7. The ASTM-R in B-P3 form a viscous gel after hydration in DI water (Fig. 2-5c), whereas the ASTM-R in B-P7 form small granules of non-viscous hydrogels after hydration in DI water (Fig. 2-5d), which are likely to be crosslinked polymer. Chimamkpam et al. (2011) reported that linear polymers when hydrated results in viscous solutions and the viscosity of these solutions can vary depending on molar mass and charge density of polymer and the quality of hydrating medium. Ahmed (2015) reported that hydrogels are formed by water-swollen, crosslinked polymers that can swell and retain a significant amount of water without dissolving in water.

2.3.1b Loss on Ignition

LOI tests were also conducted on the ASTM-P and ASTM-R samples prepared following ASTM D5890 to quantify the polymer loading. The LOI results for ASTM-P

and ASTM-R samples for the Na-B and the seven B-P composites are shown in Fig. 2-6. Na-B has LOI of 1.3 %, which is similar to the LOI of Na-B reported by previous researchers (~1.6 %) (Tian et al. 2016.). LOI for the ASTM-P samples of the B-P composites containing linear polymer (i.e., B-P1, B-P2, B-P3, and B-P4) is similar to LOI of Na-B (1.2 to 1.3 %), whereas the LOI of ASTM-P samples for B-P composites containing crosslinked polymer (i.e., B-P5, B-P6, and B-P7) ranged approximately from 1.8 to 4%. The higher LOI of ASTM-P of B-P5 to B-P7 may be attributed to the relatively smaller size of these polymers in B-P composites, i.e., smaller polymer particles may be able to pass the #100 sieve during the grinding and sieving process. The ASTM-R specimens for all the B-P composites showed significantly higher LOI (>40%) in comparison with LOI of ASTM-P. The significantly high LOI of ASTM-R of B-P indicates that ASTM-R was primarily composed of the polymer that was burnt (combusted) during LOI tests, which agreed with the SI test results that ASTM-R had much higher SI than ASTM-P.

Images analysis of ASTM-P and ASTM-R specimens for Na-B and B-P6 before and after the LOI test support this assumption that polymer were segregated during grinding and sieving process (Fig. 2-7). ASTM-P of Na-B samples before and after the LOI test looked similar and no ash was seen in the ignited sample, as shown in Fig. 2-7 (a) and (d). Limited ash residues are observed for ASTM-P specimens of B-P6 after the LOI test (Fig. 2-7e), whereas ASTM-R of B-P6 turned from white-gray granules to black ash after the LOI test, indicating the burning of the polymer. These observations correlate with the LOI results seen in Fig. 2-6, i.e., LOI of ASTM-P for B-P composites is similar to Na-B,

whereas ASTM-R of B-P samples has significantly higher LOI in comparison to ASTM-P samples. Overall, these observations support the hypothesis that the polymer was segregated by the #100 sieve during crushing and sieving as per ASTM D5890 sample preparation method, which may lead to inaccuracy of SI due to the preparation of the samples. Alternative tests and/or procedures should be developed and investigated.

2.3.2 Alternative Methods

Two alternative methods have been adopted for sample preparation. The SI and LOI results obtained from the alternative method 1 (AL1-As-is) and alternative method 2 (AL2-P and AL2-R) are compared with SI and LOI results of ASTM-P to further investigate the impact of #100 sieve on polymer segregation. The SI and LOI results of the ASTM-P specimens and the alternative methods (AL1-As-is, AL2-P, and AL2-R) for Na-B and B-P are summarized in Table 2-4.

2.3.2a Swell Index

The SI of Na-B prepared with all different methods had very similar results, ranging from 28.5 mL/2 g to 31 mL/2 g (Fig. 2-8). Scalia et al. (2018) also showed that the SI of Na-B is not sensitive to the granule size of the sample. In contrast, the B-P samples prepared by AL1-As-is were higher than those for AL2-P samples but lower than the AL-R samples, as shown in Fig. 2-8. The swell indices of ASTM-P and AL2-P of B-P composites containing liner polymer (e.g., B-P1, B-P2, B-P3, and B-P4) are very close to SI of Na-B, whereas the AL1-As-is and AL2-R samples had slightly higher swelling value. Images of Na-B and B-P3 after SI test were shown in Fig. 2-9. No gel was sticky on the glass rod of Na-B samples prepared as ASTM-P and AL-As-is (Figs. 2-9a and 2-9b),

indicating that Na-B formed a low viscosity gel after swelling. For the B-P3, more As-is samples were sticky on the glass rod than ASTM-P sample (Fig 2-9c and 2-9d), indicating that As-is specimen formed a high viscosity gel and contained more polymer than ASTM-P specimen.

B-P composites containing crosslinked polymer (B-P5, B-P6, and B-P7) had various SI for specimens prepared with a different method (Fig. 2-8). For example, ASTM-P of B-P5 and B-P7 composite had similar SI to that of Na-B, but the AL1-As-is and AL2-R had much higher SI than that of Na-B. The high SI of AL1-As-is and AL2-R B-P were contributed to the crosslinked polymers that form three-dimensional hydrogels and increase the total swell (Fig. 2-9f). In contrast, limited three-dimensional polymer hydrogel was observed after SI test for ASTM-P of B-P7 (Fig. 2-9e), because the polymer was filtered by #100 sieve during the sieving process. For the B-P6, the AL2-R had the highest SI, but the ASTM-P had higher swelling than AL1-As-is.

2.3.2b Loss on Ignition

LOI of the specimens prepared by ASTM method and alternative methods are shown in Table 2-4. The LOI of Na-B specimen prepared following the ASTM standard method (ASTM-P) was similar to LOI of specimens obtained following alternative method 1 (AL1-As-is) and alternative method 2 (AL2-P and AL2-R), which confirms that different sample preparation methods did not impact the LOI of Na-B samples. On the other hand, for all the B-P composites, the LOI of AL2-R is much higher than the LOI of the specimens prepared by ASTM-P and AL2-P. The LOI of B-P samples prepared by AL1-As-is method is between the retained and passing samples.

Images of B-P samples before and after the LOI test are shown in Fig. 2-11. AL2-P specimens before and after LOI test (Fig. 2-11e) looked similar, which was the same observation for Na-B samples after LOI test (Fig. 2-7d), whereas AL1-As-is and AL2-R specimens had a significant amount of ash residues after LOI test (Fig. 2-11d and f).

LOI of AL1-As-is for Na-B and the B-P samples were compared with the LOI of samples from ASTM standard (ASTM-P) and alternative method 2 (AL2-P and AL2-R) in Fig. 2-12. LOI of ASTM-P (7 to 30%) and AL2-P (15 to 70%) were lower than the AL1-As, which is attributed to segregation of polymer from these samples during crushing and sieving through #100 sieve. In contrast, the LOI of AL2-R (\approx 50 to 60%) were much higher than AL1-As-is, especially for B-P composites having LOI greater than 3%, indicating that polymer was retained on #100 sieve during crushing and sieving. Thus, the specimens prepared following the ASTM standard method (ASTM-P) and alternative method 2 (AL2-P and AL2-R) may provide unrepresentative samples for the index test. Alternative method 1 (AL1-As-is) may be considered as the most suitable method of sample preparation to characterize the SI and LOI test for polymer modified GCLs.

2.4 Summary and Conclusion

The study was conducted to investigate the effects of crushing and sieving on the swell index (SI) and loss on ignition (LOI) of B-P GCLs. SI and LOI of seven B-P GCLs and Na-B GCL were conducted using the ASTM standard method (D5890) and two alternative methods. Based on the results of the SI and LOI tests, the following conclusions can be deduced:

1. Limitations were observed for SI test of bentonite polymer (B-P) GCL in accordance with ASTM D5890. The B-P samples cannot pass through the #100 sieve completely. For Na-B GCL, approximately 0.2% of the total mass cannot pass the #100 sieve. For B-P GCLs, up to 4% of the samples can be retained on the #100 sieve, which was primarily consisting of polymer particles.
2. SI and LOI tests of the portion of the B-P samples passing #100 sieve had similar or slightly higher SI and LOI in comparison to Na-B, whereas the sample retained on #100 sieve had very high swell (~50 to 550 mL/2 g) and LOI (~ 40 to 84%). These observations indicate that the grinding and sieving of the samples in according to ASTM D5890 lead to the segregation of B-P composites, resulting in unrepresentative samples for index tests.
3. Sample preparation methods investigated in this study showed that the influence of crushing and sieving on SI of B-P GCLs depends on the type and size of polymer in B-P. The polymer with smaller size had higher possibility to pass the #100 sieve (e.g., B-P5, B-P6, and B-P7), whereas the polymer with big size had limited chance to pass the #100 sieve.
4. Alternative sample preparation method for the index test was investigated in this study. The result showed that samples directly received from the manufacturer or retrieved from GCLs without grinding or sieving were most representative to be used to characterize the index properties of B-P.

Tables:

Table 2-1: Amount of Na-B and B-P sample retained and passing #100 sieve after grinding in according to ASTM D5890.

Material	Initial mass (g)	Mass retained #100 sieve (g)	Mass passing # 100 sieve (g)	Percentage mass retained # 100 sieve (%)
Na-B	25.0	0.05	24.95	0.2
B-P1	25.0	0.03	24.97	0.1
B-P2	25.0	0.54	24.46	2.2
B-P3	25.0	0.41	24.59	1.6
B-P4	25.0	0.99	24.01	4.0
B-P5	25.0	0.56	24.44	2.2
B-P6	25.0	0.60	24.40	2.4
B-P7	25.0	0.50	24.50	2.0

Table 2-2: Sample preparation methods used in this study.

Sr. No.	Method	Method Components	Designation	Crushing and Sieving
1	ASTM Standard	ASTM-Passing #100	ASTM-P	Passing #100 sieve (min 60% passing # 200 sieve)
		ASTM-Remnants #100	ASTM-R	Retained #100 sieve (Remnants of ASTM sample)
2	Alternative 1	Alternative 1-As-is	AL1-As-is	None
3	Alternative 2	Alternative 2-Passing #100	AL2-P	Passing #100 sieve (50% of total AL2 sample)
		Alternative 2-Retained #100	AL2-R	Retained #100 sieve (50% of total AL2 sample)

Table 2-3: Swell index and loss on ignition (LOI) test results of samples prepared following ASTM standard method.

Material	ASTM-P		ASTM-R		
	Swell Index	LOI	Swell Index	Estimated Swell Index	LOI
	(mL/2 g)	(%)	(mL/0.2 g)	(mL/2 g)	(%)
Na-B	28.7	1.3	NM	NM	NM
B-P1	28.7	1.2	NM	NM	50.0
B-P2	30.3	1.2	5.0	50.0	45.9
B-P3	30.3	1.4	9.0	90.0	72.0
B-P4	31.0	1.3	15.0	150.0	70.6
B-P5	31.0	1.9	7.0	70.0	44.4
B-P6	50.1	2.9	40.0	400.0	54.4
B-P7	46.3	4.0	55.0	550.0	83.7

Note: NM = Not measured due to limited quantity of sample

Table 2-4: Swell index and loss on ignition results of Na-B and B-P GCL samples prepared following the alternative methods 1 and 2.

Material	AL1-As-is		AL2-P		AL2-R	
	Swell Index	LOI	Swell Index	LOI	Swell Index	LOI
	(mL/2 g)	(%)	(mL/2 g)	(%)	(mL/2 g)	(%)
Na-B	28.5	0.9	31.0	1.2	29.3	1.1
B-P1	30.6	1.3	29.2	1.1	31.3	2.0
B-P2	31.4	2.0	29.3	1.4	35.5	3.5
B-P3	31.8	2.2	29.0	1.4	34.2	3.5
B-P4	37.7	4.5	29.2	1.9	35.2	7.7
B-P5	40.1	2.5	29.5	1.4	40.3	6.4
B-P6	51.4	4.6	29.7	1.4	61.8	8.7
B-P7	52.4	5.9	30.7	1.8	66.3	11.2

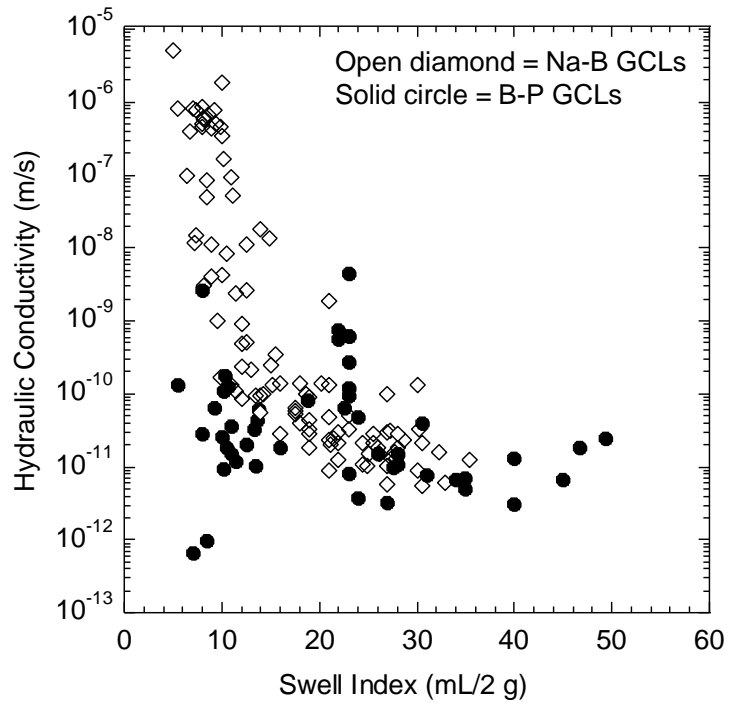


Figure 2-1: Relationship between swell index and hydraulic conductivity of Na-B and B-P GCLs (Note: Na-B GCLs data from Jo et al. 2001; Kolstad et al. 2004a; Lee et al. 2005; Katsumi et al. 2008; Scalia et al. 2014; Setz et al. 2017; Tian et al. 2017; and B-P GCLs data from Katsumi et al. 2008; Scalia et al. 2014; Tian et al. 2016; Tian and Benson 2017; Tian et al. 2017)

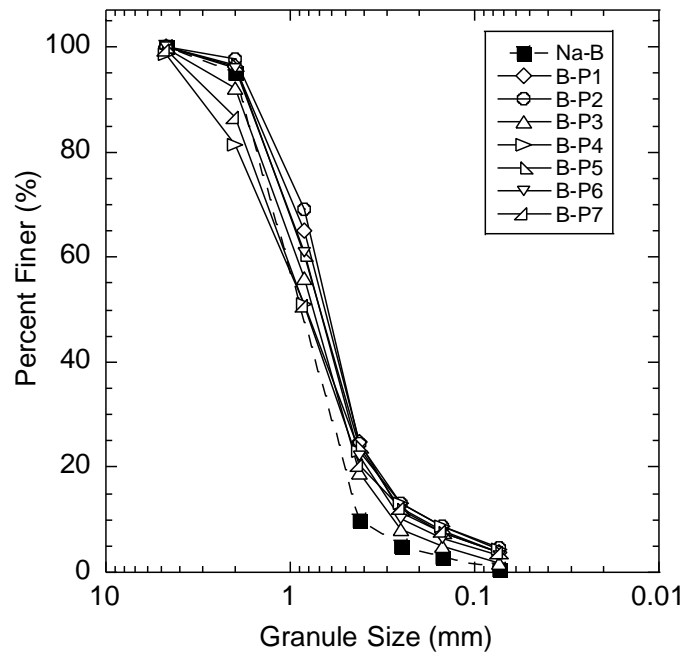


Figure 2-2: Granule size distribution of Na-B and B-P GCL samples used in this study.

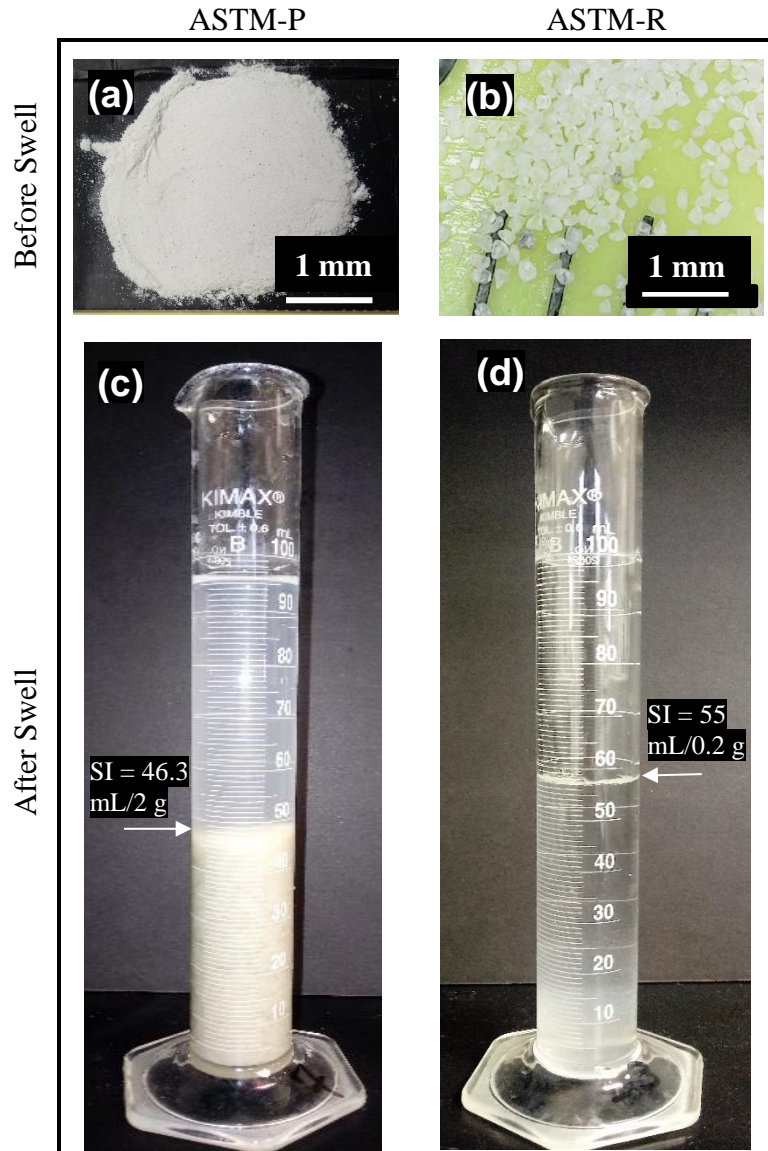


Figure 2-3: Comparison of swell indices of B-P7 samples before (a and b) and after (c and d) swell test, prepared following ASTM standard method that includes the specimens passing the #100 sieve (ASTM-P) and remaining on the #100 sieve (ASTM-R).

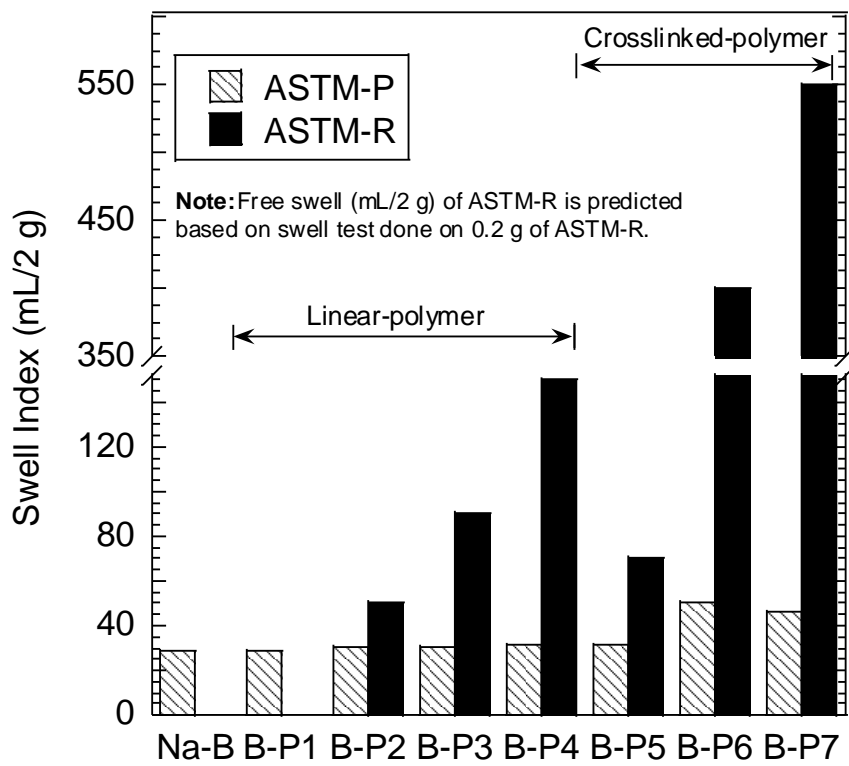


Figure 2-4: Comparison of swell indices of ASTM-P and ASTM-R for the Na-B and B-P samples prepared following ASTM standard method (Note: Swell test not done on Na-B and B-P1-ASTM-R due to limited quantity of sample retained on #100 sieve).

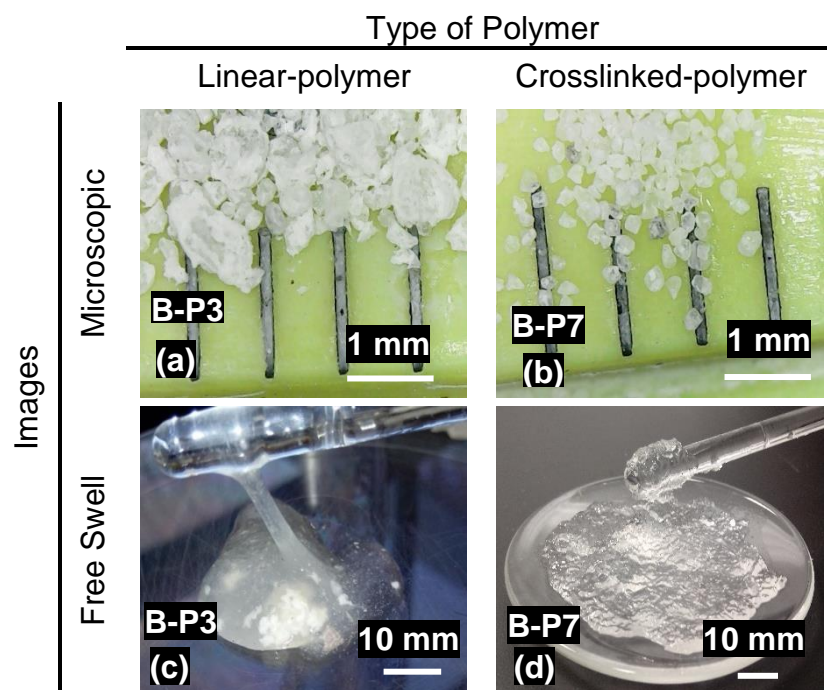


Figure 2-5: Images of ASTM-Remnants #100 (ASTM-R) specimens of B-P3 and B-P7 before (a and b) and after (c and d) swell index test.

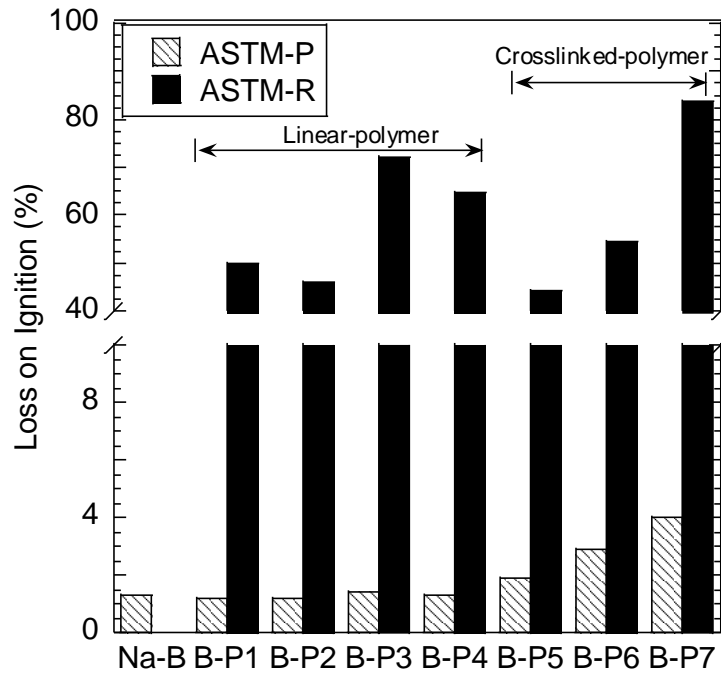


Figure 2-6: Loss on ignition (LOI) of Na-B and B-P samples prepared following ASTM standard method for the specimen passing the #100 sieve (ASTM-P) and remnants on the #100 sieve (ASTM-R).

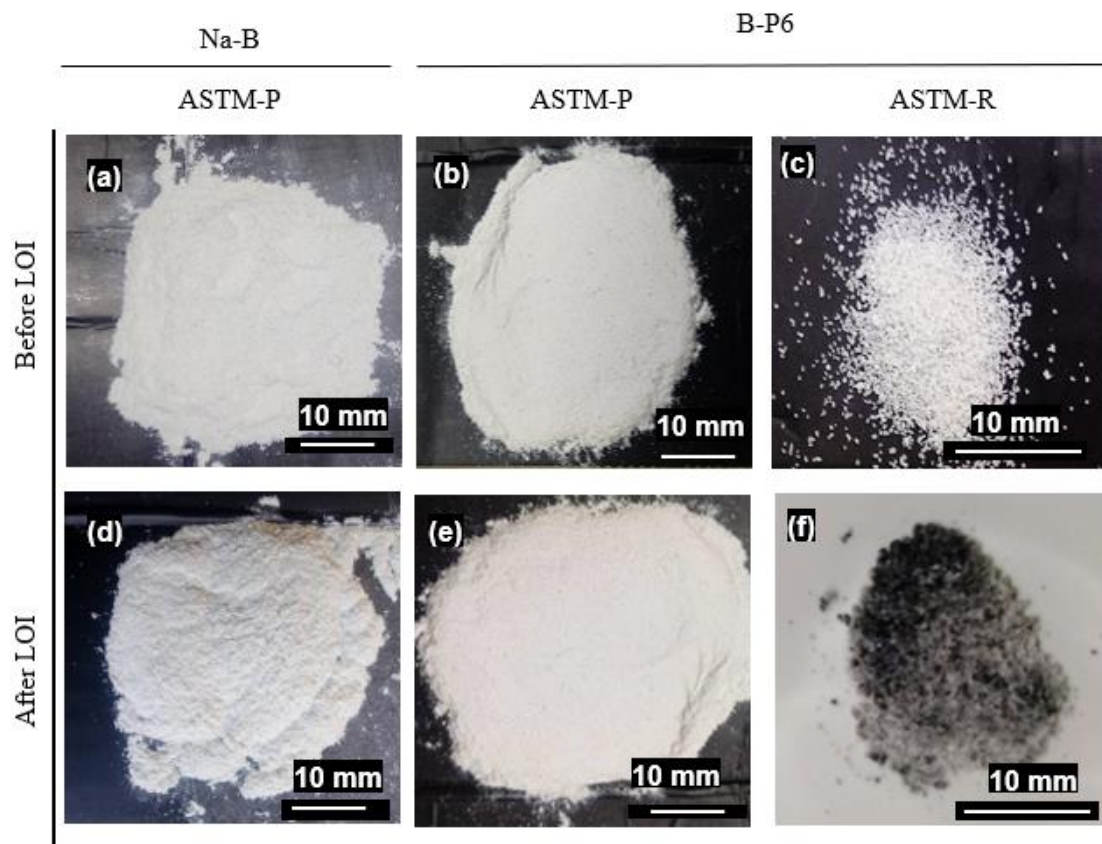


Figure 2-7: Images of Na-B and B-P6 specimens prepared following ASTM standard method for the specimens passing the #100 sieve (ASTM-P) and remnants on the #100 sieve (ASTM-R) before and after loss on ignition test.

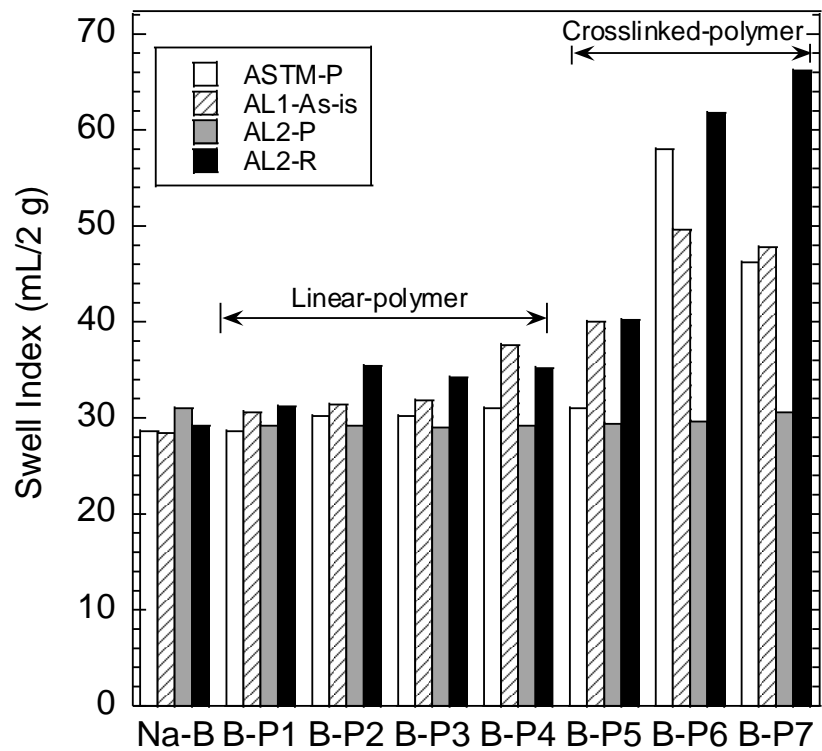


Figure 2-8: Comparison of swell indices of Na-B and B-P samples prepared following ASTM standard method (ASTM-P) with the alternative method 1 (AL1-As-is) and alternative method 2 passing #100 (AL2-P) and retained #100 (AL2-R).

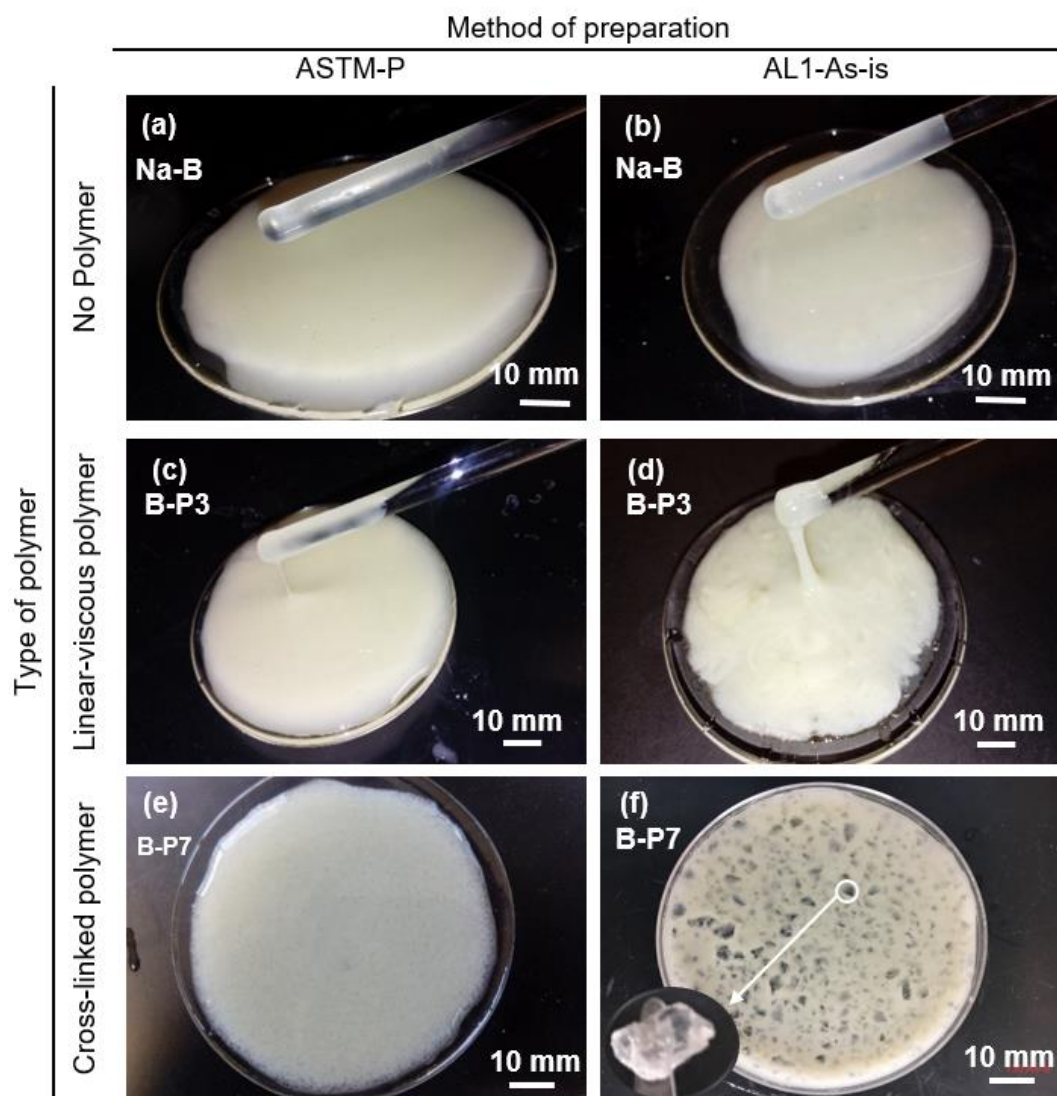


Figure 2-9: Images of Na-B, B-P3 and B-P7 prepared following the ASTM standard method (ASTM-P) and the alternative method 1 (AL1-As-is) after swell index test on specimens.

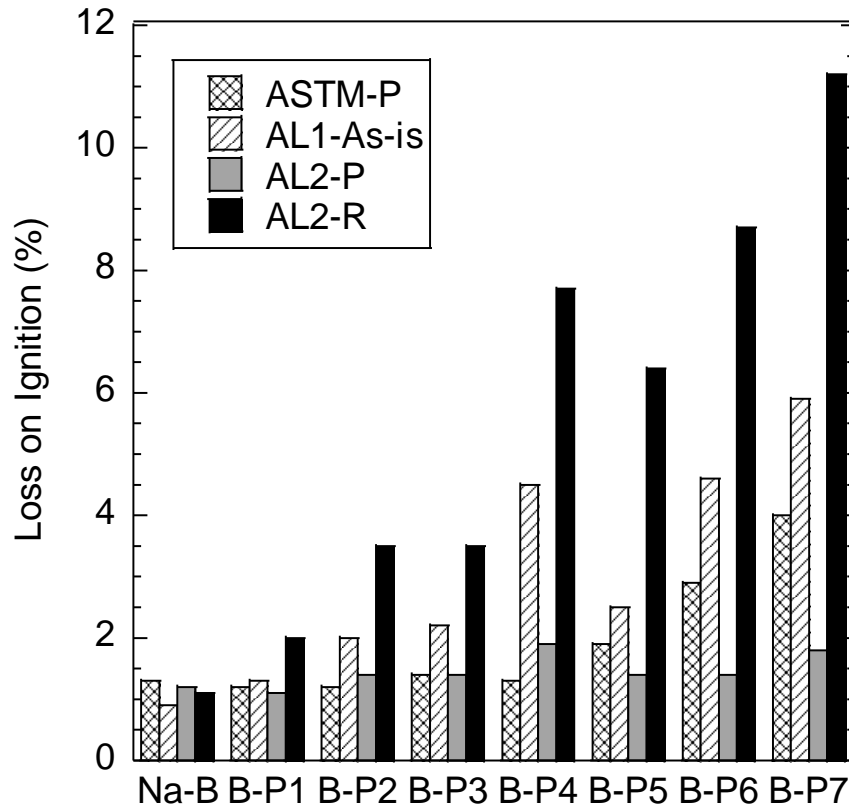


Figure 2-10: Comparison of loss on ignition values of Na-B and B-P samples prepared following ASTM standard method (ASTM-P) with the alternative method 1 (AL1-As-is) and alternative method 2 [i.e. passing #100 (AL2-P) and retained #100 (AL2-R)].

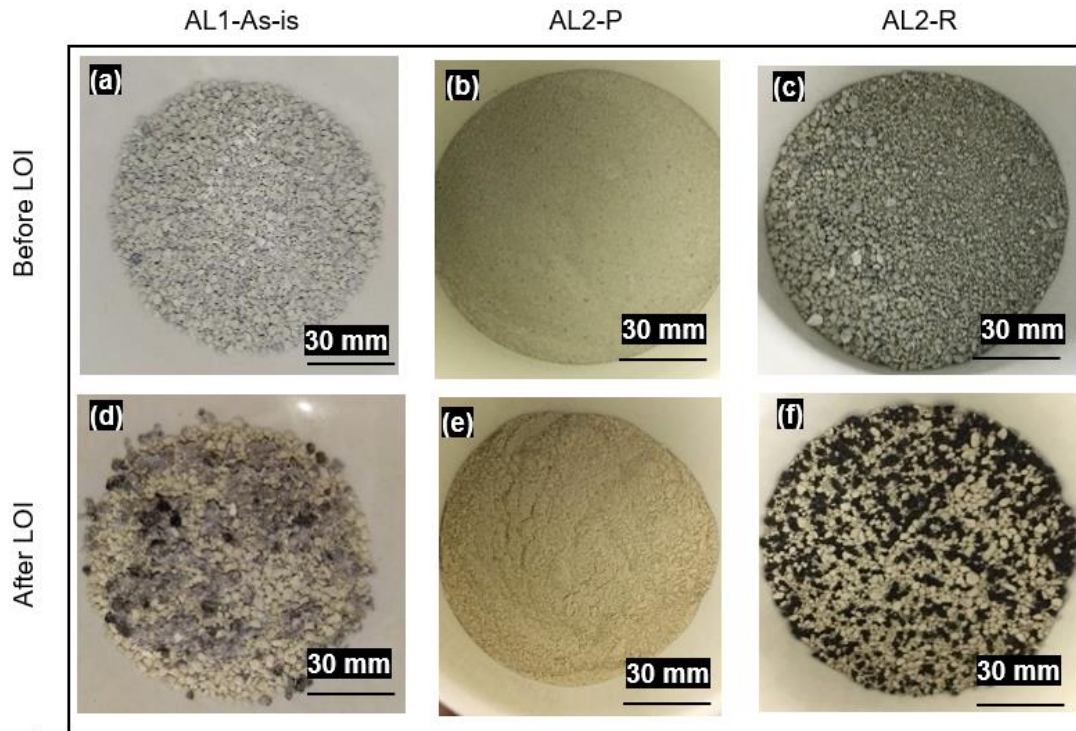


Figure 2-11: Images of B-P6 specimens prepared following alternative method 1(AL1-As-is) and alternative method 2 (AL2-P and AL2-R) before and after loss on ignition test.

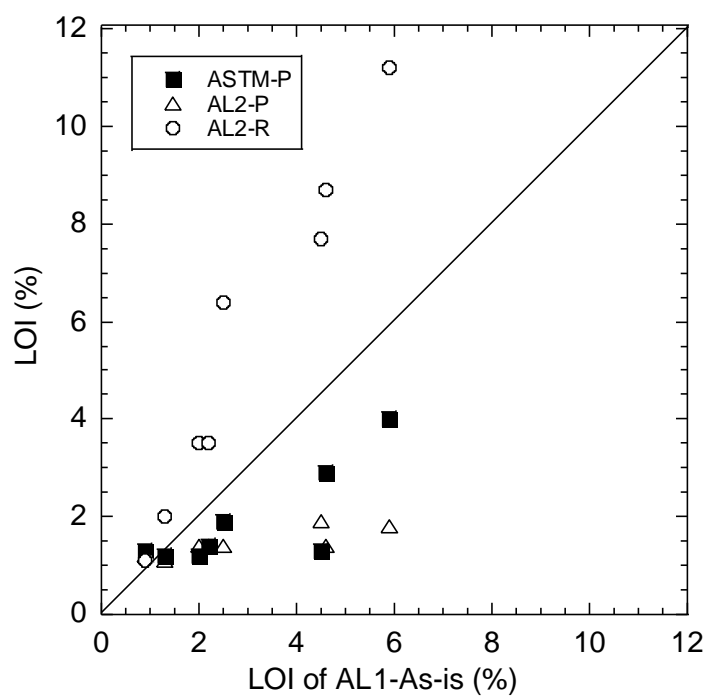


Figure 2-12: Comparison of loss on ignition (LOI) of Na-B and B-P samples prepared following the alternative method 1 (AL1-As-is), prepared following ASTM standard method (ASTM-P), and the alternative method 2 passing (AL2-P) and retained (AL2-R) on #100 sieve.

CHAPTER 3 : HYDRAULIC CONDUCTIVITY OF BENTONITE-POLYMER GEOSYNTHETIC CLAY LINERS TO AGGRESSIVE COAL COMBUSTION PRODUCT LEACHATES

Hydraulic conductivity was evaluated for seven commercially available geosynthetic clay liners (GCLs) permeated with six synthetic coal combustion product (CCP) leachates representative of typical and worse scenarios observed in the CCP landfills with ionic strength (I) ranging from 50 mM to 4676 mM (TCCP-50, LRMD-96, TFGDS-473, LR-2577, HI-3179 and HR-4676). One of the GCLs contained conventional sodium bentonite (Na-B) and the other six contained bentonite-polymer (B-P) mixture with polymer loading (P) ranging from 0.5% to 12.7% (B-P-0.5, B-P-1.5, B-P-3.4, B-P-3.7, B-P-5.5 and B-P-12.7). Hydraulic conductivity tests were conducted on all the GCLs with six synthetic CCP leachates at an effective stress of 20 kPa. Hydraulic conductivity of Na-B GCL was measured to be $>10^{-10}$ m/s for all the CCP leachates whereas, the hydraulic conductivity of B-P GCLs was dependent on leachate chemistry and polymer loading. All the B-P GCLs showed low hydraulic conductivity ($<10^{-10}$ m/s) to low ionic strength leachates (TCCP-50, I= 50 mM and LRMD-96, I= 96 mM). Hydraulic conductivity of B-P GCLs to aggressive CCP leachates (I = 473 mM to 3179 mM) varied from 10^{-7} m/s to 10^{-12} m/s with varying polymer loading (P = 0.5% to 12.7%). B-P GCLs with P < 5% showed high hydraulic conductivity ($>10^{-10}$ m/s) and B-P GCLs with P > 5% showed low hydraulic conductivity ($<10^{-10}$ m/s). These results suggest that B-P GCL with sufficient polymer loading (i.e., > 5%) can be used to manage aggressive CCP leachates.

3.1 Introduction

Coal Combustion Products (CCPs) also known as coal ash/residues are generated when coal is burnt to generate electricity or steam. CCPs include fly ash, bottom ash, flue gas desulfurization (FGD) materials (FGD solids, FGD Gypsum), spray dryer ash etc. In 2012, approximately 40 percent of the CCPs generated in U.S. were beneficially used while the remaining 60 percent of CCPs were disposed in the surface impoundments and landfills. The production of CCPs has grown from 59.5 million Mg in 1974 to 114.7 million Mg in 2013 (ACAA 2015).

USEPA (United States Environmental Protection Agency) require the CCP disposal facilities to have a composite liner consisting of a geomembrane overlying a 0.6 m thick compacted clay liner (CCLs) to prevent the potential contamination of groundwater. Hydraulic conductivity of CCLs should be $\leq 1 \times 10^{-9}$ m/s [80 Fed. Reg. 21301 (October 14, 2015)]. The regulation allows the use of alternative materials (e.g., Geosynthetic Clay Liners, GCLs) in *lieu* of CCLs, provided that they have equal or lower hydraulic conductivity than CCLs. GCLs are easy to install, save air space due to less thickness (5 to 10 mm), and have low hydraulic conductivity ($< 10^{-10}$ m/s) (Shackelford et al. 2000; Jo et al. 2001; 2005; Kolstad et al. 2004a; Bradshaw and Benson 2014).

Conventional sodium bentonite (Na-B) GCL consists of a thin layer of sodium bentonite sandwiched between two geotextiles (Shackelford et al. 2000; Jo et al. 2001, 2005). The sodium bentonite in GCLs is primarily composed of sodium montmorillonite (65 to 90%) (Shackelford et al. 2000; Jo et al. 2001, 2005; Lee et al. 2005; Kolstad et al. 2004; Bradshaw and Benson 2014). Sodium montmorillonite has high swelling capability

in aqueous solutions (Grim 1968; Mitchell 1993; Shan and Daniel 1991; Shackelford et al. 2000). The swelling of Na-B clogs the intergranular void space, resulting in narrower and tortuous flow paths for mobile water/leachate and results in low hydraulic conductivity ($\leq 10^{-10}$ m/s) (Shackelford et al. 2000; Jo et al. 2001, 2005; Ashmawy et al. 2002; Kolstad 2004; Guyonnet et al. 2005; Scalia et al. 2011; ; Bradshaw and Benson 2014; Chen et al. 2014; Athanassopoulos et al. 2015; Tian et al. 2016; Setz et al. 2017; Ören and Akar 2017; Chen et al. 2019).

Several researchers have reported that the aggressive leachates with high ionic strength, preponderance of multivalent cations, or/and extreme pH (< 3 or > 12) can inhibit the swelling of Na-B, resulting in high hydraulic conductivity ($>10^{-10}$ m/s) (Shackelford et al. 2000; Jo et al. 2001, 2005; Ashmawy et al. 2002; Katsumi et al. 2008; Scalia et al. 2014; Razakamanatsoa et al. 2014; Emidio et al. 2015; Tian et al. 2016; Chen et al. 2019).

Therefore, the conventional Na-B GCLs have been modified using different organic molecules and polymers to improve their chemical compatibility against aggressive leachates (Onikata et al. 1999; Ashmawy et al. 2002; Katsumi et al. 2008; Scalia et al. 2014). These polymer modified GCLs, also known as bentonite-polymer (B-P) GCLs have been found to have low hydraulic conductivity even in case of aggressive leachates (Ashmawy et al. 2002; Katsumi et al. 2008; Scalia et al. 2014; Razakamanatsoa et al. 2014; Emidio et al. 2015; Athanassopoulos et al. 2015; Tian et al. 2016; Setz et al. 2017; Chen et al. 2019, Tian et al. 2019). Scalia et al (2014), polymerized acrylic acid within the bentonite slurry to create a bentonite polymer composite (BPC) that can give low hydraulic conductivity even when permeated with aggressive inorganic solutions. Tests were

conducted on BPC as well as on pure Na-B using deionized water (as control solution), CaCl_2 (5 to 500 mM), NaOH (1 M with pH 13.1) and HNO_3 (1 M with pH 0.3) as permeant solutions. BPC maintained low hydraulic conductivity ($k < 10^{-11}$ m/s) in all permeant solutions whereas, Na-B showed three orders of magnitude higher hydraulic conductivity than BPC (except in < 5 mM CaCl_2). Athanassopoulos et al. (2015) also reported that B-P GCLs permeated with bauxite residue liquor (pH = 13, ionic strength = 2.35 M) showed low hydraulic conductivity ($< 1 \times 10^{-11}$ m/s). Tian et al. (2016) studied the effect of low level radioactive leachates (LLW) on the hydraulic conductivity of BP-GCLs. The hydraulic conductivity of B-P GCLs (polymer loading $> 5\%$) to LLW leachates was found to be similar or lower than, the hydraulic conductivity to DI water i.e., in order of 10^{-12} m/s. Tian et al. 2016 also proposed the low hydraulic conductivity of the B-P GCLs to liquid like glutinous hydrogels which coats the bentonite particles together and result in clogging of voids. Chen et al. (2019) studied the effect of CCP leachates on the hydraulic conductivity of B-P GCLs and found that the hydraulic conductivity of B-P GCLs with polymer loading $\geq 1.9\%$ was primarily controlled by polymer hydrogel instead of bentonite swell. Hydraulic conductivity of conventional Na-B GCLs was $> 10^{-10}$ m/s with all the CCP leachates ($I = 39.5$ mM to 755 mM). B-P GCLs with $P < 1.9\%$ to CCP leachates was similar to the hydraulic conductivity of Na-B GCL ($\geq 10^{-10}$ m/s) whereas B-P GCL with $P \geq 1.9\%$ typically showed low hydraulic conductivity ($< 10^{-10}$ m/s) to CCP leachates ($I = 39.5$ mM to 755 mM). Chen et al. (2019) also conducted hydraulic conductivity tests on two B-P GCLs (polymer loading = 2.1% and 5.1%) with CCP leachate of $I = 975$ mM and found that both the GCLs resulted in high hydraulic conductivity ($> 10^{-10}$ m/s).

Leachate data collected from more than 130 coal-fired power plants has revealed many waste streams that generate leachates much more aggressive than those studied by previous researchers (4.6 M vs. 0.975 M). The increase in aggressiveness of the CCP leachates can be linked to the closure of all CCP surface impoundments operating without a proper liner system. Largely, by leaving all the CCPs in place in the surface impoundment and covering it with a cap or by excavating the CCPs from surface impoundments (wet storage) and re-disposing it into the CCP lined landfills (ACCA, 2016). Excavation and re-disposing of CCPs from surface impoundments to landfills can take long time resulting in longer period of infiltration of CCP contaminants to groundwater. Evaluating the hydraulic conductivity of B-P GCLs to current aggressive CCP leachates is necessary for the selection of GCLs as liner material in the CCP disposal facilities.

The objective of this study is to evaluate the hydraulic conductivity of B-P GCLs to aggressive CCP leachates ($I = 50$ to 4676 mM). Hydraulic conductivity of seven GCLs (both Na-B and B-P GCLs) to CCP leachates was evaluated in this study. Tests were conducted on B-P GCLs with various polymer loading ranging from 0.5 to 12.7 % to evaluate the effect of polymer loading on the chemical compatibility of the GCLs. Six synthetic CCP leachates were created from data collected from 130 CCP disposal facilities to represent the typical and worse scenarios observed in the field. Control tests were also conducted with deionized water (DI).

3.2 Materials

3.2.1 Geosynthetic Clay Liners

Seven commercially available GCLs were evaluated in this study. One of the GCLs contained conventional Na-B and the other six contained B-P mixtures with varying

polymer loading, ranging from 0.5% to 12.7%. Herein, named as B-P-0.5, B-P-1.5, B-P-3.4, B-P-3.7, B-P-5.5 and B-P-12.7. The numeric digits in the GCL designation indicates the polymer loading of the GCLs. The B-P GCLs contained a dry mixture of Na-B and proprietary polymer.

Polymer loading was determined following the loss on ignition (LOI) method adopted by Scalia et al. (2014) and Tian et al. (2016). Polymer loading was determined based on the assumption that polymer completely burns out at 550 °C in 4 hours and the difference between LOI of Na-B and B-P is equal to amount of polymer present in the B-P mixture.

The granule size distribution of the GCLs was determined by mechanical sieve analysis following ASTM D6913. All the GCLs had similar grain size distribution (D50 ≈ 0.9 mm, medium to fine sand) as shown in Fig. 3-1. Mass per unit area, thickness and polymer loading of the GCLs is given in Table 3-1.

3.2.2 Permeant Solutions

Ionic strength (I), relative abundance of monovalent and polyvalent cations (RMD) and pH are the master variables known to affect the hydraulic properties of GCLs (Jo et al. 2001, 2005; Kolstad et al. 2004). Ionic strength is the measure of concentration of ions, defined by

$$I = \frac{1}{2} \sum_{i=1}^n c_i z_i^2 \quad \text{Equation 3-1: Ionic strength}$$

where c_i = molar concentration of i th ion in solution; and z_i = valence of the i th ion. RMD is defined as follows (Kolstad et al. 2004):

$$\text{RMD} = \frac{M_M}{\sqrt{M_D}} \quad \text{Equation 3-2: RMD}$$

where M_M = total molarity of monovalent cations; and M_D = total molarity of divalent cations.

Leachates with high ionic strength and preponderance of polyvalent cations (low RMD) can inhibit the swelling of bentonite resulting in high hydraulic conductivity of GCLs (Jo et al 2001; Kolstad et al. 2004a; Lee et al. 2005; Katsumi 2008; Scalia et al 2011; Tian et al. 2016; Chen et al. 2019). Tian et al. (2017), also related the sensitivity of the B-P GCL to anion ratio ($R = \text{Cl}^-/\text{SO}_4^{2-}$) and attributed it to the collapse of the polymer. When the Cl^- concentration increases, it opens the intergranular pores and results in higher hydraulic conductivity.

The concentration of major cations, anions and the bulk properties (I, RMD, R and pH) of the six synthetic CCP leachates selected for this study are given in Table 3-2. Na^+ , K^+ and Mg^{2+} , Cl^- and SO_4^{2-} are the dominant ions present in the synthetic CCP leachates. I ranges from 50 mM to 4676 mM, RMD from 0.005 to ∞ (no divalent cations), R from 0.01 (sulphate rich) to 122.29 (chloride rich) and the pH of the synthetic leachates ranges from 5.5 to 8.4.

The comparison between the CCP leachate used by previous researchers (Chen et al. 2018, 2019 i.e., based on EPRI database) and the leachate data recently collected from more than 130 CCP disposal facilities located within United States is shown in Fig. 3-2. The synthetic CCP leachate represents the six synthetic CCP leachates used in this study, selected from the new data set to represent the typical and worse scenarios observed in the field. (1) High anion ratio (HR) leachate (I = 4676 mM, RMD = ∞ , R = 122.3) represents

the most aggressive leachate with highest ionic strength and highest concentration of chloride ions. (2) High ionic strength (HI) leachate ($I = 3179 \text{ mM}$, $\text{RMD} = 32.0 \text{ M}^{1/2}$, $R = 0.53$) represents the leachate with high ionic strength but relatively less aggressive RMD and R. (3) Low anion ratio (LR) leachate ($I = 2577 \text{ mM}$, $\text{RMD} = 0.27 \text{ M}^{1/2}$, $R = 0.01$) represents the leachate with minimum anion ratio i.e., with the highest concentration of sulphate ions. (4) Typical FGD solids (TFGDS) leachate ($I = 473 \text{ mM}$, $\text{RMD} = 0.65 \text{ M}^{1/2}$, $R = 0.56$) represents the most aggressive CCP type leachate obtained by taking geometric mean of all the leachates collected from FGD solids disposal facilities. (5) Low RMD (LRMD) leachate ($I = 96 \text{ mM}$, $\text{RMD} = 0.005 \text{ M}^{1/2}$, $R = 0.55$) represents the leachate with highest amount of divalent cations in comparison to monovalent cations and is obtained by taking geometric mean of all the leachates collected from FGD gypsum disposal facilities. (5) Typical CCP (TCCP) leachate ($I = 50 \text{ mM}$, $\text{RMD} = 0.1 \text{ M}^{1/2}$, $R = 0.25$) represents the typical CCP leachate found in the field, obtained by taking geometric mean of all the CCP leachates. Fig. 3-2 shows that the synthetic CCP leachates selected for this study are much more aggressive than the synthetic leachate used by previous researchers (EPRI) both in terms of high ionic strength (e.g., $I = 4.6 \text{ M}$ versus 0.755 M) and low RMD (e.g., 0.005 versus $0.014 \text{ M}^{1/2}$).

All the synthetic CCP leachates were prepared by dissolving reagent-grade NaCl, KCl, Na_2SO_4 , MgCl, MgSO_4 and K_2SO_4 in Type II DI water as per ASTM D1193. The synthetic leachates were stored in sealed carboys to prevent interaction with atmosphere (CO_2). The electrical conductivity (EC) and pH of the synthetic leachates was checked periodically to assure no changes in the leachate chemistry.

3.3 Methods

3.3.1 Hydraulic Conductivity

Hydraulic conductivity tests were conducted on 152.4 mm (6-inch) circular GCL samples in flexible wall permeameters following the falling headwater and constant tailwater method as per ASTM D6766. All the GCL samples were first hydrated in the permeameter with the specific leachate at an effective stress of 20 kPa for 48 hours. After hydration tests were continued at an effective stress of 20 kPa and at an average hydraulic gradient of approximately 150. 50 mL graduated glass burettes were used as influent reservoir. No back pressure was applied to collect the effluent. Effluent was collected in 70 mL polyethylene bottles and its pH and EC was periodically measured to check chemical equilibrium. The tests were continued until the hydraulic and chemical equilibrium was achieved as per ASTM D6766. Tests were conducted on all the seven GCLs permeated with six synthetic CCP leachates and DI water.

Termination Criteria

Tests were terminated only when the hydraulic and chemical equilibrium was achieved as per ASTM D6766. Hydraulic equilibrium is achieved when, no temporal trend is observed in the hydraulic conductivity, hydraulic conductivity of three consecutive values is within the 25% of the mean hydraulic conductivity and the ratio of inflow over outflow (Q_{in}/Q_{out}) is within 0.75 and 1.25. The chemical equilibrium is achieved when EC of effluent is within 10% of influent EC (ASTM D6766). In addition to EC, pH of the effluent was also measured to check whether pH of effluent is within 10% of influent pH (Tian et al. 2016; Chen et al. 2019).

Concentration of major cations (Na^+ , K^+ and Mg^{2+}) in the influent and effluent was also measured periodically for elemental analysis using inductively coupled plasma-optical emission spectroscopy (ICP-OES) as per EPA Method 6010C (USEPA). Samples preserved in 1% nitric acid were stored at temperature of 4 °C and were filtered using 0.2- μm filter before analyzing in ICP-OES.

3.3.2 Swell Index

Swell index was measured for all the six B-P GCLs and Na-B GCL using DI water and the six synthetic CCP leachate following the test method as per ASTM D5890. The samples were first crushed using a pastel and mortar such that 100% passes #100 sieve and at least 65% passes #200 sieve. The tests were conducted using 2 g of oven dried sample, added into a 100 mL graduated cylinder filled with 90 mL of solution (DI water and six synthetic CCP leachates). The sample was added in graduated cylinder with an increment of 0.1 g. After adding 2 g of sample, the cylinder was filled to the 100 mL with the solution (DI water and six synthetic CCP leachates). The SI was measured as the volume of the swollen specimen in the graduated cylinder after 24 h (in mL/2 g).

3.4 Results and Discussion

3.4.1 Hydraulic Conductivity

A summary of hydraulic conductivity tests on Na-B and B-P GCLs is given in Table 3-3. All the GCLs (six B-P GCLs and one Na-B) were tested with DI water and six synthetic CCP leachates. Tests on GCLs with hydraulic conductivity $< 10^{-10}$ m/s are still running to measure their long-term hydraulic conductivity. The number of days and pore volumes of flow (PVF) reported in the Table 3-3 are to the time this paper was prepared.

Temporal behavior of the B-P-0.5 permeated with LRMD-96 leachate is shown in Fig. 3-3. The hydraulic conductivity of B-P-0.5 to LRMD-96 drastically decreased at a PVF of 4 to 6, which can be due to polymer elution resulting in clogging of the tubes leading to low hydraulic conductivity. Similar observations were made by Tian et al. (2019). To remove polymer clogging the influent and effluent tubes were regularly flushed and the hydraulic conductivity of B-P-0.5 to LRMD-96 increased from 10^{-12} m/s to 10^{-11} m/s and remained constant. At approximately 6 PVF the EC of the effluent levelled off and fall within the range associated with chemical equilibrium based on EC termination criteria as per ASTM D6766 (i.e., effluent EC within 10% of the influent EC). The test is running as the pH is still higher than the 10% of influent pH (Tian et al. 2016; Chen et al. 2019).

Hydraulic conductivity of all the GCLs permeated with DI water and six synthetic CCP leachates as a function of ionic strength of the permeant solutions, at an effective stress of 20 kPa is shown in Fig. 3-4. Ionic strength was found to have much greater effect on hydraulic conductivity than RMD, similar findings were reported by previous researchers when the ionic strength of the leachates varied over a broad range in comparison to RMD (Benson et al. 2014; Chen et al. 2019).

Na-B GCL showed low hydraulic conductivity ($< 10^{-10}$ m/s) when permeated with DI water whereas, the hydraulic conductivity of Na-B was greater than 10^{-10} m/s for all the CCP leachates (I = 50 mM to 4676 mM). Hydraulic conductivity of the B-P GCLs to CCP leachates varied with varying polymer loading and ionic strength. All the B-P GCLs (B-P-0.5, B-P-1.5, B-P-3.4, B-P-3.7, B-P-5.5, and B-P-12.7) showed low hydraulic conductivity ($< 10^{-10}$ m/s) to TCCP-50 (I = 50 mM) and LRMD-96 (I = 96 mM). The low hydraulic

conductivity ($<10^{-10}$ m/s) of B-P GCLs to CCP leachates can be attributed to polymer clogging (Tian et al. 2016). B-P GCLs contain super absorbent polymers such as Na-carboxymethylcellulos, Na-polyacrylate and Na-polyacrylamide that absorbs high amount of water, results in formation of swollen, viscous polymer hydrogels which clogs the void spaces present between the bentonite granules resulting in narrower and tortuous flow paths and low hydraulic conductivity (Tian et al. 2016; Chen et al. 2019). The water molecules attached to the polymer hydrogels hydraulically act as solid, immobile water (Tian et al. 2016) similar to water molecules attached to bentonite when it undergoes osmotic swell. Hydraulic conductivity of B-P GCLs varied with varying polymer loading when the ionic strength of CCP leachates increased to 473 mM to 4676 mM. B-P GCLs with polymer loading less than 5 % (i.e., B-P-0.5, B-P-1.5, B-P-3.4, and B-P-3.7) showed high hydraulic conductivity ($> 10^{-10}$ m/s) to TFGDS-473, LR-2577, HI-3179 and HR-4676 (I = 473 mM to 4676 mM). High ionic strength leachates can limit the water absorption capacity and swelling of polymer hydrogels, therefore if polymer loading is not sufficient enough then it can lead to wider flow channels and high hydraulic conductivity (Tian et al. 2016, 2019; Chen et al. 2019). B-P GCL with 5.5 % polymer loading (B-P-5.5) showed low hydraulic conductivity (1.4×10^{-11} m/s to 3.7×10^{-11} m/s) to TFGDS-473 and LR-2577 leachates and B-P-12.7 with 12.7 % polymer loading showed low hydraulic conductivity ($\approx 10^{-12}$ m/s) to all the CCP leachates (I = 50 mM to 3179 mM) except HR-4676 (I = 4676 mM). This suggests that with increase in polymer loading, low hydraulic conductivity can be achieved against aggressive CCP leachates. The maximum polymer loading of the GCLs used in this study was up to 12.7%. Hydraulic conductivity of all the GCLs (Na-B and B-P GCLs) to

HR-4676 leachate ($I = 4676$ mM) was greater than 10^{-10} m/s. The B-P GCLs used in this study may not have sufficient polymer loading for such an aggressive leachate. Further studies with higher polymer loading (> 12.7 %) is recommended, as the hydraulic conductivity may decrease with the increase in polymer loading.

3.4.2 Swelling

Swell index tests were also conducted on all the GCLs (Na-B and B-P GCLs) with six synthetic CCP leachates and DI water. The relationship between hydraulic conductivity and swell index is shown in Fig. 3-5. The hydraulic conductivity of Na-B decreased significantly with the increase in swell index. Na-B resulted in low hydraulic conductivity ($< 10^{-10}$ m/s) when permeated with DI water at a swell of 28.7 mL/2 g, indicating that the hydraulic conductivity of Na-B GCLs has a strong inverse relationship with SI and bentonite swelling is primarily responsible for the hydraulic conductivity of Na-B GCLs (Jo et al. 2001; Kolstad et al. 2004; Lee et al. 2005; Katsumi et al. 2008; Scalia et al. 2014; Tian et al. 2016; Chen et al. 2018). The hydraulic conductivity of B-P GCLs with polymer loading < 5 % (B-P-0.5, B-P-1.5, B-P-3.4, B-P-3.7) also showed a decreasing trend in hydraulic conductivity with the increase in SI and the hydraulic conductivity is $< 10^{-10}$ m/s at a lower swell than Na-B (i.e., 15.5 mL/2 g versus 28.7 mL/2 g), suggesting that for B-P GCLs with low polymer loading (< 5 %) both Na-B swelling and polymer clogging mechanism contribute towards the low hydraulic conductivity (Tian et al. 2016; Chen et al. 2019). The hydraulic conductivity of B-P GCLs with polymer loading > 5 % did not show a trend with SI as both low ($< 10^{-10}$ m/s) and high ($> 10^{-10}$ m/s) hydraulic conductivities were observed at a similar SI (≈ 6 mL/2 g), suggesting that with increase in

polymer loading the hydraulic conductivity of B-P GCLs is primarily controlled by polymer clogging rather than Na-B swelling (Tian et al. 2016). Similar findings were observed by previous researchers. Scalia et al (2014) observed that B-P GCL when permeated with 0 to 500 mM CaCl₂ solutions showed low hydraulic conductivity ($<10^{-10}$ m/s) even at a swell of 7 mL/2 g. Chen et al. (2019) conducted hydraulic conductivity and swell index tests on B-P GCLs permeated with CCP leachates (I= 39.5 mM to 975 mM) and observed that B-P GCL with P = 5.1 showed both low ($<10^{-10}$ m/s) and high ($>10^{-10}$ m/s) hydraulic conductivity at SI \approx 16 mL/2 g.

3.4.3 Polymer Loading

The hydraulic conductivity of B-P GCLs varies with varying polymer loading as indicated from previous discussion based on the relationship between hydraulic conductivity and ionic strength (Fig. 3-5) and hydraulic conductivity and swell index (Fig. 3-5). Hydraulic conductivity of B-P GCLs is primarily controlled by polymer clogging when the polymer loading is high ($>5\%$) whereas, for B-P GCLs with low polymer loading ($<5\%$) both Na-B swelling and polymer clogging contribute towards the hydraulic conductivity. The 5% polymer loading criteria is based on the results obtained in this study and may change when B-P GCLs are permeated with other leachates.

The relationship between polymer loading and hydraulic conductivity is shown in Fig. 3-6. Na-B is shown with black symbols whereas for B-P GCLs blue represents $P < 5\%$ and red $P > 5\%$. There exists a direct trend between polymer loading and hydraulic conductivity i.e., with increase in polymer loading hydraulic conductivity is decreasing. At low polymer loading ($P < 5\%$) most of the GCLs show high hydraulic conductivity to CCP

leachates whereas, with $P > 5\%$, hydraulic conductivity has substantially decreased that can be attributed to polymers being more resilient to chemicals than Na-B (Ashmawy et al. 2002; Kolstad et al. 2004; Katsumi et al. 2008; Scalia et al. 2014; Razakamanatsoa et al. 2014; Emidio et al. 2015; Athanassopoulos et al. 2015; Tian et al. 2016; Setz et al. 2017; Chen et al. 2019; Tian et al. 2019).

3.4.4 Polymer Type

Visual examination of the B-P samples after the swell index test showed that the B-P GCLs used in this study may contain two different types of polymers. B-P-0.5, B-P-1.5 and B-P-3.7 formed a viscous gel after hydration in leachates as shown in Fig. 3-7a, whereas B-P-3.4, B-P-5.5 and B-P-12.7 formed small granules of non-viscous hydrogels after hydration, which are likely to be crosslinked polymer (Fig. 3-7b). Chimamkpam et al. (2011) reported that linear polymers when hydrated results in viscous solutions and the viscosity of these solutions can vary depending on molar mass and charge density of polymer and the quality of hydrating medium. Ahmed (2015) reported that hydrogels are formed by water-swollen, crosslinked polymers that can swell and retain a significant amount of water without dissolving in water.

These different types of polymer may affect the mechanism controlling the hydraulic conductivity of B-P GCLs. The linear polymers forming a viscous glue-like substance may help to keep the bentonite particles together whereas, the crosslinked polymer forming small 3 dimensional hydrogels helps to clog the void spaces present between the bentonite particles resulting in low hydraulic conductivity of the B-P GCLs.

Further studies are needed to evaluate the effect and behavior of these two different types of polymers in detail.

Out of six B-P GCLs used in this study three contained linear polymer (B-P-0.5, B-P-1.5 and B-P-3.7) and three contained crosslinked polymers (B-P-3.4, B-P-5.5, B-P-12.7). All the linear B-P GCLs used in this study had polymer loading less than 5% whereas only one of the crosslinked B-P GCL had polymer loading less than 5% (i.e., B-P-3.4). Therefore, it is difficult to make a comparison between the hydraulic conductivity of two different types of B-P GCLs due to different polymer loadings. Comparison between B-P GCLs with different polymer type (B-P-3.4, crosslinked and B-P-3.7, linear) but similar polymer loadings ($P = 3.4\%$ and 3.7%) is shown in Fig. 3-8. The two GCLs showed similar trends of low ($< 10^{-10}$ m/s) and high ($> 10^{-10}$ m/s) hydraulic conductivity to CCP leachates (low for TCCP-50, LRMD-96 and high for TFGDS-473, LR-2179, HI-3179 and HR-4676). Which suggests that polymer loading plays a significant role towards the low hydraulic conductivity of B-P GCLs. Higher polymer results in lower hydraulic conductivity against aggressive CCP leachates. To further understand the effect of polymer type on the hydraulic conductivity of B-P GCLs, tests on B-P GCLs with same polymer loading but different polymer type should be conducted.

3.4.5 Polymer Elution - Preferential Flow

The temporal trend of hydraulic conductivity of B-P-0.5 to LR-2577 leachate ($I = 2577$ mM) is shown in Fig. 3-9a. The hydraulic conductivity of the B-P GCL decreased to 10^{-10} m/s and remained constant for approximately 10 PVF but after 10 PVF the hydraulic conductivity of the GCL sample increased drastically to 10^{-8} m/s. Dye test was conducted

on the GCL sample by adding dye to the permeant liquid following the procedure adopted by Scalia and Benson (2010) to determine the possibility of side wall leakage or preferential flow (Fig. 3-9b). The dye test showed no signs of side wall leakage but showed stains of dye at a small region on the effluent side (Fig. 3-9b) of the GCL sample coinciding with preferential flow pathways for the flow through the GCL, leading to sudden increase in the hydraulic conductivity of the GCL sample from 10^{-10} m/s to 10^{-8} m/s. The potential cause for the preferential flow after 10 PVF can be polymer elution due to polymer being washed away with the effluent from the GCL sample leading to open flow channels and high hydraulic conductivity. Viscous glue like stands of polymer forming on the effluent side of the GCL are also shown in Fig. 3-10. Temporal trend of hydraulic conductivity of B-P-3.4 permeated to LR-2577 leachate is also shown in Fig. 3-9c that shows a constant hydraulic conductivity throughout and when the dye test was conducted on the sample (shown in Fig. 3-9d) it further shows that the dye was uniformly spread over the GCL sample (effluent side) indicating that the GCL had uniform high permeability throughout.. Tian et al. (2019) also related polymer elution from B-P GCL to high hydraulic conductivities ($>10^{-10}$ m/s). Similarly, Chen et al. (2019) reported three different regions of hydraulic conductivities from 10^{-12} m/s to 10^{-8} m/s within one B-P GCL sample due to uneven distribution of polymer loading.

3.5 Summary and Conclusions

Hydraulic conductivity of Na-B and B-P GCLs to six synthetic CCP leachates (I=50 mM to 4676 mM) was evaluated in this study. The B-P GCLs used in this study contained a dry mixture of sodium bentonite and proprietary polymer with polymer loading ranging

from 0.5 % to 12.7%. Hydraulic conductivity tests were conducted at an effective stress of 20 kPa and were continued until the hydraulic and chemical equilibrium was achieved as per ASTM D6766. Tests were also conducted with DI water as control. Swell index and solution retention capacity tests were also conducted on Na-B and B-P GCLs with six synthetic CCP leachates and DI water.

Based on the findings from these tests, the following conclusions and recommendations are drawn:

- B-P GCLs showed much lower hydraulic conductivity to CCP leachates than Na-B GCL. Na-B GCLs can be very permeable to CCP leachates as it resulted in high hydraulic conductivity ($>10^{-10}$ m/s) to all the six synthetic CCP leachates (I = 50 mM to 4676 mM) used in this study. Hydraulic conductivity of B-P GCLs is dependent on the leachate chemistry and polymer loading. All the B-P GCLs can be used for dilute CCP leachates (e.g., TCCP-50 and LRMD-96) whereas, for aggressive CCP leachates (e.g., TFGDS-473, LR-2577 and HI-3179) B-P GCLs with high polymer loading $> 5\%$ should be used. More study is needed to determine whether B-P GCLs with polymer loading $> 12.7\%$ can give low hydraulic conductivity against very aggressive leachates such as HR-4676 (I=4676 mM).
- Typically, two different types of polymers can be found in the B-P GCLs. (1) Polymers that form viscous glue like substance (linear) and (2) polymers that form 3-D polymer hydrogels (crosslinked). The mechanism controlling the hydraulic conductivity of B-P GCLs can vary depending on the type of polymer present. Further studies with B-P GCLs having same polymer loading but different polymer types are needed.

- The mechanism controlling the hydraulic conductivity of Na-B GCLs and B-P GCLs differ depending on the polymer loading. Hydraulic conductivity of Na-B GCLs is controlled by osmotic swelling that is inhibited in the presence of aggressive CCP leachates whereas, for B-P GCLs with low polymer loading (< 5%) both swelling of bentonite and polymer clogging controls the hydraulic conductivity. Hydraulic conductivity of B-P GCLs with polymer loading > 5% appears to be controlled by polymer clogging. B-P GCLs with higher polymer loading also tend to retain higher amount of water.
- Hydraulic conductivity of B-P GCLs can be effected due to polymer elution as it leads to open flow channels for preferential flow paths.

Hydraulic conductivity tests on B-P GCLs with $k < 10^{-10}$ m/s are still running to study their long term hydraulic conductivity. Factors such as effective stress, polymer type and polymer elution needs to be evaluated in more detail.

Tables:

Table 3-1: Mass per unit area, initial thickness and polymer loading of sodium bentonite (Na-B) and bentonite-polymer (B-P) GCLs used in this study.

GCL	Mass per unit area (kg/m ²)	Thickness (mm)	Polymer loading (%)
Na-B	3.6	5.0	-
B-P-0.5	5.7	7.0	0.5
B-P-1.5	6.8	8.9	1.5
B-P-3.4	6.8	7.0	3.4
B-P-3.7	6.1	7.9	3.7
B-P-5.5	6.0	8.1	5.5
B-P-12.7	4.8	7.0	12.7

Note: Polymer loading is calculated based on loss on ignition as per ASTM D7348 and Scalia et al. 2014. Mass per unit area is measured as per ASTM D5993. “-” indicates not applicable. The numeric digits with B-P GCLs represent their polymer loading.

Table 3-2. Properties of selected synthetic CCP leachates.

Leachate	Major cations			Major anions		Bulk properties			
	Na ⁺ (M)	K ⁺ (M)	Mg ²⁺ (M)	Cl ⁻ (M)	SO ₄ ²⁻ (M)	I (mM)	RMD (M ^{1/2})	R= Cl ⁻ /SO ₄ ²⁻	pH
TCCP	0.01	0.00	0.01	0.003	0.01	50	0.10	0.25	6.8
LRMD	0.001	0.00	0.03	0.01	0.02	96	0.005	0.55	6.6
TFGDS	0.17	0.00	0.06	0.06	0.11	473	0.65	0.56	6.5
LR	0.19	0.01	0.57	0.01	0.67	2577	0.27	0.01	5.5
HI	2.23	0.03	0.005	0.47	0.90	3179	32.02	0.53	7.4
HR	3.30	1.34	0.00	4.56	0.04	4676	∞ ^a	122.3	8.4

Note: R = Anion ratio, I = Ionic strength, RMD = Relative abundance of monovalent and divalent cations, HR = High anion ratio, HI = High ionic strength, LR = Low anion ratio, TFGDS = Typical FGD solids, LRMD = Low RMD and TCCP = Typical CCP leachate.

^a ∞ = No divalent cations present.

Table 3-3. Hydraulic conductivity of GCLs permeated with CCP leachates and DI water.

GCL	Permeant liquid	PVF	Total test time (days)	Termination criteria satisfied		Hydraulic conductivity (m/s)
				Hydraulic	Chemical	
Na-B	DI	12.8	110	Yes	No	2.2×10^{-11}
	TCCP-50	30.6	78	Yes	Yes	2.3×10^{-9}
	LRMD-96	7.3	12	Yes	Yes	4.9×10^{-9}
	TFGDS-473	5.7	5	Yes	Yes	1.7×10^{-7}
	LR-2577	4.3	5	Yes	Yes	3.1×10^{-7}
	HI-3179	11.6	17	Yes	Yes	7.9×10^{-7}
	HR-4676	7.5	7	Yes	Yes	7.6×10^{-7}
B-P-0.5	DI	4.6	119	Yes	No	2.2×10^{-11}
	TCCP-50	7.4	160	Yes	No	1.5×10^{-11}
	LRMD-96	77.1	438	Yes	No	2.8×10^{-11}
	TFGDS-473	11.8	33	Yes	Yes	1.4×10^{-7}
	LR-2577	16.3	89	Yes	Yes	4.4×10^{-8}
	HI-3179	17.5	48	Yes	Yes	2.5×10^{-7}
	HR-4676	6.0	15	Yes	Yes	6.0×10^{-7}
B-P-1.5	DI	10.8	395	Yes	No	7.8×10^{-12}
	TCCP-50	9.1	424	Yes	No	5.3×10^{-12}
	LRMD-96	37.1	410	Yes	No	1.2×10^{-11}
	TFGDS-473	25.2	142	Yes	Yes	6.0×10^{-8}
	LR-2577	6.8	16	Yes	Yes	8.5×10^{-9}
	HI-3179	2.3	15	Yes	Yes	4.0×10^{-8}
	HR-4676	4.8	9	Yes	Yes	6.4×10^{-7}
B-P-3.4	DI	3.4	102	Yes	No	5.1×10^{-12}
	TCCP-50	5.2	105	Yes	No	5.4×10^{-12}
	LRMD-96	4.6	106	Yes	No	5.0×10^{-12}
	TFGDS-473	20.9	71	Yes	Yes	6.3×10^{-9}
	LR-2577	9.2	33	Yes	Yes	1.6×10^{-8}
	HI-3179	18.0	62	Yes	Yes	3.2×10^{-7}
	HR-4676	50	60	Yes	Yes	1.0×10^{-8}
B-P-3.7	DI	2.0	127	Yes	No	2.4×10^{-12}
	TCCP-50	2.7	137	Yes	No	3.0×10^{-12}
	LRMD-96	2.8	150	Yes	No	1.5×10^{-12}
	TFGDS-473	5.8	42	Yes	No	2.7×10^{-9}
	LR-2577	33.9	256	Yes	Yes	7.9×10^{-10}
	HI-3179	7.1	56	Yes	Yes	3.0×10^{-8}
	HR-4676	13.7	71	Yes	Yes	9.5×10^{-8}
B-P-5.5	DI	13.0	388	Yes	No	9.4×10^{-12}
	TCCP-50	11.8	423	Yes	No	6.3×10^{-12}
	LRMD-96	7.4	411	Yes	No	4.5×10^{-12}
	TFGDS-473	27.4	431	Yes	Yes	1.4×10^{-11}
	LR-2577	34.3	380	Yes	Yes	3.7×10^{-11}
	HI-3179	3.8	5	Yes	Yes	4.7×10^{-8}
	HR-4676	2.2	4	Yes	Yes	7.6×10^{-8}
B-P-12.7	DI	1.9	37	Yes	No	6.7×10^{-12}
	TCCP-50	2.3	70	Yes	No	2.4×10^{-12}
	LRMD-96	10.2	414	Yes	No	5.0×10^{-12}
	TFGDS-473	5	50	Yes	No	3.18×10^{-12}
	LR-2577	-	-	-	-	-
	HI-3179	37.8	388	Yes	Yes	8.6×10^{-12}
	HR-4676	10.1	10	Yes	Yes	5.0×10^{-7}

Note: PVF = Pore volumes of flow. The numeric digits with CCP leachates represent their ionic strength in mM.

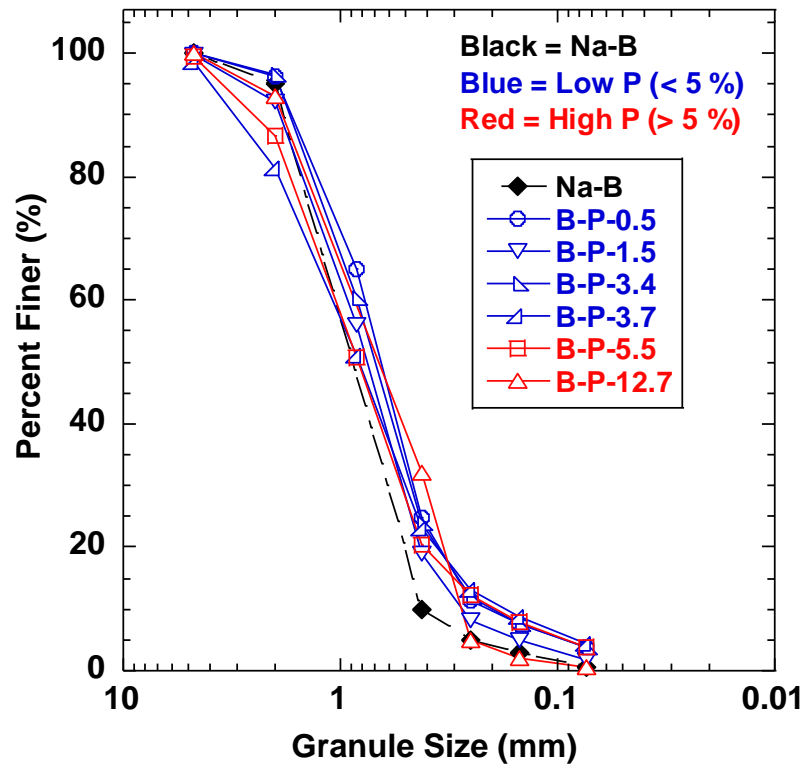


Figure 3-1: Grain size distribution of sodium bentonite (Na-B) and bentonite polymer (B-P) GCLs used in this study. Note: Na-B = conventional sodium bentonite GCL with polymer loading = 0%, P = polymer loading.

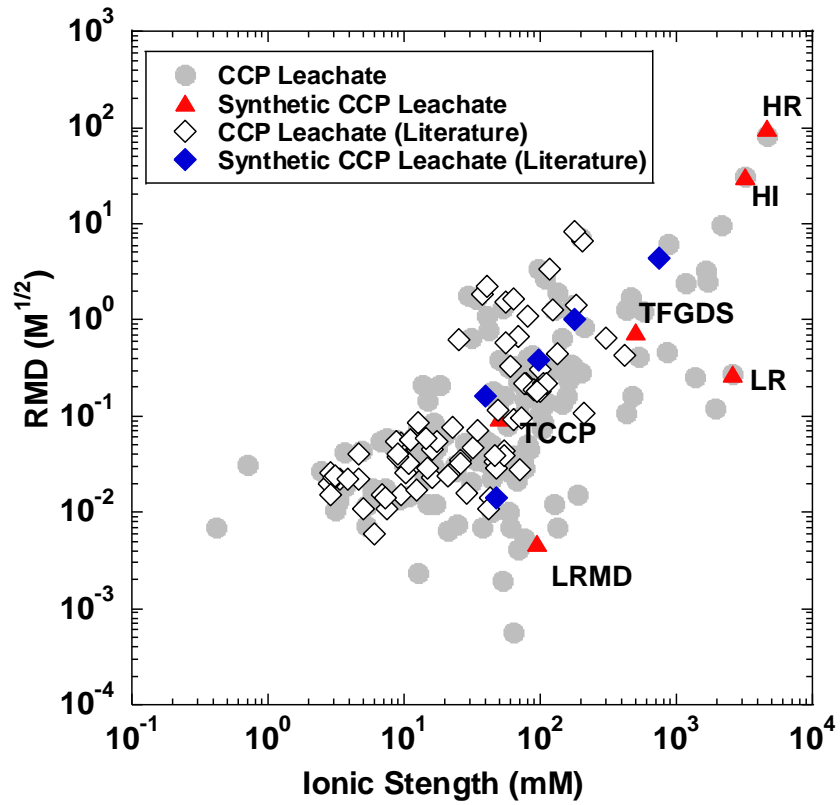


Figure 3-2: Comparison of selected synthetic CCP leachate with CCP leachate used by previous researchers (Chen et al. 2019). Note: The maximum RMD observed in case of CCP leachate data was ∞ (i.e. only monovalent cations present) but to represent that data in figure RMD = 100 has been used.

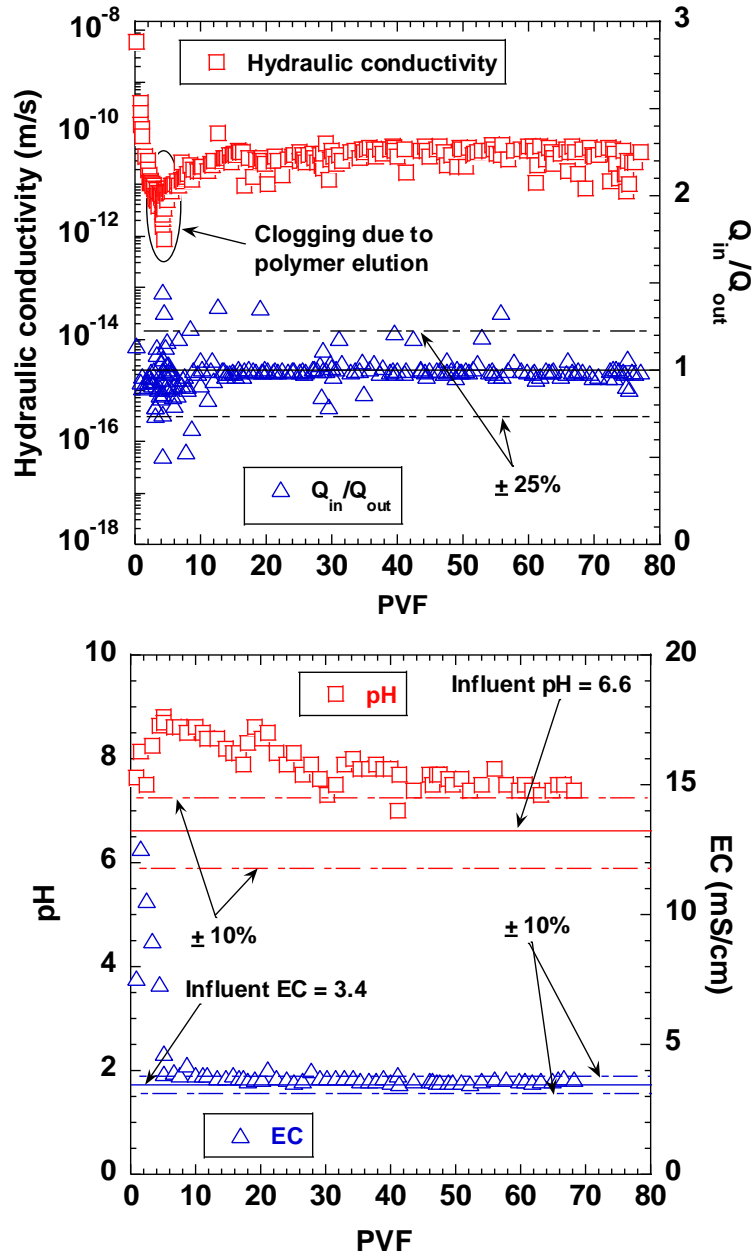


Figure 3-3: Hydraulic conductivity, ratio of inflow to outflow (Q_{in}/Q_{out}), pH, and EC from test on B-P-0.5 permeated to LRMD-96 leachate.

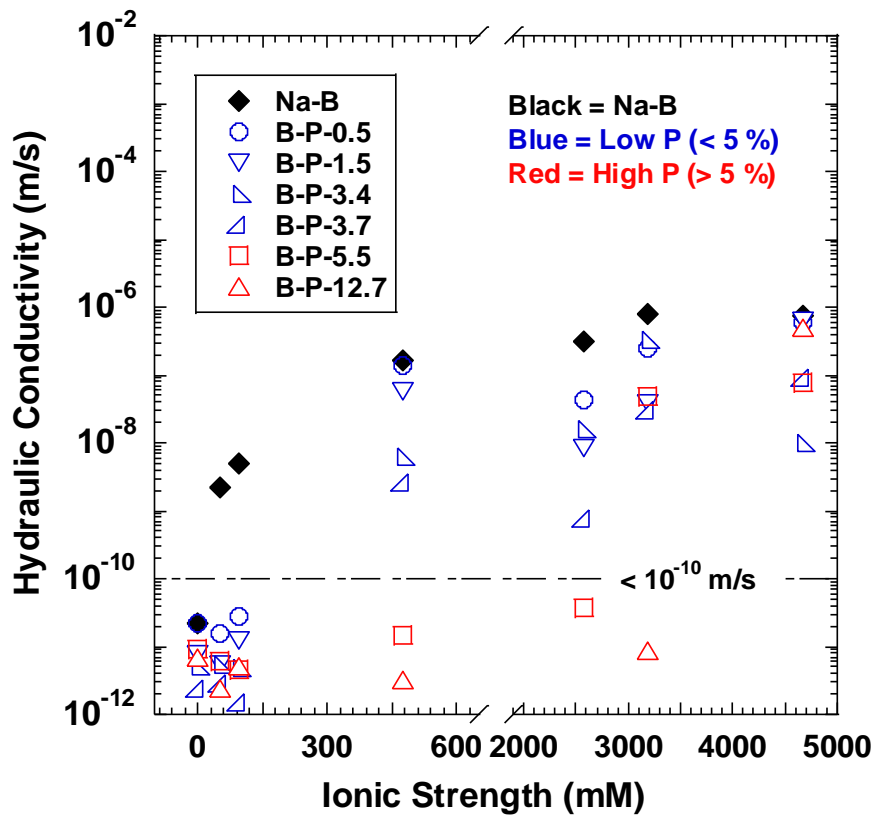


Figure 3-4: Hydraulic conductivity of GCLs as a function of ionic strength.

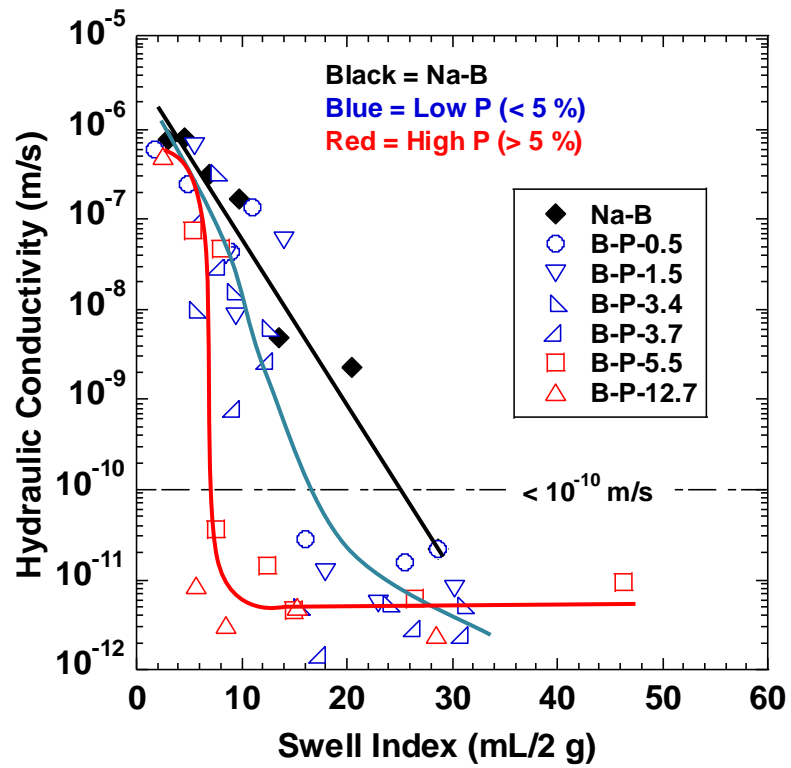


Figure 3-5: Hydraulic conductivity versus swell index of Na-B and B-P GCLs in CCP leachates and DI water.

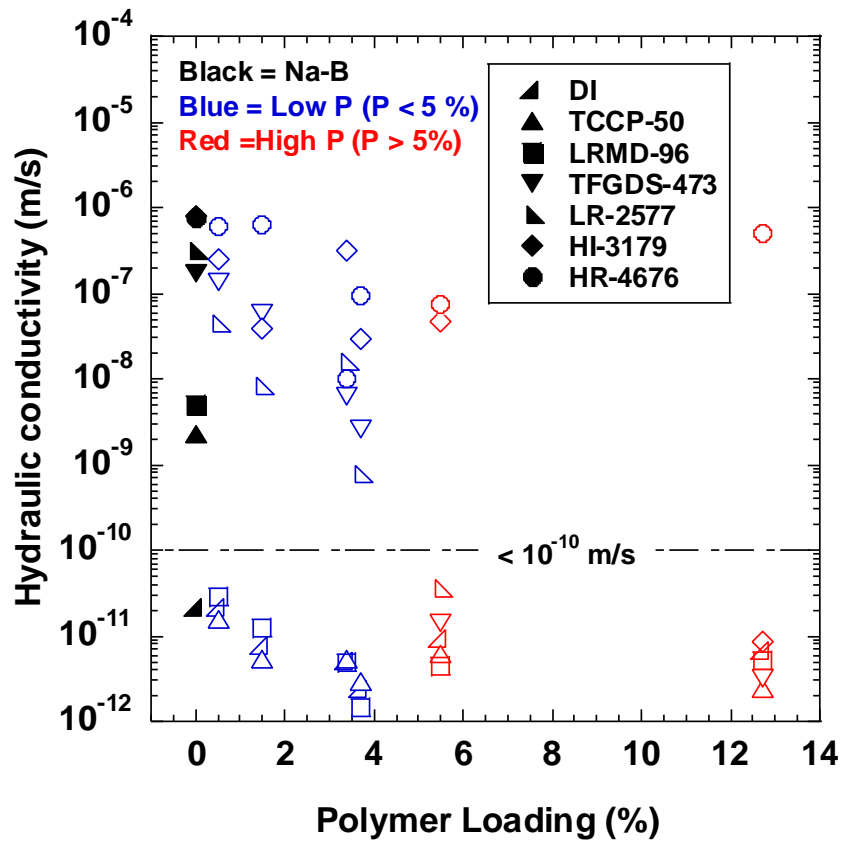


Figure 3-6: Hydraulic conductivity of GCLs as a function of polymer loading.

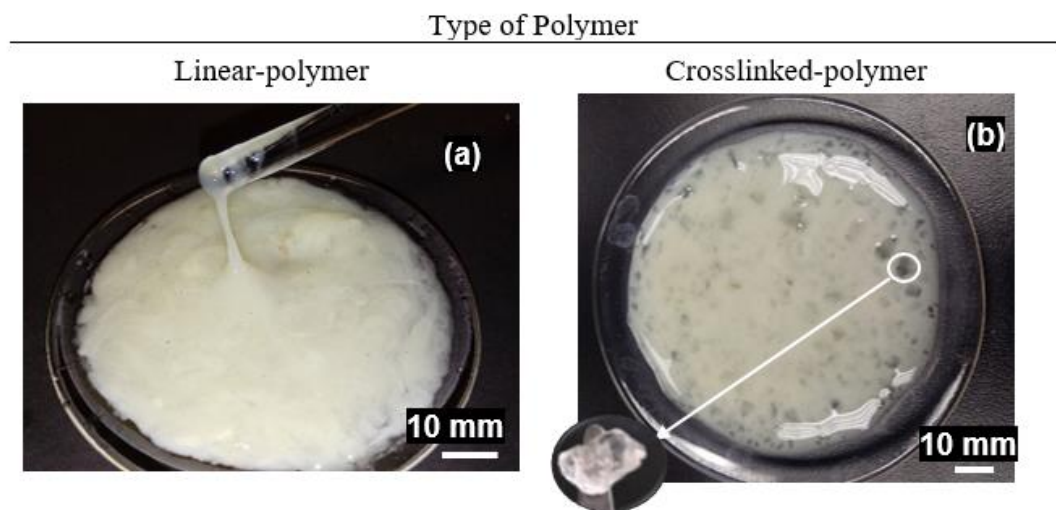


Figure 3-7: Images of two different types of polymers found in BP-GCLs. (a) B-P-3.7 and (b) B-P-5.5.

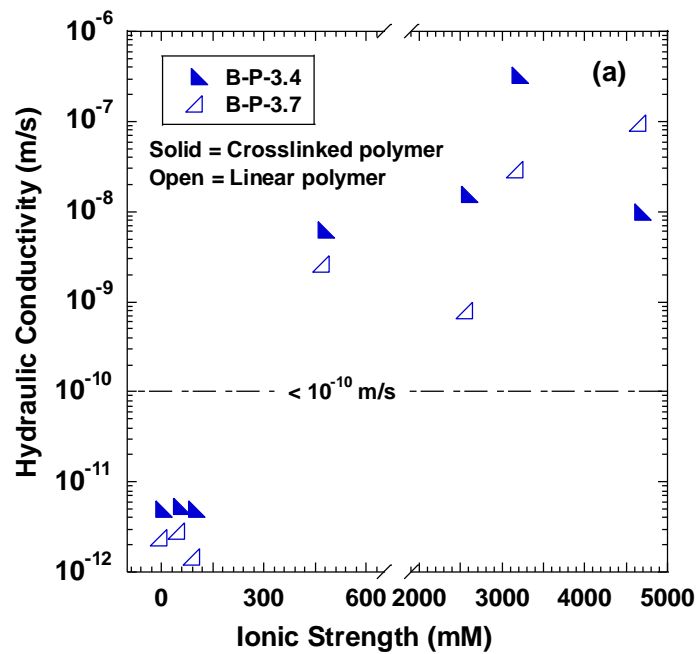


Figure 3-8: Comparison of hydraulic conductivity of B-P GCLs with similar polymer loading but different polymer type (linear vs. crosslinked polymers).

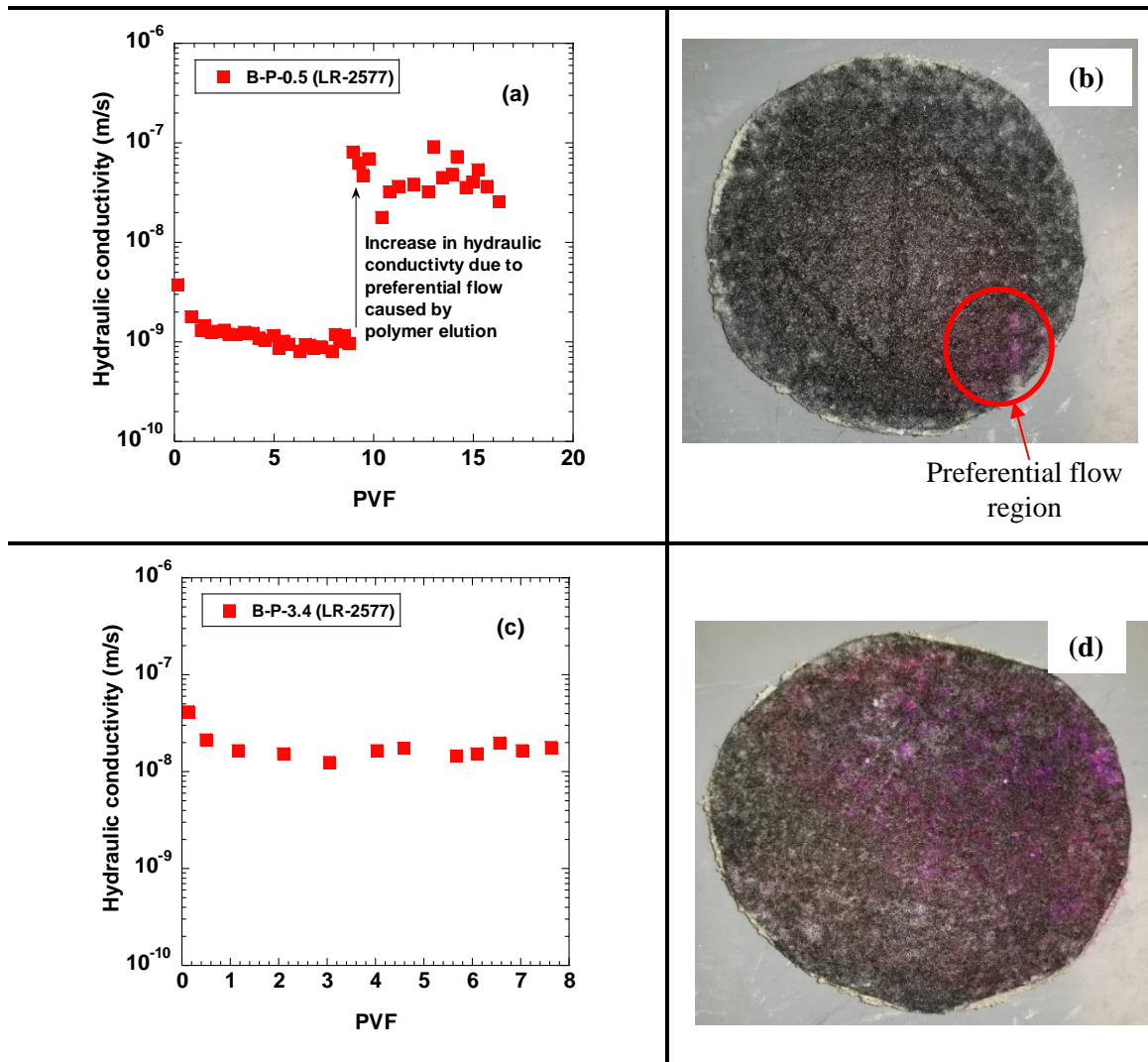


Figure 3-9: (a) Temporal behavior of B-P-0.5 permeated to LR-2577 leachate (b) dye test conducted on B-P-0.5 (LR-2577) indicating preferential flow on the effluent side of GCL (c) Temporal behavior of B-P-3.4 permeated with LR-2577 and (d) dye test on B-P-3.4 (LR-2577) showing uniform flow distribution on effluent side of GCL.

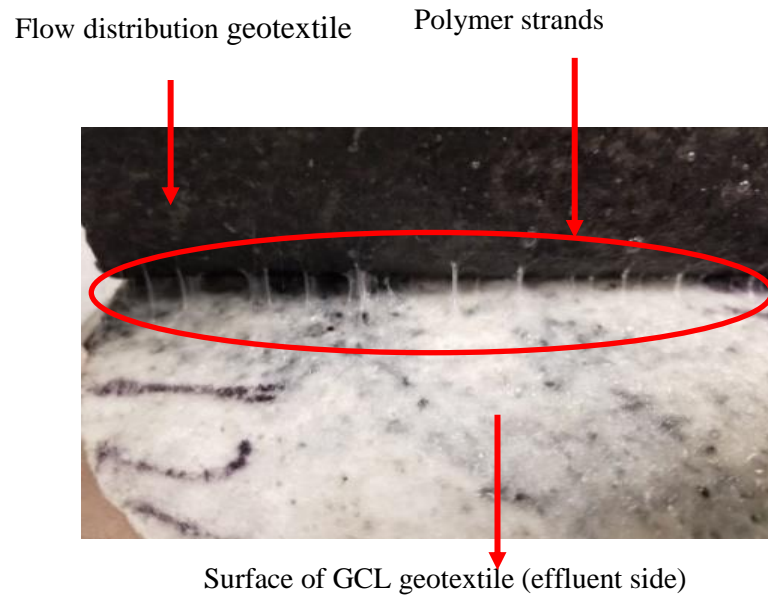


Figure 3-10: Polymer elution from B-P GCL during permeation with CCP leachate

CHAPTER 4 : FINAL REMARKS AND CONCLUSION

Based on the findings and results explained in the previous chapters following conclusions can be made:

As discussed in chapter 2, sieving and crushing of bentonite polymer mixtures as per ASTM D5890 (standard test method for swell index) resulted in segregation of bentonite and polymer on #100 sieve. It indicates that ASTM D5890 swell test has some limitations particularly for B-P GCLs that can lead to inaccurate measurement of swell and polymer loading of the B-P GCLs and there is a need for a new and modified swell test for B-P GCLs. Results also showed that as-is method of sample preparation (i.e., without crushing and sieving) can prevent the segregation of B-P mixtures hence, it is recommended that index test of B-P GCLs should be performed using as is samples.

Moreover, swell index and loss on ignition test conducted on material retained on #100 sieve showed that it was primarily the polymer and visual examination after swell test conducted on the polymers retained on #100 sieve showed that the B-P GCLs used in this study mainly consisted of two different types of polymer i.e., linear and crosslinked polymer.

The hydraulic conductivity test results discussed in chapter 3 showed that Na-B GCL with zero polymer loading resulted in high hydraulic conductivity $> 10^{-10}$ m/s to all CCP leachates whereas, for B-P GCLs the hydraulic conductivity to CCP leachates is dependent on leachate chemistry and polymer loading. For dilute leachates (TCCP-50 and LRMD-96) all the B-P GCLs showed low hydraulic conductivity. B-P GCLs with high

polymer loading (> 5%) are needed to give low hydraulic conductivity ($< 10^{-10}$ m/s) to aggressive CCP leachates ($I = 2577$ and 3179 mM). In addition to polymer loading effect of polymer type may also affect the hydraulic conductivity of B-P GCLs. In this study, polymer loading was found to have greater impact than polymer type but to study the behavior of polymer type in more detail hydraulic conductivity tests on B-P GCLs with same polymer loading but different polymer type needs to be conducted.

Future Research

In landfills the waste is generally placed in layers and each layer applies a different effective stress on the GCLs. Hydraulic conductivity tests with varying effective stress from 20 kPa to 100, 250 and 500 kPa (replicating field loads) are being conducted to study the effect of effective stress on hydraulic conductivity of GCLs.

A series of loss on ignition (LOI) tests are being conducted on B-P mixtures with different types of polymers and with varying polymer loadings at varying temperatures and time of burning to find the best approach to determine the polymer loading of the B-P mixtures. As it is very important for quality control purposes to determine the exact polymer loading of the B-P GCLs used in the field as increase in polymer loading decreases the hydraulic conductivity but also increases the cost of the material. Loss on ignition test conducted on B-P GCLs to determine polymer loading involves assumptions such as 100% polymer burns at 550 °C within 4 hours but these assumptions may not be accurate for all the polymer used in B-P GCLs.

REFERENCES

- Ahmed, E. M. (2015). Hydrogel: Preparation, characterization, and applications: A review. *Journal of advanced research*, 6(2), 105-121.
- Americal Coal Ash Association, (2015). *Key findings 2015, Coal Combustion Products Utilization, U.S. Historical Perspective and Forecast*. ACAA.
- Ashmawy, A. K., El-Hajji, D., Sotelo, N., & Muhammad, N. (2002). Hydraulic performance of untreated and polymer-treated bentonite in inorganic landfill leachates. *Clays and Clay Minerals*, 50(5), 546-552.
- Athanassopoulos, C., Benson, C., Donovan, M. & Chen, J. (2015). Hydraulic conductivity of a polymer-modified gcl permeated with high-ph solutions. *Proceedings of the Geosynthetics 2015 Conf*, Portland, OR, 2015.
- Benson, C. H., Ören, A. H., & Gates, W. P. (2010). Hydraulic conductivity of two geosynthetic clay liners permeated with a hyperalkaline solution. *Geotextiles and Geomembranes*, 28(2), 206-218.
- Benson, C., J. Chen, and T. Edil. 2014. Engineering properties of geosynthetic clay liners permeated with coal combustion product leachates. Rep. No. 3002003770. Palo Alto, CA: Electric Power Research Institute.
- Bouazza, A., and Bowders, J. (2010). *Geosynthetic clay liners for waste containment facilities*, CRC Press, Leiden, Netherlands.
- Bradshaw, S.L. & Benson, C.H. (2014). Effect of municipal solid waste leachate on hydraulic conductivity and exchange complex of geosynthetic clay liners. *Journal of Geotechnical and Geoenvironmental Engineering*, 140(4), 04013038.
- Bradshaw, S.L., Benson, C.H. & Rauen, T.L. (2016). Hydraulic conductivity of geosynthetic clay liners to recirculated municipal solid waste leachates. *Journal of Geotechnical and Geoenvironmental Engineering*, 142(2), 04015074.
- Chen, J. N., Bradshaw, S. L., Likos, W. J., Benson, C. H., & Edil, T. B. (2014). Hydraulic conductivity of geosynthetic clay liners to synthetic coal combustion product leachates. In *Geo-Congress 2014: Geo-characterization and Modeling for Sustainability* (pp. 334-342).
- Chen, J.N., Benson, C.H. & Edil, T.B. (2018). Hydraulic conductivity of geosynthetic clay liners with sodium bentonite to coal combustion product leachates. *Journal of Geotechnical and Geoenvironmental Engineering*, 144(3), 04018008.
- Chen, Jiannan & Salihoglu, Hulya & Benson, Craig & J. Likos, William & Edil, Tuncer. (2019). Hydraulic Conductivity of Bentonite-Polymer Composite Geosynthetic Clay Liners Permeated with Coal Combustion Product Leachates. *Journal of*

Geotechnical and Geoenvironmental Engineering. 145. 10.1061/(ASCE)GT.1943-5606.0002105.

- Chimamkpm, T. O., Rasteiro, M. G., Garcia, F. A. P., Antunes, E., Ferreira, P., Hunkeler, D., & Wandrey, C. (2011). Solution viscosity and flocculation characteristics of linear polymeric flocculants in various media. *Chemical Engineering Research and Design*, 89(7), 1037-1044.
- Di Emidio, G., Mazzieri, F., Verastegui-Flores, R. D., Van Impe, W., & Bezuijen, A. (2015). Polymer-treated bentonite clay for chemical-resistant geosynthetic clay liners. *Geosynthetics International*, 22(1), 125-137.
- Donovan, M.S., Valorio, R. & Gebka, B (2017). Polymer enhanced geosynthetic clay liners for bauxite storage. *Proceedings of the Proceedings of 35th International ICSOBA Conference*, Hamburg, Germany, 2017, Pp. 478.
- Grim, R. E. (1968). *Clay mineralogy*. McGraw-Hill, New York.
- Guyonnet, D., Gaucher, E., Gaboriau, H., Pons, C. H., Clinard, C., Norotte, V., & Didier, G. (2005). Geosynthetic clay liner interaction with leachate: correlation between permeability, microstructure, and surface chemistry. *Journal of Geotechnical and Geoenvironmental Engineering*, 131(6), 740-749.
- Heebink, L. V., Buckley, T. D., Hassett, D. J., Zacher, E. J., Pflughoeft-Hassett, D. F., & Dockter, B. A. (2007). Current status of spray dryer absorber material characterization and utilization. *World of Coal Ash (WOCA)*.
- Jo, H.Y., Katsumi, T., Benson, C.H. & Edil, T.B. (2001). Hydraulic conductivity and swelling of nonprehydrated gcls permeated with single-species salt solutions. *Journal of Geotechnical and Geoenvironmental Engineering*, 127, 557-567.
- Jo, H.Y., Benson, C.H. & Edil, T.B. (2004). Hydraulic conductivity and cation exchange in non-prehydrated and prehydrated bentonite permeated with weak inorganic salt solutions. *Clays and Clay Minerals*, 52, 661-679.
- Jo, H.Y., Benson, C.H., Shackelford, C.D., Lee, J.-M. & Edil, T.B. (2005). Long-term hydraulic conductivity of a geosynthetic clay liner permeated with inorganic salt solutions. *Journal of Geotechnical Geoenvironmental Engineering*, 131, 405-417.
- Katsumi, T., Ishimori, H., Onikata, M. & Fukagawa, R. (2008). Long-term barrier performance of modified bentonite materials against sodium and calcium permeant solutions. *Geotextiles and Geomembranes*, 26, 14-30.
- Koerner, R.M. (2012). *Designing with geosynthetics*. 5 Edition. Pearson Prentice Hall, Upper Saddle River, New Jersey 07458.
- Kolstad, D. C. (2000). Compatibility of geosynthetic clay liners (GCLs) with multi-species inorganic solutions. MS Thesis, University of Wisconsin at Madison.

- Kolstad, D.C., Benson, C.H. & Edil, T.B. (2004a). Hydraulic conductivity and swell of nonprehydrated geosynthetic clay liners permeated with multispecies inorganic solutions. *Journal of Geotechnical and Geoenvironmental Engineering*, 130, 1236-1249.
- Kolstad, D. C., Benson, C. H., Edil, T. B., & Jo, H. Y. (2004b). Hydraulic conductivity of a dense prehydrated GCL permeated with aggressive inorganic. *Geosynthetics International*, 11(3), 233-241.
- Lee, J.-M., Shackelford, C.D., Benson, C.H., Jo, H.-Y., Edil, T.B. (2005) Correlating index properties and hydraulic conductivity of geosynthetic clay liners. *Journal of Geotechnical and Geoenvironmental Engineering*, 131(11), 1319-1329.
- Mesri, G. & Olson, R.E. (1971). Mechanisms controlling the permeability of clays. *Clays and Clay Minerals*, 19, 151-158.
- Onikata, M., Kondo, M., Hayashi, N., Yamanaka, S.J.C. & Minerals, C. (1999). Complex formation of cation-exchanged montmorillonites with propylene carbonate: Osmotic swelling in aqueous electrolyte solutions. *Clays and Clay Minerals*, 47(5), 672-677.
- Ören, A. H., & Akar, R. Ç. (2017). Swelling and hydraulic conductivity of bentonites permeated with landfill leachates. *Applied Clay Science*, 142, 81-89.
- Petrov, R.J. & Rowe, R.K. (1997). Geosynthetic clay liner (gcl)-chemical compatibility by hydraulic conductivity testing and factors impacting its performance. *Canadian Geotechnical Journal*, 34, 863-885.
- Razakamanantsoa, A.R. & Djeran-Maigre, I. (2016). Long term chemo-hydro-mechanical behavior of compacted soil bentonite polymer complex submitted to synthetic leachate. *Waste Manag*, 53, 92-104.
- Salihoglu, H., Chen, J.N., Likos, W.J. & Benson, C.H. (2016). Hydraulic conductivity of bentonite-polymer geosynthetic clay liners in coal combustion product leachates. *Geo-Chicago 2016*, Pp. 438-447.
- Sari, K. & Chai, J. (2013). Self healing capacity of geosynthetic clay liners and influencing factors. *Geotextiles and Geomembranes*, 41, 64-71.
- Scalia, J., Benson, C. H., Edil, T. B., Bohnhoff, G. L., & Shackelford, C. D. (2011). Geosynthetic clay liners containing bentonite polymer nanocomposite. In *Geo-Frontiers 2011: Advances in geotechnical engineering* (pp. 2001-2009).
- Scalia, J., Benson, C. H., Bohnhoff, G. L., Edil, T. B., & Shackelford, C. D. (2014). Long-term hydraulic conductivity of a bentonite-polymer composite permeated with aggressive inorganic solutions. *Journal of Geotechnical and Geoenvironmental Engineering*, 140(3), 04013025.

- Scalia, J., Benson, C. & Finnegan, M. (2018). Alternate procedures for swell index testing of granular bentonite from GCLs. *Geotechnical Testing Journal* 42 (in press), <https://doi.org/10.1520/GTJ20180075>.
- Setz, M. C., Tian, K., Benson, C. H., & Bradshaw, S. L. (2017). Effect of ammonium on the hydraulic conductivity of geosynthetic clay liners. *Geotextiles and Geomembranes*, 45(6), 665-673.
- Shackelford, C.D., Benson, C.H., Katsumi, T., Edil, T.B. & Lin, L. (2000). Evaluating the hydraulic conductivity of gcls permeated with non-standard liquids. *Geotextiles and Geomembranes*, 18, 133-161.
- Shan, H., and Daniel, D. (1991). "Results of laboratory tests on a geotextile/bentonite liner material." *Proc., Geosynthetics, Industrial Fabrics Association International, St. Paul, MN*, 517–535.
- Tian, K., Benson, C.H. & Likos, W.J. (2016). Hydraulic conductivity of geosynthetic clay liners to low-level radioactive waste leachate. *Journal of Geotechnical and Geoenvironmental Engineering*, 142, 04016037.
- Tian, K. & Benson, C.H. (2017). Chemical compatibility of geosynthetic clay liners to aggressive bauxite liquor. *Proceedings of the Proceedings of 35th International ICSOBA Conference, Hamburg, Germany*, Pp. 479-484.
- Tian, K., Benson, C.H. & Likos, W.J. (2017). Effect of an anion ratio on the hydraulic conductivity of a bentonite-polymer geosynthetic clay liner. *Geotechnical Frontiers 2017*, Pp. 180-189.
- Tian, K., Likos, W. J., & Benson, C. H. (2019). Polymer Elution and Hydraulic Conductivity of Bentonite–Polymer Composite Geosynthetic Clay Liners. *Journal of Geotechnical and Geoenvironmental Engineering*, 145(10), 04019071.
- Yun, K. K., Kim, K. K., Choi, W., & Yeon, J. (2017). Hygral behavior of superabsorbent polymers with various particle sizes and cross-linking densities. *Polymers*, 9(11), 600.

BIOGRAPHY

Binte Zainab is Pakistani-born civil engineer who did her Bachelor of Civil Engineering from one of the renowned universities of Pakistan, University of Engineering and Technology (UET) Lahore, Pakistan. Zainab graduated among top 5 % students of her civil engineering batch of 2016. After completion of her bachelors she worked in a geotechnical consultancy company as a trainee engineer. She then started her master's in civil environmental and Infrastructure Engineering in spring 2018 at George Mason University (GMU) Fairfax, VA. During that she also got the opportunity of working as a graduate research assistant with Dr. Kuo Tian as her adviser. Her research topic is to evaluate the hydraulic conductivity of bentonite-polymer geosynthetic clay liners to aggressive coal combustion product leachates.